

Copyright

by

Andres Jose Jasso

2012

**The Thesis Committee for Andres Jose Jasso  
Certifies that this is the approved version of the following thesis:**

**Characterization of Fly Ash for Evaluating the Alkali-Silica Reaction  
Resistance of Concrete**

**APPROVED BY  
SUPERVISING COMMITTEE:**

**Supervisor:**

---

Kevin J. Folliard

**Co-Supervisor:**

---

Raissa Ferron

**Characterization of Fly Ash for Evaluating the Alkali-Silica Reaction  
Resistance of Concrete**

**by**

**Andres Jose Jasso, B.S.C.E.**

**Thesis**

Presented to the Faculty of the Graduate School of

The University of Texas at Austin

in Partial Fulfillment

of the Requirements

for the Degree of

**Master of Science in Engineering**

**The University of Texas at Austin**

**December 2012**

## **Acknowledgements**

I would like to sincerely thank several individuals that took part and assisted in this project. I would first like to thank my family for their support throughout the years. To my son, Andy Jr., thank you for having fun with me during my writing breaks.

My sincere gratitude goes to my project advisor Dr. Kevin Folliard for the opportunity of this research. Thank you for your continuous support throughout graduate school and before.

I would also like to thank my co-advisor Dr. Raissa Ferron for your assistance in and guidance with this research. You were very helpful with the many questions.

To my colleague Karla, thanks for your help and insight with everything. You made the experiments and the lab a fun place.

Thank you TxDOT for both your financial support and laboratory assistance when our equipment was not cooperating.

Finally, I would also like to thank the faculty and staff of the Concrete Durability Center. My sincere thanks also goes to Thanos Drimalas for helping with the everyday questions and the fun fishing breaks. Thank you Sherian and Mike for your help at the lab the past four years. Thank you Dr. Juenger for always being a part of the meetings and for your assistance with the many chemistry discussions.

## **Abstract**

### **Characterization of Fly Ash for Evaluating the Alkali-Silica Reaction Resistance of Concrete**

Andres Jose Jasso M.S.E.

The University of Texas at Austin, 2012

Co-Supervisors: Kevin J. Folliard & Raissa Ferron

Fly ash has been used extensively to control deleterious alkali-silica reaction in concrete. The majority of fly ashes can be used to control ASR induced expansion. Fly ashes with high CaO contents are less effective at reducing expansion and fly ashes with high alkali contents can be counter active. Class C fly ashes are less effective at reducing the pH of the pore solution because they are less pozzolanic. The pozzolanic reaction in Class F fly ashes enhances the ability for the hydration products to bind alkalis. This prevents the availability of these alkalis for ASR. This project aims to characterize fly ash in a way that best predicts how it will perform in concrete with an emphasis on ASR. Fly ashes with a variety of chemical compositions were evaluated using a range of analytical and characterization techniques. Research data from several universities were used to correlate their long term data with this project's accelerated tests. This research aimed at evaluating the mineralogical, chemical, and physical characteristics that most affect the ability of a given fly ash to prevent ASR-induced expansion and cracking.

## Table of Contents

List of Tables .....	ix
List of Figures .....	x
List of Notation .....	xiv
Chapter 1: Introduction .....	1
1.1 Introduction.....	1
1.2 Scope and Objective .....	1
Chapter 2: Literature Review.....	3
2.1 Alkali – Aggregate Reaction.....	3
2.1.1 Alkali – Carbonate Reaction.....	3
2.1.2 Alkali – Silica Reaction .....	4
2.2 Fly Ash.....	7
2.2.1 Background.....	8
2.2.2 Effects on Concrete.....	10
2.3 Effects of Fly Ash on Alkali – Silica Reaction.....	11
2.3.1 Fly ash effectiveness .....	11
2.3.2 Available Alkalis .....	14
2.3.3 Pore Solution Chemistry .....	18
2.4 Testing of Expansion due to Alkali – Silica Reaction .....	23
2.4.1 ASTM C 1260, 1567.....	24
2.4.2 ASTM C 1293.....	24
2.4.3 Outdoor Exposure Blocks .....	25
Chapter 3: Materials and Testing Methods .....	27
3.1 Materials .....	27
3.2 Testing Methods.....	30
3.2.1 X-Ray Fluorescence.....	30
3.2.2 Particle Size Distribution .....	32
3.2.2.1 ASTM C 430 Residue Retained on No. 325 Sieve.....	32

3.2.2.2 Laser Diffraction .....	32
3.2.3 Total Alkalis (Acid-Soluble).....	33
3.2.4 Available Alkalis .....	33
3.2.5 Pore Solution Extraction .....	34
3.2.6 ASTM C 1260, 1567.....	35
3.2.7 Leaching Test.....	36
3.2.8 Flame Photometer .....	37
Chapter 4: Results and Analysis .....	39
4.1 Raw Materials .....	39
4.1.1 Particle Size Distribution .....	39
4.1.1.1 Wet No. 325 Sieve .....	39
4.1.1.2 Laser Diffraction.....	40
4.1.2 X-Ray Fluorescence.....	44
4.1.3 Total Alkalis (Acid-Soluble).....	48
4.2 ASTM C 1260, 1567.....	53
4.3 Paste .....	62
4.3.1 Pore Solution Extraction .....	62
4.3.2 Leaching.....	68
4.3.3 Available Alkalis .....	76
Chapter 5: Discussion .....	81
Chapter 6: Conclusion.....	88
6.1 Summary .....	88
6.2 Conclusions.....	88
6.3 Recommendations for Further Study .....	90

Appendix A: ASTM C 1260 Testing Results .....	92
Appendix B: XRF Trends .....	101
Appendix C: Trends for Total Alkalis, Available Alkalis, Pore Solution, and Leaching .....	104
References .....	108



## **List of Tables**

Table 1: Chemical Composition for ASR Gel Formed (Monteiro et al, 1997) .....	7
Table 2: Fly Ash Classification.....	9
Table 3: C-S-H Composition .....	11
Table 4: Original Proposal Fly Ashes .....	29
Table 5: Cement ID.....	29
Table 6: Thesis ID and Proposal ID.....	30
Table 7: Fly Ash XRF Results .....	46
Table 8: Cement XRF .....	46
Table 9: Chemical Composition of FA-7 & 10 .....	85

## List of Figures

Figure 1: Effect of SCM and Replacement Level on the Pore Solution [OH-] (Thomas, 2011) .....	13
Figure 2: Effect of SCM Replacement on ASR Expansion (Thomas, 2011) .....	14
Figure 3: Long-Term Available Alkalis (Lee et al., 1985) .....	16
Figure 4: Effect of Fly Ash on Available Alkalis (Thomas, Shehata, 2006) .....	18
Figure 5: Sources of Alkalis in Pore Solution (Shehata, 2001) .....	19
Figure 6: Pore Solution Concentrations (Diamond, 1981) .....	20
Figure 7: Alkalis in Pore Solution (Duchesne, Berube, 1994) .....	21
Figure 8: Effect of % Fly ash on Pore Solution (Hooton et al, 2009) .....	22
Figure 9: Effect of 25% Fly Ash on Pore Solution (Hooton et al, 2009) .....	23
Figure 10: XRF Sample Preparation .....	31
Figure 11: Pore Press Apparatus .....	34
Figure 12: Dual Flame Photometer (Cole Parmer) .....	38
Figure 13: The Process Involved in Flame Photometry (Sherwood Scientific) ....	38
Figure 14: Percent Passing No. 325 Sieve .....	40
Figure 15: Fly Ash Particle Size Distribution .....	41
Figure 16: Particle Size Distribution (CaO<20%) .....	42
Figure 17: Particle Size Distribution (CaO>20%) .....	42
Figure 18: Average Particle Diameter by Mass .....	43
Figure 19: CaO and Na <sub>2</sub> Oe Percentages .....	45
Figure 20: Sum of Oxides, CaO Percentages .....	47
Figure 21: Acid-Soluble Results .....	49
Figure 22: Acid-Soluble Alkalis (CaO) .....	50

Figure 23: Acid-Soluble/Total Alkalis (CaO).....	51
Figure 24: Acid-Soluble Alkalis (Na <sub>2</sub> O <sub>e</sub> ) .....	51
Figure 25: Acid-Soluble Compositional Parameter .....	53
Figure 26: ASTM 1260 14 Day Similar Chemical Compositions.....	54
Figure 27: ASTM C 1260 28 Day Similar Chemical Compositions .....	56
Figure 28: ASTM 14 Day FA-8.....	57
Figure 29: ASTM C 1260 14 Day Expansion - Wide Range of CaO.....	58
Figure 30: ASTM 1260 14 Day Expansion - CaO Relationship .....	59
Figure 31: ASTM 1260 14 Day Expansion - Na <sub>2</sub> O <sub>e</sub> Relationship.....	60
Figure 32: ASTM 1260 14 Day Expansion - SiO <sub>2</sub> Relationship .....	60
Figure 33: ASTM 1260 14 Day Expansion - Chemical Index.....	61
Figure 34: Pore Solution Alkali Concentrations .....	63
Figure 35: Pore Solution Concentration (CaO) .....	65
Figure 36: Pore Solution Concentration (SiO <sub>2</sub> ) .....	65
Figure 37: Pore Solution Concentration (Na <sub>2</sub> O <sub>e</sub> ).....	66
Figure 38: Pore Solution Concentration (CaO/SiO <sub>2</sub> ).....	67
Figure 39: Pore Solution Concentration (Na <sub>2</sub> O <sub>e</sub> xCaO/SiO <sub>2</sub> ).....	67
Figure 40: Pore Solution Concentration (Chemical Index) .....	68
Figure 41: Leaching at 0 M OH-.....	69
Figure 42: Leaching at 0 M OH- (CaO).....	70
Figure 43: Leaching at 0 M OH- (SiO <sub>2</sub> ) .....	71
Figure 44: Leaching at 0 M OH- (Na <sub>2</sub> O <sub>e</sub> ).....	71
Figure 45: Leaching at 0 M OH- (Chemical Index) .....	72
Figure 46: Leaching at 0.1 M OH- (Chemical Index) .....	73
Figure 47: Leaching at 0.2 M OH - (Chemical Index) .....	73

Figure 48: Leaching at 0.3 M OH- (Chemical Index) .....	74
Figure 49: Leaching at 0.6 M OH- (Chemical Index) .....	75
Figure 50: Overall Data Set for Leaching Experiment .....	76
Figure 51: Available Alkalis .....	77
Figure 52: Available Alkalis (SiO <sub>2</sub> ).....	78
Figure 53: Available Alkalis/Total (SiO <sub>2</sub> ) .....	79
Figure 54: Available Alkalis (Na <sub>2</sub> O <sub>e</sub> ) .....	80
Figure 55: ASTM C 1293 35% Fly Ash Expansion with Pore Solution Study .....	82
Figure 56: ASTM C 1260 Expansion with Pore Solution Study .....	83
Figure 57: Exposure Block Data with Chemical Index .....	84
Figure 58: Pore Solution Study with Chemical Composition Change of Fly Ash .....	85
Figure 59: Comparison of ASTM C 1293 Pore Solution .....	86
Figure A - 1: C-1 (Control).....	92
Figure A - 2: FA-8 (1).....	92
Figure A - 3: FA-8 (2).....	93
Figure A - 4: FA-5 .....	93
Figure A - 5: FA-9 .....	94
Figure A - 6: FA-7 .....	94
Figure A - 7: FA-17 .....	95
Figure A - 8: FA-12 .....	95
Figure A - 9: FA-2 .....	96
Figure A - 10: FA-16 .....	96
Figure A - 11: FA-11 .....	97
Figure A - 12: FA-6 .....	97
Figure A - 13: FA-3 .....	98

Figure A - 14: ASTM C 1260 28 Day (CaO) .....	98
Figure A - 15: ASTM C 1260 28 Day (SiO <sub>2</sub> ) .....	99
Figure A - 16: ASTM C 1260 28 Day (Na <sub>2</sub> O <sub>e</sub> ).....	99
Figure A - 17: ASTM C 1260 28 Day Chemical Index .....	100
Figure B - 1: CaO vs. SiO <sub>2</sub> .....	101
Figure B - 2: CaO vs. Al <sub>2</sub> O <sub>3</sub> .....	101
Figure B - 3: CaO vs. MgO.....	102
Figure B - 4: CaO vs. Fe <sub>2</sub> O <sub>3</sub> .....	102
Figure B - 5: CaO vs. Na <sub>2</sub> O <sub>e</sub> .....	103
Figure C - 1: Acid-Soluble Alkalis (SiO <sub>2</sub> ).....	104
Figure C - 2: Acid-Soluble/Total Alkalis (SiO <sub>2</sub> ) .....	104
Figure C - 3: Acid-Soluble/Total Alkalis (Chemical Index) .....	105
Figure C - 4: Acid-Soluble/Total Alkalis (Na <sub>2</sub> O <sub>e</sub> ).....	105
Figure C - 5: Leaching at 0.1 M OH-.....	106
Figure C - 6: Leaching at 0.2 M OH-.....	106
Figure C - 7: Leaching at 0.3 M OH-.....	107
Figure C - 8: Leaching at 0.6 M OH-.....	107

## **List of Notation**

AAR	Alkali-aggregate reaction
ACR	Alkali-carbonate reaction
ASR	Alkali-silica reaction
ASTM	American Society for Testing and Materials
BEI	Backscattered Electron Image
C-A-S-H	Calcium aluminosilicate hydrate
CMRG	Construction Materials Research Group
CSA	Canadian Standards Association
C-S-H	Calcium silicate hydrate
EDS	Energy Dispersive Spectroscopy
FA	Fly ash
M	mol/L
$\text{Na}_2\text{O}_e$	Sodium equivalent ( $\text{Na}_2\text{O}_e = \text{Na}_2\text{O} + 0.658\text{K}_2\text{O}$ )
PC	Portland cement
QXRD	Quantitative X-Ray Diffraction
SCM	Supplementary Cementitious Materials
SEM	Scanning Electron Microscopy
TxDOT	Texas Department of Transportation
XRD	X-Ray Diffraction
XRF	X-ray Fluorescence

## **Chapter 1: Introduction**

### **1.1 INTRODUCTION**

Alkali-silica reaction (ASR) is the general name given to a series of chemical reactions involving the interaction of reactive silica, alkalis, and water that results in premature distress and loss in serviceability of concrete structures. The first case of ASR was discovered by Thomas Stanton in the 1930s in southern California (Stanton 1940). Although ASR still remains a problem today, its reaction is better understood and there are now several preventive measures that one can take to limit ASR from occurring and/or mitigating its effects once ASR has occurred. One preventive measure is the replacement of cement with fly ash, a supplementary cementing material (SCM).

Today, the use of SCMs such as fly ash is one of the most popular ways to prevent ASR induced expansion. Fly ash is a by-product from the combustion of pulverized coal in power station furnaces; however not all fly ashes are the same when it comes to ASR. Rather, there are several factors, including the mineralogical, chemical, and physical composition of the fly ash that plays a role in the effectiveness of fly ash to controlling ASR.

### **1.2 SCOPE AND OBJECTIVE**

Incorporating fly ash into concrete is one of the most economical and simplest ways the concrete industry has to prevent ASR. However, the properties of fly ash vary from source to source, and the chemical, mineralogical and physical properties of an ash taken today from a power plant can be considerably different from the ash obtained from the same power plant just a few years ago. Furthermore, environmental regulations on the coal combustion industry continue to evolve and this can affect the quality of ash that is produced. Because of this, it is becoming important to be able to characterize fly ash in

order to predict its performance and behavior in concrete. The objective of the research in this thesis is to characterize fly ash and relate these findings to fresh, hardened, and durability properties of concrete with respect to ASR. The results of this project will provide a way to relate short-term characterization techniques to long-term data. With these results, fly ash will be able to be characterized with simple and accurate short-term techniques.



## **Chapter 2: Literature Review**

Since ASR was first discovered in the 1930s, there have been many studies focusing on ASR. Within this literature there are hundreds of research papers concerning the use of fly ash as a means to mitigate ASR. This chapter surveys a portion of the literature regarding ASR, focusing in on articles dealing with what is important for this project. Topics such as ASR, fly ash, pore solution chemistry, and testing methods will be discussed.

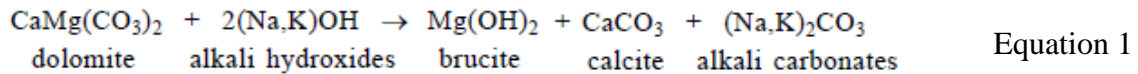
### **2.1 ALKALI – AGGREGATE REACTION**

Alkali-aggregate reaction (AAR) is a chemical reaction that occurs in concrete that induce stress. The pores within concrete are filled with highly basic solutions that consist of many dissolved ions, mostly  $K^+$ ,  $Na^+$ , and  $OH^-$ . Other ions include  $Ca^{2+}$ , and  $SO_4^{2-}$  but these are not as important to AAR as the ions mentions before. There are a variety of fine and coarse aggregates that contain chemically unstable mineral phases that can react deleteriously in the high pH environment in concrete. This then can cause internal expansion, cracking, and loss of serviceability which can lead to failure of the concrete element (Fournier, Berube, 2000). There are two types of AAR, alkali-carbonate reaction (ACR) and alkali-silica reaction (ASR), which will be discussed in the following two sections.

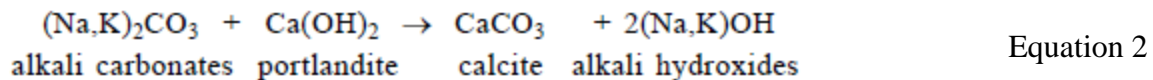
#### **2.1.1 Alkali – Carbonate Reaction**

ACR is similar to ASR but requires a different set of aggregate for reaction. ACR has been observed to occur with certain dolomitic rocks and the reaction with the high pH solution in the pores of the concrete. The first case of ACR was reported in the late 1950s in Canada and since then has been greatly studied (Swenson, 1957), (Farbriar, Carrasquillo, 1986), (Fournier, Berube, 2000).

The alkali hydroxides in the concrete pore solution attack the dolomite crystals of the aggregate and begin the process of dedolomitization. It is believed that this process, the breakdown of dolomite, is responsible with expansion. Equation 1 shows the breakdown of dolomite with the alkali hydroxides to form brucite, calcite, and alkali carbonates.



The ACR mechanism occurs in the two steps in Equations 1 and 2. In Equation 2, the alkali carbonates and portlandite react to form brucite and additional alkalis, which in turn will increase or maintain a high pH and cause more reaction. This can mean that ACR could continue to proceed almost indefinitely if a source of reactive aggregate is present. It is this recycling of alkalis that makes it very difficult, if not impossible, to prevent ACR-susceptible aggregates from reacting in concrete, even at very low alkali loadings.



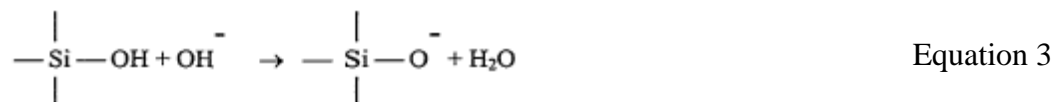
ACR is far less common than ASR because the type of aggregate needed for ACR is quite rare, and because of this, occurrences of ACR in concrete structures are very limited around the world.

### 2.1.2 Alkali – Silica Reaction

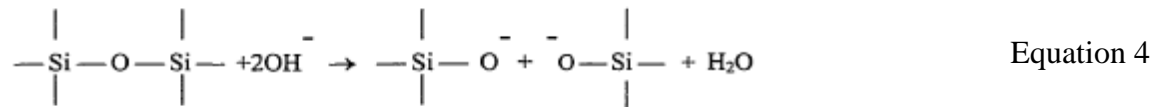
ASR is much more common than ACR because of the abundance of reactive siliceous aggregates worldwide. It is a reaction that occurs between the high pH pore

solution in concrete and certain types of aggregates with poorly crystalline silica. The reaction causes the formation of a gel and that expands when it absorbs water.

The mechanism of ASR and the chemistry behind it was studied greatly by Glasser and Katakoka (1981). Glasser and Katakoka stated that when poorly-crystalline hydrous silica is exposed to a strong alkaline solution, there is an acid-base reaction. This reaction can be described in Equation 3. As shown in the equation, the first step is the silica being attacked by the hydroxyl ion. This results in the negatively charged oxygen terminal that is shown on the right hand side of the equation being balanced by alkali cations ( $\text{Na}^+$  and  $\text{K}^+$ ) from the solution.



If a strong alkaline solution continues to be present, then further hydroxide reaction with reactive silica particles can occur and the siloxane linkages can also be attacked. Equation 4 depicts the reaction between the hydroxyl ions and siloxane linkages. If there are still sufficient amounts of alkali hydroxides available, then the process continues to produce an alkaline silicate solution.



Thomas (2011) states that the extent or rate of dissolution is controlled by the alkalinity of the solution, the structure of the silica, and the influence of the pH increase on the solubility of the poorly crystalline/amorphous silica. The dissolution of silica from reactive particles caused by hydroxide ions in solution forms the alkali-silicate gel which is accompanied by an increase of volume (Glasser, Kataoka 1981)

There have been various studies performed to determine the minimum hydroxide concentration in pore solution for ASR to occur in concrete, and concentrations within the range of 0.20 M to 0.30M are believed to be the minimum threshold. Research by Diamond et al., (1981), Kollek et al., (1986), and Thomas, Shehata, (2006) have generated data with values within this range. One reason why the concentration range varies by 0.10 M could be because of the different types of reactive aggregates used by the different researchers. However, it is important to realize that the minimum hydroxide concentration ranges are just estimates, and that it may be possible for a more reactive aggregate to react at a threshold lower than 0.20M or an aggregate that is not too reactive to have a minimum threshold closer to 0.30M.

Monteiro et al (1997) conducted studies on ASR gel chemical composition on 30 day old mortar bars. Mortar bars were cast, soaked 1M NaOH, and then the expansion was measured in accordance to ASTM C 1260 Standard Test Method for Potential Alkali Reactivity of Aggregates (Mortar-Bar Method). The mortar bars were mixed with different SCMs and cements. After 30 days, the mortar bars were examined with an SEM with BEI and EDS analysis. More specifically the chemical composition of the ASR gel found within the mortar bars was determined. Table 1 shows the results from this analysis.

Table 1: Chemical Composition for ASR Gel Formed (Monteiro et al, 1997)

Sample	CaO%	SiO <sub>2</sub> %	Na <sub>2</sub> O <sub>e</sub> %	Ca/Si	CaO/Na <sub>2</sub> O <sub>e</sub>	Expansion
OPC 1, Na <sub>2</sub> O <sub>e</sub> = 1.37%	30.32	53.40	11.06	0.61	3.10	0.145%
OPC 1 + 25% Pozzolan	24.27	60.18	9.17	0.43	3.49	0.079%
OPC 1 + 25% FA	28.84	58.05	8.03	0.54	3.59	0.078%
OPC 2, Na <sub>2</sub> O <sub>e</sub> = 0.68%	20.52	51.51	9.89	0.43	2.16	0.155%
OPC 2 + 45% Slag	29.83	67.18	6.76	0.47	4.80	0.166%
OPC 2 + 55% Slag	37.92	51.07	3.7	0.79	12.15	0.032%

The Ca/Si within the ASR gel plays a role in expansion. The highest ratio was 0.79 and is associated with the least amount of expansion of 0.032%. Although the mix with the lowest ratio did not have the high expansion measurement, generally speaking, mixes with lower Ca/Si ratios displayed higher expansion. Monteiro et al. (1997) concluded that not all alkali silica gels are equally expansive, and the alkali and calcium contents in ASR gel factor the expansion mechanism. Additionally, the higher the CaO/Na<sub>2</sub>O<sub>e</sub> ratio in the ASR gel, the less expansive the gel.

The amount of ASR-induced expansion is dependent on several parameters. According to Thomas (2011), they include the availability of alkalis in the system, the nature and amount of reactive silica in the aggregate, exposure conditions (temperature and moisture availability) and the degree of internal and external restraint to movement (e.g. amount and distribution of reinforcing steel). Fly ash is only involved in one parameter, the availability of alkalis in the system, although fly ash also reduces permeability, which can keep water from entering concrete.

## 2.2 FLY ASH

Fly ash is a by-product of the process of coal combustion in power generating stations. Coal is a complex and heterogeneous material used around the world as an energy source. When this coal is burnt to generate electrical power, large quantities of

fly ash is produced and can be collected. Fly ash and bottom ash are produced but it is the finely-graded fly ash that is important especially in the concrete industry.

Fly ashes are divided into two categories in the United States, Class C and Class F. Class F fly ash is produced from burning anthracite or bituminous coal and has pozzolanic properties. Class C fly ash is produced from burning lignite or sub-bituminous coal and can have both pozzolanic and cementitious properties.

The glass content, silica content, alkali content, and particle size all assist in determining which fly ash is efficient for preventing ASR. ASR is mainly fueled by alkalis from the cement but fly ash can also contribute alkalis in some instances. Some fly ashes with higher alkali contents require higher replacement levels but some have excessive amounts of alkali that they are totally ineffective.

Currently, there is no standardized test that can correctly predict the amount of alkalis released from fly ash into the concrete pore solution. Some of the alkalis in fly ashes can be trapped in crystalline phases and are not available for reaction. Both classes of fly ashes can lower the amount of alkalis released, but Class C fly ashes generally release more alkalis than Class F fly ashes. In other words, Class F fly ashes are more efficient at reducing ASR expansion. This project used accelerated tests with characterization techniques to correlate with long-term expansion results.

### **2.2.1 Background**

Fly ash is a solid, fine-grained material collected from the combustion of coal in power plants. The physical and chemical properties of fly ash can vary significantly and largely depend of the composition of the coal and the burning conditions in the furnace. Fly ashes that react with  $\text{Ca}(\text{OH})_2$  at room temperature can be classified as a pozzolan. These fly ashes act as pozzolan because of the higher amounts of  $\text{SiO}_2$  and  $\text{Al}_2\text{O}_3$  in their

amorphous form. Fly ashes can be divided into two groups by the American Standard for Testing and Materials (ASTM) (ASTM C 618). Table 2 displays the classes and their chemical requirements. Class F fly ashes are normally produced from burning anthracite or bituminous coal and are required to have the sum of the silicon, aluminum, and iron oxides percentage greater than or equal to 70% as shown in Table 2. Also, Class F fly ashes generally have pozzolanic properties. Class C ashes are normally produced from lignite or sub-bituminous coal and have both pozzolanic and cementitious properties. The composition of the coal is largely dependent on the original location of the coal (Wesche, 1991). The chemical requirement for the Class C fly ash is their oxide percentage must sum up to or greater than 50%. These classifications are covered in ASTM C 618-08 Standard Specification for Coal Fly Ash and Raw or Calcined Natural Pozzolan for Use in Concrete.

Table 2: Fly Ash Classification

Class	Description	Chemical Requirements
F	Fly ash normally produced from burning anthracite or bituminous coal that meets the applicable requirements for this class as given herein. This class of fly ash has pozzolanic properties.	$\text{SiO}_2 + \text{Al}_2\text{O}_3 + \text{Fe}_2\text{O}_3 \geq 70\%$
C	Fly ash normally produced from lignite or sub-bituminous coal that meets the applicable requirements for this class as given herein. This class of fly ash, in addition to having pozzolanic properties, also has some cementitious properties.	$\text{SiO}_2 + \text{Al}_2\text{O}_3 + \text{Fe}_2\text{O}_3 \geq 50\%$

The mineralogical composition of fly ash depends characteristics and composition of the coal burned at the power plant. Because fly ash is rapidly cooled, it mostly consists of glassy particles (50-90%). A small amount of the fly ash is crystalline and also a small amount of unburned carbon can remain. The most important minerals found in fly ashes from bituminous coal are magnetite, hematite, quartz, mullite, and free calcium oxide. Other minerals found in sub-bituminous coal are anhydrite, melilite,

merwinite, periclase, and tricalcium aluminate. There are several more minerals in fly ash but are usually found in trace amounts. These minerals can be detected using X-ray diffraction because they are in fly ash in crystalline phases.

### **2.2.2 Effects on Concrete**

The proper use of fly ash improves several properties of concrete. It exhibits pozzolanic properties that react with the  $\text{Ca(OH)}_2$  produced during the hydration of Portland cement. Calcium-silicate-hydrate (C-S-H) and calcium aluminate silicate hydrates (C-A-S-H) hydrations products are formed from this pozzolanic reaction. Fly ashes with high CaO contents also show hydraulic properties as well as pozzolanic properties.

The use of fly ash is known to reduce the expansion caused by ASR. This reduction is caused by the fact the hydration products tend to bind alkalis. The pozzolanic reaction when using fly ash produces C-S-H that contains a lower Ca/Si ratio than that of just Portland cement hydration. C-S-H with a low Ca/Si ratio has the potential to bind alkalis thus removing them from the pore solution. Hong, Glasser (1999) claimed that the lower the Ca/Si ratio, the surface charge becomes more negative (or less positive) and attracts the positive alkali cations from the pore solution.

Table 3 shows the results of several studies of the chemical composition of C-S-H using a variety of SCM's in their mixtures. High CaO fly ash is less effective in reducing the Ca/Si ratio within C-S-H when compared to Class F fly ash. Also, notice how the alkali cation ( $\text{K}^+$ ,  $\text{Na}^+$ ) contents of C-S-H increase as the Ca/Si ratio decreases. The lower ratio has a higher capacity to bind these alkalis.



Table 3: C-S-H Composition

Author	sample	(Na <sub>2</sub> O <sub>e</sub> %)		Curing	SCM Level	C-S-H Composition		
		OPC	SCM			Ca/Si	Na	K
Rayment, 1982	Paste FA: F	1.07	0.75	8 days @ 20 C	0 %	1.71	**	0.58
					20%	1.55	**	0.76
Thomas et al., 1991	Conc. FA: F	1.07	3.40	7 years external	0 %	1.94	**	0.15
					20-30	1.57	**	0.68
Uchikawa et al., 1989	Paste FA: F	0.59	1.29	91 days @ 20 C	0 %	1.8	0.03	0.10
				91 days @ 20 C	25 %	1.7	0.05	0.12
				60 days @ 40 C	25 %	1.2	0.10	0.18
Thomas, 1994	Paste FA: F FA: CH	0.80	2.16 1.82	28 days @ 80 C	0 %	1.78	0.12	0.54
					25 %	1.61	0.17	0.68
					25 %	1.84	0.25	0.36
Regourd et al., 1983	Mortar with SF	0.80	2.24	28 days @ 20 C	0 % 5 %	1.70 1.43	- -	- -
Regourd et al., 1983	Conc. with SF	1.15	0.47	200 days	15%	1.3	-	0.40*
					20%	0.9	-	0.40*
Ushikawa et al., 1989	Conc. with SF	0.59	1.52	91days @ 20 C	0 %	1.8	0.03*	0.10*
					10%	1.3	0.10*	0.25*
Notes: FA: F is Type F fly ash; FA: CH is Type CH fly ash *: Below detection limit * : Expressed as Na <sub>2</sub> O% or K <sub>2</sub> O % - : Not determined.								

## 2.3 EFFECTS OF FLY ASH ON ALKALI – SILICA REACTION

The use of fly ash and other SCMs is one of the most popular solutions to suppress ASR induced expansion. Some fly ashes behave differently than others and can be very effective against ASR while others can actually contribute to the problem. There are several reasons mentioned in articles proposing various mechanisms to explain fly ashes effectiveness against ASR.

### 2.3.1 Fly ash effectiveness

Duchesne and Berube (1994) listed four of the most common mechanisms to explain the effectiveness of fly ash against ASR:

- Lower permeability and consequent lower ion mobility
- Strength improvement and higher resistance to the expansive stress developed by ASR
- Alkali dilution resulting from cement replacement, (at least for fly ashes with a lower available alkali content),
- Pozzolanic reaction producing secondary (pozzolanic) hydrates which entrap alkali ions and deplete portlandite in the cement paste, thus reducing the alkali ions and the pH in the pore solution.

Duchesne, Berube (1994) performed concrete prism expansion tests similar to ASTM C 1293 Standard Test Method for Determination of Length Change of Concrete Due to Alkali-Silica Reaction that included the use of different fly ashes. Their studies included the use of three fly ashes (two Class F and one Class C with high alkali content). They found 40% replacement with the high alkali fly ash did reduce expansion over a 2-year period with respect to the control but 20% performed worse than the control. Twenty percent of the other two fly ashes were found to be enough to control expansion. These results showed that fly ash with higher alkali content require higher replacement dosages and excessive alkali contents can possibly render the fly ash ineffective.

Thomas (2011) proposed that alkalis in the binder are released in one of three ways: dissolved within the pore solution, bound by the hydration products, or incorporated in ASR gel. If there is no reactive aggregate, then the pore solution and hydration products will reach some sort of equilibrium and the amounts are dependent on the composition of the binder. Many researchers have found that the incorporation of fly ash leads to a reduction of the alkali concentration inside of the concrete pore solution and with higher dosages the concentrations decreases. Figure 1 shows how higher replacement levels of SCM's results in lower  $\text{OH}^-$  concentrations in the pore solution.

There were three fly ashes tested (Class C, Class F, and high alkali). Notice how the high alkali fly ash had the highest concentration at all levels, followed by the Class C, and then followed by the Class F. The Class F performed the best and high the lowest  $\text{OH}^-$  concentrations. Also, notice how at higher replacements, the  $\text{OH}^-$  concentration continues to decrease.

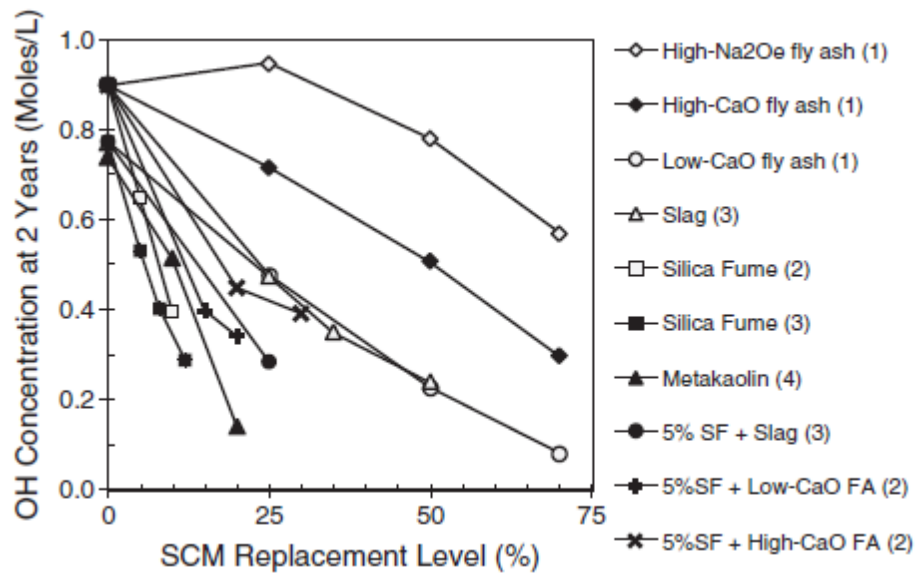


Figure 1: Effect of SCM and Replacement Level on the Pore Solution  $[\text{OH}^-]$  (Thomas, 2011)

Also, Thomas (2011) shows how not only does the  $\text{OH}^-$  concentration decrease at higher replacement level but so does ASR induced expansion. Figure 2 displays similar results from Figure 1. Performance increases as fly ash replacement level increases. Expansion can drastically be reduced with the higher replacement levels especially with a low-CaO fly ash. Notice how even the higher replacement levels with high CaO and high alkali contents performed better.

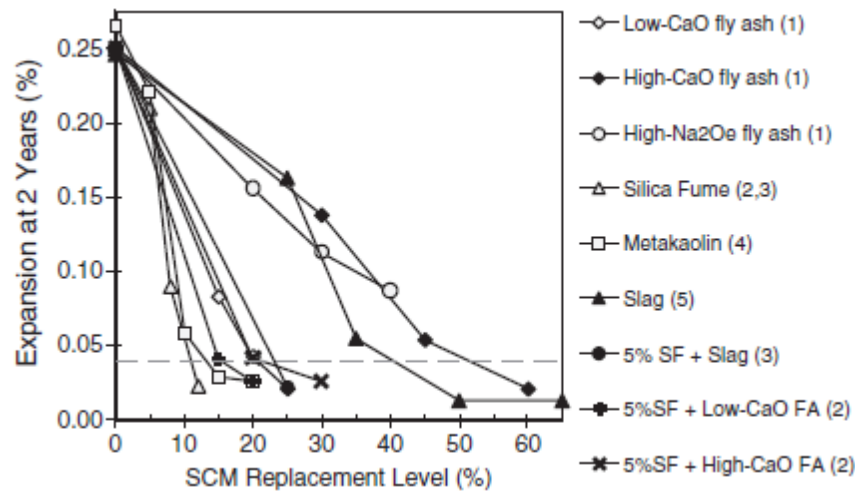


Figure 2: Effect of SCM Replacement on ASR Expansion (Thomas, 2011)

The dosage of fly ash needed to control ASR induced expansion is believed to be dependent on several variables including the alkali content of cement and possible aggregate, the alkali content of fly ash, the CaO/SiO<sub>2</sub> of fly ash, and the reactivity of the aggregate. If any or all of these variables increase so does the need for higher fly ash dosages. Thomas has developed a relationship between the chemical composition of the binder, and pore solution concentration and ASR expansion. This index  $[(Na_2O_e)^{0.33} \times CaO] / (SiO_2)^2$  clearly shows which three chemical parameters affect ASR the most. The alkalis of the binder of course contribute to ASR and so does the CaO/SiO<sub>2</sub> like many other researchers state. It is a combination of all three that influence ASR expansion the most. This relationship will be used in the later sections will the research of this thesis to determine if trends can be discovered.

### 2.3.2 Available Alkalis

The term “available alkalis” means the amount alkalis released by a fly ash into concrete pore solution that enables it to react with a reactive aggregate if available. Fly

ash contains a percentage of alkalis just as cement but not all of it is available. Some of the alkalis are trapped in non-reactive crystalline phases while others are separated between hydration products and pore solution liquid (Thomas, Shehata, 2006).

In Section 3.2.4, the ASTM C 311 method and procedure for determining the amount of available alkalis in fly ashes is described. This procedure is thought by many to be inaccurate in determining the amount of alkalis that are available for reaction with reactive aggregate. Thomas and Shehata (2006) states that the problem with this procedure is that the leaching medium is of neutral pH. The use of distilled water and not something similar to the high pH of concrete pore solution will not correctly represent available alkalis. Many researchers have shown that most of the alkalis will be released under these conditions especially if the curing period is extended past the 28 days required.

Duchesne and Berube (1994) suggested that almost all alkalis in fly ash are released over a long period of time and will remain in the concrete pore solution at least for a short period of time. It states that once the alkalis are in solution, they are either entrapped in cement hydration or pozzolanic reactions, or remain available in solution for ASR. All fly ash alkalis are released into solution at some point but only a certain amount remains available.

Work by Lee et al. (1985) states that ASTM C 311 underestimates the amount of available alkalis especially with only 28 days of curing. They tested not only at 28 days but at regular increments from 2 days to 6 months. They tested six different fly ashes and only one (a strong Class F) at 28 days had a good long term indication. The other fly ashes continued to release noticeable amounts of alkalis as time increased. Figure 3 shows a typical plot from their results. Notice how both curves continue to increase beyond the 28 days of curing. There is a significant increase beyond the normal curing

amount and under ASTM C 311, these alkalis after 28 days would not be considered available because they would not have been detected. This test is not indicative of the total amount of alkalis released into pore solution in the long-term.

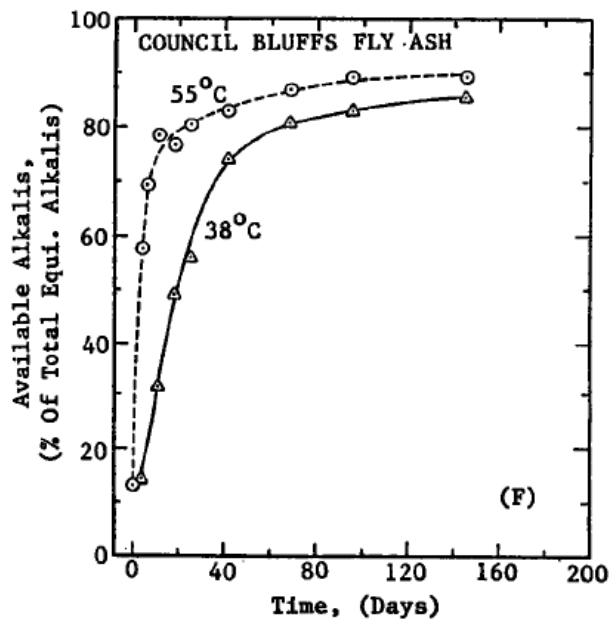


Figure 3: Long-Term Available Alkalis (Lee et al., 1985)

The experiments by Lee et al. (1985) also showed that the amount of available alkalis were about 50% of total equivalent alkalis for Class F fly ashes and 90% for Class C fly ashes after 5-6 months of curing. Although the percentages may be over or underestimated because of the test method, a relative relationship can be noticed. Class C fly ashes will have plenty of more of their alkalis available for reaction than Class F fly ashes. The numbers may not be around 90% and 50 %, respectively, but in general Class C fly ashes have more available alkalis. Also, (Lee et al., 1985) states that the test method may not be valid for high calcium fly ashes because its calcium may be reactive and interfere with the assigned fly ash to calcium hydroxide ratio (2.5:1) from ASTM C

311. Also their testing at higher temperatures to try and expedite the process resulted in the opposite, lower amounts of available alkalis.

Thomas, Shehata (2006) developed a method to determine the amounts of available alkalis from blended cements. The procedure involved mixing paste samples with different fly ashes and cements and allowing them to cure for certain period for the pore solution to reach equilibrium. Then the paste samples were crushed and a certain amount was placed in different concentrations of  $\text{OH}^-$  with the same  $\text{Na}_2\text{O}$  to  $\text{K}_2\text{O}$  ratios of its binder. They were allowed to rest in solution for a certain period of time and the concentrations before and after were taken. This method allowed for the determination of alkalis either released or bound by the paste when place into simulated pore solutions of different concentrations. This procedure was replicated during the research of this thesis and is discussed further in Sections 3.2.7 and 4.3.2. Thomas and Shehata (2006) found that the amount of available alkalis increases as the calcium and alkali contents of the blends increase and the silica content decreases. High-CaO fly ashes had more available alkalis and confirm why these fly ashes perform worse at controlling ASR. Also, they stated that fly ashes with higher amount of alkalis also contributed more alkalis into the simulated pore solution. In Figure 4, one can notice how the replacement of more fly ash in the binder decreases the amount of available alkalis for reaction with reactive aggregate. Three different fly ashes of different chemistries showed that certain fly ashes are more efficient at higher replacement dosages in terms of ASR.

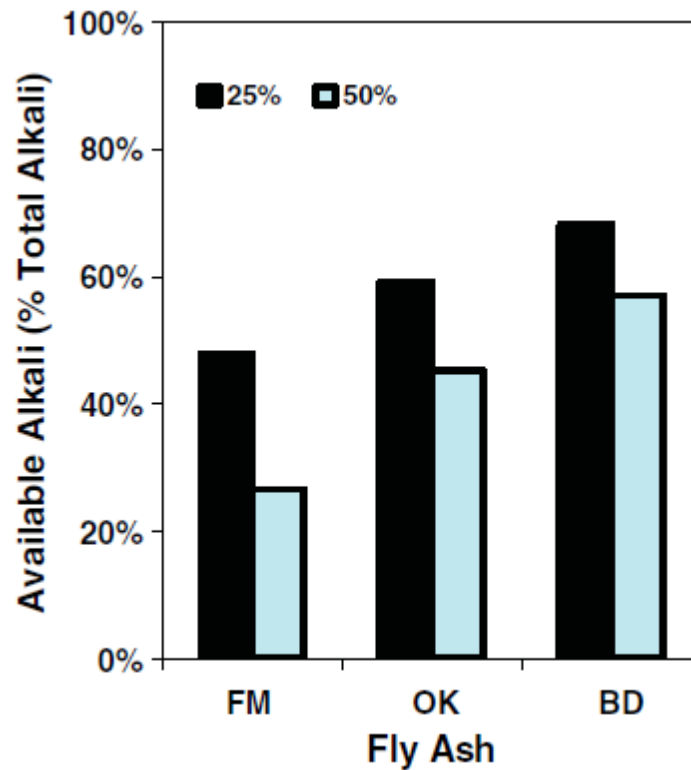


Figure 4: Effect of Fly Ash on Available Alkalis (Thomas, Shehata, 2006)

### 2.3.3 Pore Solution Chemistry

In hydrating cement paste, the concentration of the alkalis in the pore solution continuously changes. Many factors play a role in pore solution composition such as the cement, SCM, hydration products, aggregate, and potential ASR gel. Different levels and types of cement and SCM's can affect the composition as well. Figure 5 illustrates the possible sources of alkalis in the pore solution. It also shows how alkalis can be bound by hydrations products and consumed by ASR gel.



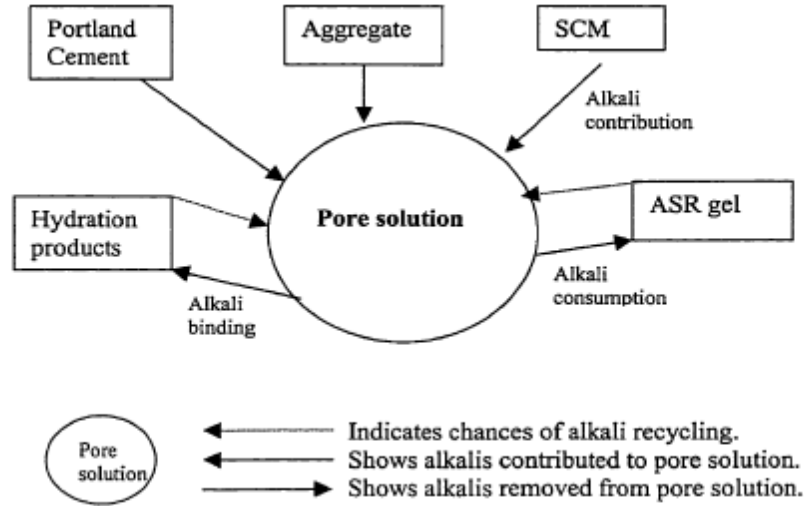


Figure 5: Sources of Alkalis in Pore Solution (Shehata, 2001)

Fly ash contains appreciable contents of potassium and sodium and a certain amount of them are available as described in the previous section. The concentration of alkalis in concrete pore solution is of importance when concerned about ASR. Certain fly ashes can reduce the alkali concentration by binding alkalis within hydration products. Other fly ashes have no effect or can increase the alkali concentration in the pore solution.

Class F fly ashes have been shown to reduce the concentration of alkali ions in the pore solution. The effectiveness of this depends on the nature of the fly ash (e.g. fineness, glass content, and alkali availability), the level of replacement, the alkali content of the Portland cement, and age (Shehata et al, 1999).

Diamond (1981) was one of the first to study the effects of fly ash on the alkali contents of pore solution. He studied the influence of two Danish fly ashes on alkali content of cement paste pore solutions. The paste samples had up to 30% replacement and were allowed to hydrate for up to six months. Both fly ashes were low in CaO

content and had moderate amount of alkalis (2.4 – 3.3%  $\text{Na}_2\text{O}_e$ ). Figure 6 displays the pore solution concentrations at several time increments. Notice how the curves usually have a maximum concentration around 10 days and after 30 days the plot sort of evens off. The left figure has potassium ion concentrations and the right has sodium ion concentrations. In both cases, the pore solution concentrations were drastically reduced with the use of both fly ashes.

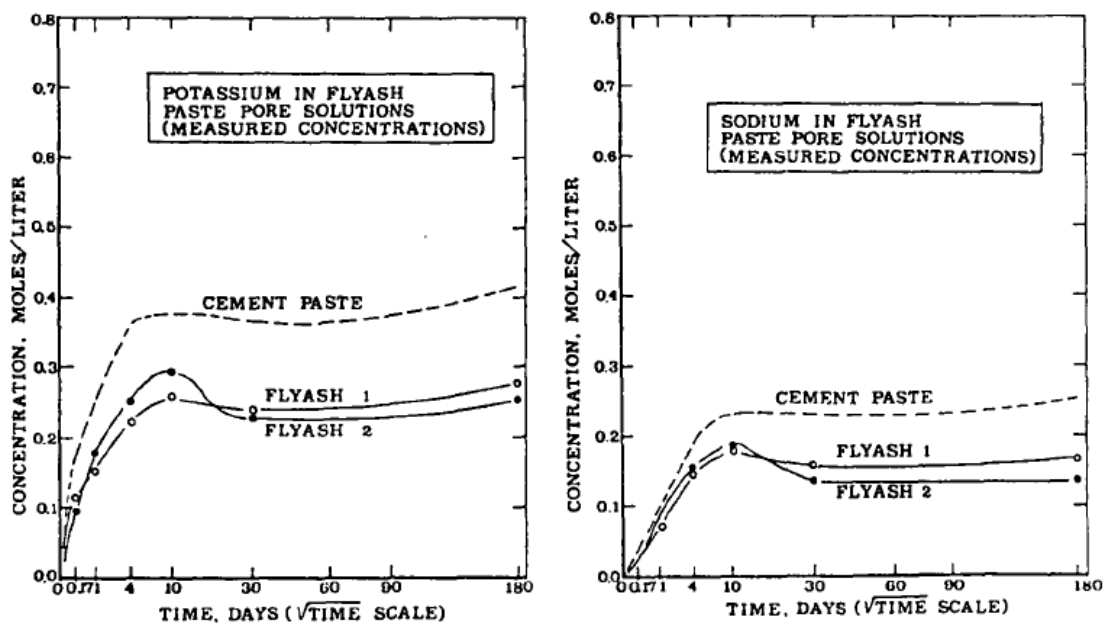


Figure 6: Pore Solution Concentrations (Diamond, 1981)

Diamond (1981) studies concluded that both fly ashes acted in an inert manner with respect to alkali concentrations. They did not contribute or remove alkalis from solution but because it replaced 30% of the cement, the alkalis were reduced by the dilution effect. The second fly ash had a slightly higher alkali content but slightly lower CaO content and showed the effect of some removal of alkalis between 10 and 30 days.

Duchesne and Berube (1994) analyzed the pore solution chemistry of several cement pastes that contained a variety of SCM's at different time periods. Three of the SCM's were fly ashes (A, B, C) with different CaO and alkali contents. The CaO and alkali contents increased from A to C with C having significant higher values at 20.7 and 8.55 respectively.

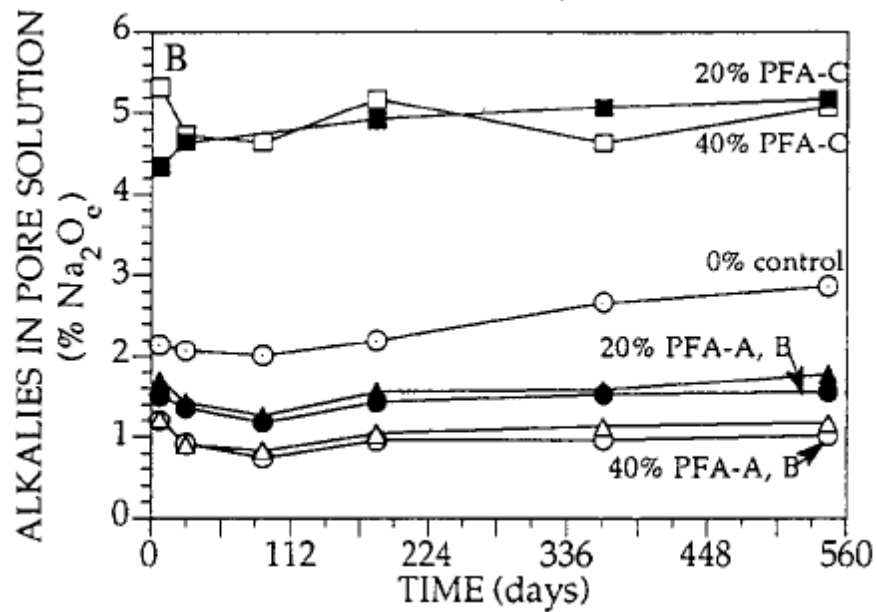


Figure 7: Alkalies in Pore Solution (Duchesne, Berube, 1994)

Figure 7 illustrates the effectiveness of certain fly ashes in reducing alkalis in the pore solution. Fly ash A and B would be classified as Class F fly ashes with moderate amounts of alkalis ( $\approx 3\%$ ). Fly ash C is a Class C fly ash with 8% alkali content and performed worse than the control. This shows how not all fly ashes even at high dosages can be effective at reducing alkalis. The Class F ashes performed better than the control and even better at replacement levels.

Hooton et al (2009) yielded similar results while they tested several fly ashes of different chemistry compositions. Figure 8 shows similar and more extensive results than Figure 7. At higher fly ash replacement levels, the OH<sup>-</sup> concentration in the pore solution decreases. The figure illustrates that this is true for both Class C and F ashes with low alkali contents. Even though the left plot contains an ash with a very high CaO content, all levels of replacement perform better than the control. Also, notice how the fly ash curves on the right plot are generally lower than the curves on the left plot. This shows that lower CaO fly ashes are more efficient at reducing alkalis in pore solution.

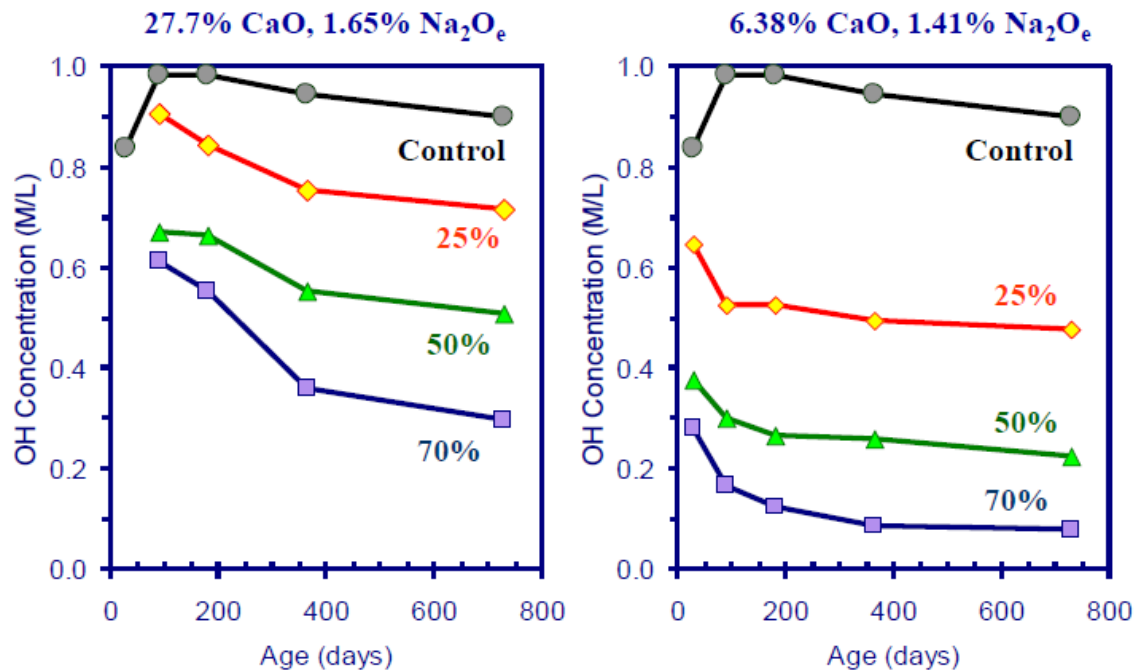


Figure 8: Effect of % Fly ash on Pore Solution (Hooton et al, 2009)

Figure 9 shows the effects of 25% fly ash with different chemistry compositions. Four fly ashes were used with low to high CaO contents and similar alkali contents. The results clearly show the efficiency of lower CaO fly ashes; as CaO decreases, so does the

OH<sup>-</sup> concentration in the pore solution. As in Figure 8, even the high CaO fly ash was more efficient than the control.

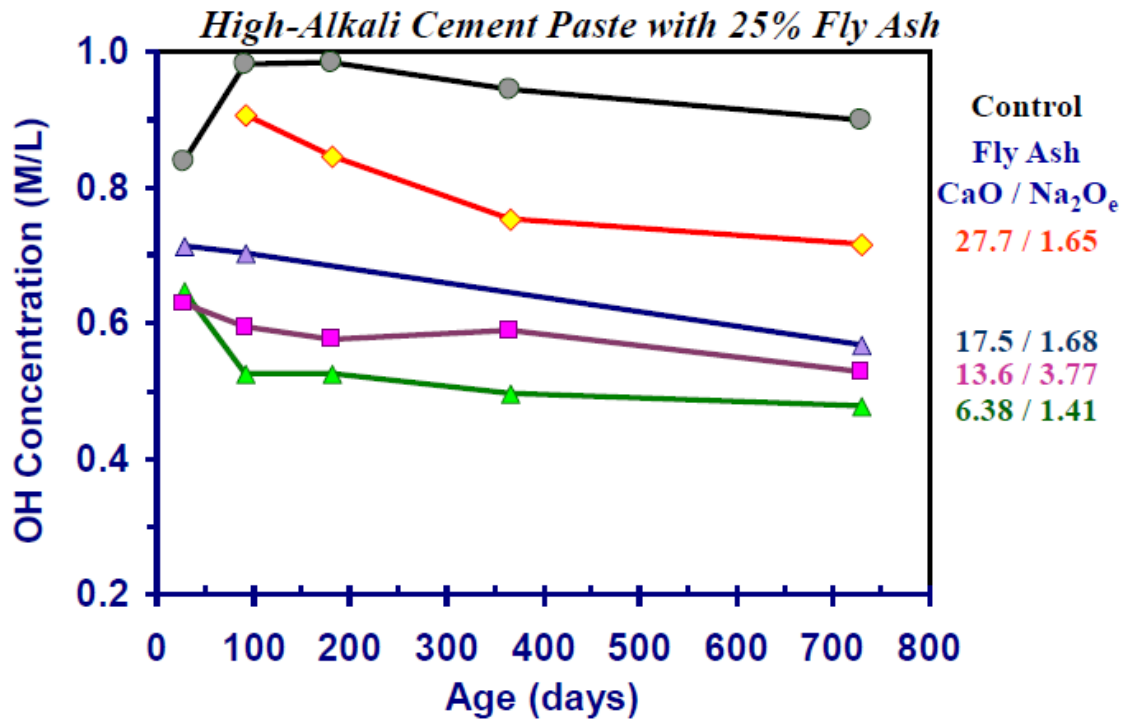


Figure 9: Effect of 25% Fly Ash on Pore Solution (Hooton et al, 2009)

## 2.4 TESTING OF EXPANSION DUE TO ALKALI – SILICA REACTION

Many different expansion tests have been used to evaluate the efficiency of the addition of fly ash in suppressing ASR induced expansion. The two most common ASTM C 1260 & 1293 that test mortar bars and concrete prisms respectively. Other methods, such as outdoor concrete block exposure sites have also been implemented to provide more realistic results. The three methods have their advantages and disadvantages, and will be discussed in the following section.

#### **2.4.1 ASTM C 1260, 1567**

ASTM C 1260 is the accelerated ASR mortar bar test that measure expansion up 16 days while placed in an 80°C 1M NaOH solution. The procedure and other matters are discussed in detail in Section 3.2.6. This test is for mortar only, so if a coarse aggregate must be tested, then it must be crushed and sieved to the appropriate size distribution. This can create different results from would be in realistic field conditions. Expansion measurements less than 0.10% at 16 days is considered indicative of innocuous behavior and expansions greater than 0.20% is indicative of potentially deleterious expansion. Expansion between 0.10% and 0.20% indicate that the aggregate ay exhibit either innocuous or deleterious performance in the field (ASTM C 1260, 2007). Similarly ASTM C 1567 states combinations of cements and SCM's that provide expansion less than 0.1% at 16 days are acceptable and anything greater indicative of potential deleterious expansion.

#### **2.4.2 ASTM C 1293**

In this test, concrete prisms are cast with square cross sections of  $3.00 \pm 0.03$  in and are 11.25 in. long. Stainless steel gauge studs are cast in both ends of each prism to give an effective gauge length of  $10.00 \pm 0.10$  in. An ASTM C150/C150M Type I cement with a  $0.9 \pm 0.1\%$  Na<sub>2</sub>O<sub>eq</sub> is specified for this test method. A sodium hydroxide solution is added to the mixing water to raise the alkali content to 1.25 Na<sub>2</sub>O<sub>eq</sub>. Prisms are demolded after  $23.5 \pm 0.5$  hours and are measured for an initial reading. Prisms are then stored at  $38.0^\circ\text{C} \pm 2.0^\circ\text{C}$  for 1 year for concrete containing no SCMs. At the University of Texas at Austin measurements are usually taken up to two years regardless if SCMs are used or not. Prior to any length change measurements, prisms are brought to  $23^\circ\text{C} \pm 2.0^\circ\text{C}$  for  $16 \pm 4$  hours. Length change measurements are performed at 1, 4, 8, and at 3, 6, 9, and 12 months. The optional additional readings are taken at 18 and 24

months for mixtures containing SCMs. An expansion of 0.04% at one year is considered potentially deleterious and the same for two year measurements when involving SCMs (ASTM C 1293, 2008).

ASTM C 1293 is considered to be more reliable than ASTM C 1260 because 1293 uses an actual concrete mix, it uses larger specimens, and is not immersed into a harsh alkali environment.

#### **2.4.3 Outdoor Exposure Blocks**

At the University of Texas at Austin, there is an outdoor exposure site with concrete block specimens created to provide realistic ASR expansion results to real world cases. The blocks measure 28 x 15 x 15 in nominally, are mixed with the same ASTM C 1293 proportions, and are wet cured for 7 days prior to outdoor exposure. Measurements are taken with two different length digital comparators at the top and all sides of the concrete block. There is no formal failure expansion measurement but cracking is noticed at 0.04% (Ideker et al, 2012).

This test method is thought be better than both ASTM C 1260 and 1293 because neither of the other two methods account for effects of outdoor exposure. Outdoor exposure provides variations in temperature, moisture availability and loading. (Ideker et al, 2012) stated that the ideal test method does not exist. ASTM C 1260 is an aggressive test that can fail specimens while they would not fail in ASTM C 1293. Also, it has been noticed that the opposite can occur; specimens can pass 1260 but show deleterious expansion in the field. ASTM C 1293 is more reliable but if SCMs are used then the test is extended to two years while 1260 is only a 16 day test. ASTM C 1293 correlates better to field conditions but two years is a long period of time to access ASR. The same can be

said for the outdoor exposure blocks, where expansions may not be observed for several years, and significant resources and space are required for a site.



## **Chapter 3: Materials and Testing Methods**

This chapter will discuss the materials and testing methods used throughout the duration of the project. The majority of the materials used were already in possession by the University of Texas at Austin and some had to be procured from other locations. The testing methods were mostly performed at the CMRG laboratory, but some testing was performed at the TxDOT materials laboratory.

### **3.1 MATERIALS**

The fly ashes selected covered a wide range of chemical and mineralogical compositions. Also, many of the fly ashes selected have been used before in different projects at the University of Texas at Austin, allowing for a comparison between the short-term testing performed under this project and the long-term testing performed under previous projects. Because this project was sponsored by the TxDOT, most of the fly ashes are from Texas sources. Eleven of the original fourteen fly ashes are from Texas while three are from outside but were brought in to extend the ranges of chemical properties. In addition to these fourteen, TxDOT provided the research team with four more fly ashes during the project.

Table 4 has the original fourteen fly ashes that were described in the proposal. This table also lists which experiments had been previously conducted on the fly ashes. The chemical compositions of these fly ashes are also located on the table but may differ from the values used for calculations because these values may be from older or different samples. Because four fly additional fly ashes were added to the project, it was decided to have the order of the fly ash identification numbers increase with increasing calcium oxide content; as such, the proposal ID and this thesis ID vary, as shown in Table 6. Please note that this thesis will have the number system located on the left column of this

table. Table 5 shows the two cements used during this project and because this thesis focuses mainly on ASR, only cement 1 was used because of its high alkali content.

Table 4: Original Proposal Fly Ashes

Fly Ash	Chemical Composition						Physical Property	ASR			External Sulfate Attack Test Methods			DEF	AEA* demand
ID	CaO	Al <sub>2</sub> O <sub>3</sub>	SiO <sub>2</sub>	Fe <sub>2</sub> O <sub>3</sub>	MgO	Na <sub>2</sub> O <sub>eq</sub>	LOI	ASTM 1567	ASTM 1293	Exposure Block	ASTM 1012	Exposure site		Kelham/ Fu	
												UT	W. Texas		
FA-1	1.1	30.6	55.8	5.1	0.7	1.78	1.99	X	X	X	X				X
FA-2	9.9	20.4	56.2	6.8	2.6	1.2	0.19								X
FA-3	12.8	23.7	52.1	4.6	2.0	0.84	0.95	X	X	X	X	X	X	X	X
FA-4	14.4	18.9	51.0	7.9	2.91	1.19	0.46				X				X
FA-5	14.6	22.8	47.2	4.6	3.5	2.2	0.51		X	X	X				X
FA-6	15.8	21.2	40.7	4.5	3.5	8.46	0.53	X	X	X					
FA-7	18.9	19	32.7	5.8	4.3	8.7	1.2	X	X	X					
FA-8	21.6	19.3	41.3	6.5	4.4	1.94	0.16				X				
FA-9	23.5	18.8	38.6	6.7	4.8	2.1	0.28				X	X	X		
FA-10	25.3	21.4	36.5	5.2	4.5	1.78	0.15		X	X					
FA-11	25.4	21.2	34.6	5.7	4.6	2.1	0.55	X	X	X	X				X
FA-12	25.8	20.6	37.2	6.1	4.3	1.93	0.13		X	X	X				
FA-13	27.5	18.1	33.1	6.6	5.5	2.1	0.4	X	X	X	X			X	X
FA-14	28.9	17.8	30.7	5.9	6.6	2.35	0.44		X	X	X		X		

Table 5: Cement ID

Cement ID	SiO2	Al2O3	Fe2O3	CaO	MgO	SO3	Na2O	K2O	TiO2	Mn2O3	P2O5	Cl	ZnO	Cr2O3	LOI	CO2	C3S	C2S	C3A	C4AF
C-1	18.95	5.35	2.57	63.87	1.14	3.27	0.113	0.9	0.23	0.049	0.34	0.007	0.0108	0.0122	2.99	1.806	58	11	10	8
C-2	20.04	4.49	3.63	63.8	0.72	3.02	0.037	0.62	0.21	0.096	0.305	0.0063	0.007	0.0149	2.75	1.759	54	16	6	11

Table 6: Thesis ID and Proposal ID

Thesis ID	Proposal ID
FA-1	1
FA-2	
FA-3	2
FA-4	3
FA-5	7
FA-6	4
FA-7	5
FA-8	6
FA-9	8
FA-10	10
FA-11	9
FA-12	
FA-13	13
FA-14	12
FA-15	11
FA-16	
FA-17	
FA-18	14

## 3.2 TESTING METHODS

This chapter will contain the different experiments conducted on the fly ashes as well as their procedures. Many of the procedures were followed in accordance to ASTM and others followed procedures from previous work done by researchers.

### 3.2.1 X-Ray Fluorescence

All the eighteen fly ashes and the two cements were sent to the TxDOT materials laboratory to be analyzed using their XRF instrument, as the CMRG laboratory does not have an XRF instrument.

The use of XRF helped to determine the chemical compositions of the samples. XRF analysis involved an x-ray beam to be aimed at the sample while some of these

beams cause more to form in the sample and escape. An x-ray detector collects the x-rays and measures the different amount of energy sent off. The energies are a function of the atomic number of the atom so we then can determine the element it was from (Wirth, Barth 2012).

The samples were analyzed on a 1kW Wavelength Dispersive S4 Explorer manufactured by Bruker-AXS. The samples were prepared for XRF analysis using fused bead method. This method consisted of heating a mixture of the sample with a flux and heating to 800°C to 1200°C. The flux then melts and sample dissolves creating a homogeneous glass. Figure 10 shows the apparatus used for the XRF sample preparation. This image was taken after the heating process and during the pouring process when the homogeneous sample is allowed to cool to become a glass.



Figure 10: XRF Sample Preparation

The XRF procedure and analysis was conducted in accordance to ASTM C 114, The Chemical Analysis of Hydraulic Cement.

### 3.2.2 Particle Size Distribution

This section discusses the two methods used to analyze the particle size distribution of the samples. The particle size distributions of the samples were analyzed with the wet No. 325 sieve technique and laser diffraction technique.

#### 3.2.2.1 ASTM C 430 Residue Retained on No. 325 Sieve

This method measures the percentage of fly ash coarser than the No. 325 sieve as it is generally believed that fly ash particles larger than this will not react in concrete. The standard calls for 1.000 g sample to be placed on a clean and dry No. 325 sieve. Then, the sample is wet with a gentle stream of water for one minute until it is saturated. Next, the sample is rinsed with 50 ml of deionized water, dried in an oven, allowed to cool, and then weighed. Equation 5 explains how the fineness of the sample is determined.  $F$  is fineness of the sample expressed as percentage passing the No. 325 sieve,  $R_c$  is the corrected residue,  $R_s$  is the residue retained on sieve, and  $C$  is a correction factor for the sieve used (ASTM C 430).

$$\begin{aligned} R_c &= R_s \times (100 + C) \\ F &= 100 - R_c \end{aligned} \quad \text{Equation 5}$$

#### 3.2.2.2 Laser Diffraction

Laser diffraction involves a light from a laser passed into a group of particles suspended in air. The particles scatter the light while different size particles scatter the light at different angles. The instrument has several photo detectors at different angles to measure the light. The light patterns can then be converted to particle size using scattering theory (Malvern 2012).

The laser diffraction machine used for this project was a Spraytec by Malvern Instruments, Inc. with Spraytec software. The material refractive index was 2.5 with an imaginary index of 0.1 and the instrument used isopropyl alcohol as the dispersive agent. The instrument calculated the diameter of 10%, 50%, and 90% numerically and produced a particle size distribution plot.

### **3.2.3 Total Alkalis (Acid-Soluble)**

The total alkalis of our samples were determined using the XRF method. The total alkali percentage was also measured in accordance to ASTM C 114/311. This standard has a section that covers the determination of sodium oxide and potassium oxide of our samples.

The procedure requires that 1.000 g of sample be placed in a 150-mL beaker and dispersed with 20 mL of water while swirling. Then 5.0 mL of concentrated HCl is added and then diluted to 50 mL. Next, the sample is digested and stirred on a hot plate for 15 minutes and filter into a 100-mL volumetric flask. The sample is then allowed to cool and then diluted to the 100-mL line with water (ASTM C114). The concentrations of sodium oxide and potassium oxide are then determined using the flame photometry method discussed in section 3.2.8.

### **3.2.4 Available Alkalis**

The available alkali experiment followed the procedure from ASTM C 311. This experiment was conducted on all eighteen fly ashes as well as C-1.

ASTM C 311 states to weigh 5.0 g of the sample along with 2.0 g of hydrated lime and mix with 10 mL of water in a 25-mL vial. The sample is then shaken, sealed and stored in an oven at 35°C for 28 days. Then, the vial is opened and the sample is ground with a small amount of water. The total volume is raised to 200 mL and then let

to stand at room temperature for one hour. The sample is then filtered into a 500-mL volumetric flask and neutralized with dilute HCl while using phenolphthalein as the pH indicator. The remaining volume is then diluted with water and the alkali concentrations are then measured using the flame photometer.

### 3.2.5 Pore Solution Extraction

This experiment involves the extraction of pore solution from a cement paste. The procedure followed is one conducted by students and researchers at the University of Texas at Austin. In this method, the steel apparatus is placed in a compression machine to extract pore solution from concrete, mortar, and paste. Figure 11 shows a diagram with two views of the pore press apparatus.

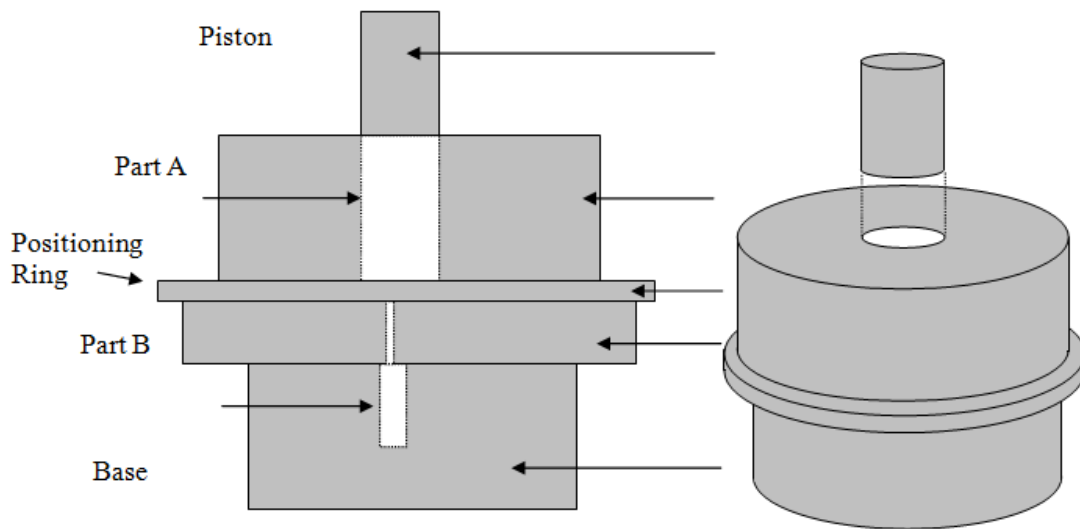


Figure 11: Pore Press Apparatus

The following procedure was used for this experiment for the use of cement paste. The procedure varies slightly for mortar and concrete. First, the sample is placed in a heavy duty plastic bag and crushed with a hammer roughly to fragments of less than



0.375 inches. Approximately 250 g of material is placed on a Teflon disc in a 200-mL beaker and the mass is recorded. Then, the steel apparatus must be assembled as in Figure 11 and placed inside of the compression machine. A plastic vial is placed inside of the base part to collect the pore solution. The sample is placed in 3 layers and compacted inside of part A. The Teflon disc is placed above the sample and the piston above that. Next, load is applied at a rate of about 35,000 lbs/min to a maximum of 500,000 lbs depending on the sample size. These sample sizes were small that only a maximum load of roughly 250,000 lbs was used because the piston would become almost flush with part A. The sample was then removed, along with the Teflon disc and weighed out. Then, the sample was placed in an oven for 24 hours and weighed again. The plastic vial within the base contains pore solution from the sample, and its alkali concentration is measured using the flame photometer.

### **3.2.6 ASTM C 1260, 1567**

ASTM C 1260 and 1567 permit the detection of the potential alkali-silica reactivity of aggregate and combinations of cementitious materials. The goal using these experiments was to not test the reactivity of an aggregate but the usefulness of fly ash additions. Because of this, one of our most reactive fine aggregate was used for all the mixes.

The first step of this procedure is to batch the materials and place at room temperature for 24 hours prior to mixing. The standard calls for batching material for three prisms but four prisms were batched because of the possibility of one breaking during demolding. 586.7 g of cementitious material and 1320 g of graded fine aggregate were used with a w/cm of 0.47. Next, the materials are mixed in accordance to ASTM C 305 for mortar mixes and placed in assembled prism molds. The prisms are demolded

after 24 hours, initial comparator readings are taken, and placed back in containers filled with water in the 80°C oven. The following day, length measurements are taken again and then placed in an 80°C 1 M NaOH solution. The standard then calls for at least three intermediate measurements before 14 days. Measurements were taken at 3, 7, 10, 14, 21 and 28 days. Expansion beyond 0.1% at 14 days is considered a failure (ASTM C 1260).

### **3.2.7 Leaching Test**

This leaching experiment was conducted to determine the amount of available alkalis in a cementitious binder. Similar experiments have been performed by many researchers but the procedure developed by Dr. M. Thomas of the University of New Brunswick was used.

This test involved the use of the fourteen original fly ashes proposed and C-1 yielding 15 samples. A 25% cement replacement was used for all mixes except the control at a w/cm . Paste samples were created using a high shear mixer at 40 RPM with a mix sequence of 1 min mixing and a 1 min rest period repeated twice for three total minutes mixing. Each sample was placed in a polyethylene cylinder. The samples were rotated for the first 24 hours to prevent segregation. Next, the samples were placed in an enclosed bucket over water in a 100°F oven for 90 days. The samples were removed and crushed. Large samples were saved for pore solution and others to determine evaporable and non-evaporable water contents. The remainder was ground and sieved between a No.16 and No. 80 sieve (.180mm-1.18mm).

In some cases, before removing the samples from the oven, simulated pore solutions were created using NaOH and KOH. The pore solutions were created to have the same Na<sub>2</sub>O to K<sub>2</sub>O ratios as the cementing materials used in each sample. This was done at OH<sup>-</sup> concentrations of 0.0, 0.1, 0.2, 0.3, 0.6 mol/L. 1.5 g of the sieved paste

sample was placed into 15 mL of its corresponding simulated pore solution in a 20-mL vial, sealed with silicone and weighed. Fifteen paste samples were used at five different concentrations yielding a total of 75 samples but it was done twice in this project to yield 150 samples. The samples were allowed to rest in solution for 90 days and then weighed again. This was done to check for any evaporation that might factor into concentration calculations. The samples were vacuum filtered and alkali concentrations were produced using the flame photometer. It was thus possible to know the difference in alkali concentrations before and after the paste was placed in the simulated pore solutions to determine how much was bound or released by the paste.

### **3.2.8 Flame Photometer**

The flame photometer test was not an experiment on its own but rather assisted with other experiments such as total alkali, available alkali, pore solution extraction, and leaching. The flame photometer apparatus allowed us to determine the concentrations of sodium and potassium ions in solution.

The flame photometer used for our experiments was the Cole Parmer Dual-Channel Flame Photometer, Figure 12, which allowed us to obtain  $\text{Na}^+$  and  $\text{K}^+$  results simultaneously. Figure 13 describes the process involved during flame photometry. A solution is aspirated into a low temperature flame where the water evaporates leaving solid residue of evaporation. The solid breaks down to form atomic species where the atoms are excited by the flame and its electrons move to a higher energy state. The electrons eventually return to ground state and the loss of energy creates a discrete wavelength of light. The amount of light is proportional to the number of atoms in the flame and the concentration in the original solution. This light is measured by a photo detector and the concentrations are displayed in a digital readout (Parmer 2008).



Figure 12: Dual Flame Photometer (Cole Parmer)

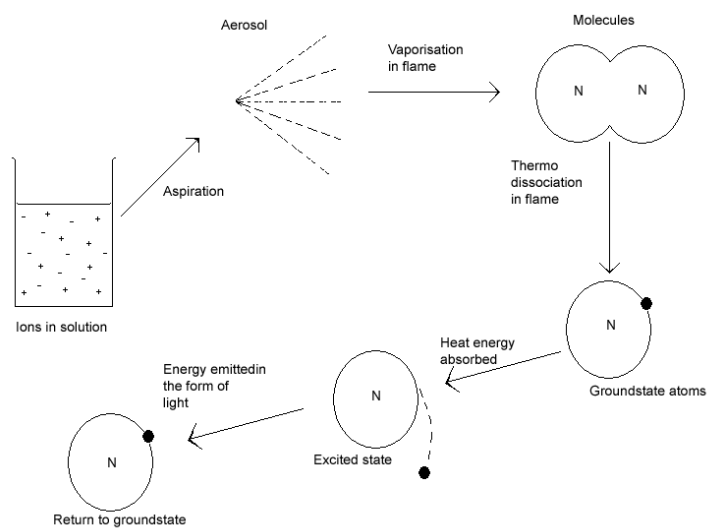


Figure 13: The Process Involved in Flame Photometry (Sherwood Scientific)

## **Chapter 4: Results and Analysis**

### **4.1 RAW MATERIALS**

This section describes the results and analysis of the experiments conducted on the raw materials. These tests only involved the different fly ashes and cements and did not involve their hydration into paste, mortar, or concrete.

#### **4.1.1 Particle Size Distribution**

Fineness of fly ash is thought to be one important characteristic that determines its efficiency in preventing ASR. Finer pozzolans are more efficient in reducing ASR expansion because fineness affects the pozzolanic activity. It has been shown that the use of ultra fine fly ash (UFFA), even with a CaO of 11.8% is very effective in terms of ASR (Malver, Lenke, 2006). Particle size distribution was evaluated using the wet No. 325 sieve method and the laser diffraction methods.

##### ***4.1.1.1 Wet No. 325 Sieve***

This test was conducted with accordance to ASTM C 430 Residue Retained on No. 325 Sieve. ASTM C 618 requires all fly ashes to have a maximum of 34% retained when wet-sieved on a No. 325 sieve. Figure 14 illustrates the results from this testing. The entire group of fly ashes was well above 34% retained or 66% passing mark. The fly ashes were arranged throughout the x-axis from low to high CaO contents. A general trend is noticeable, as CaO content increases so does the percent passing the #325 sieve, except for FA-5 and FA-8. These two fly ashes are distinct from the group because of their extremely high alkali content ( $\text{Na}_2\text{O}_e > 8\%$ ).

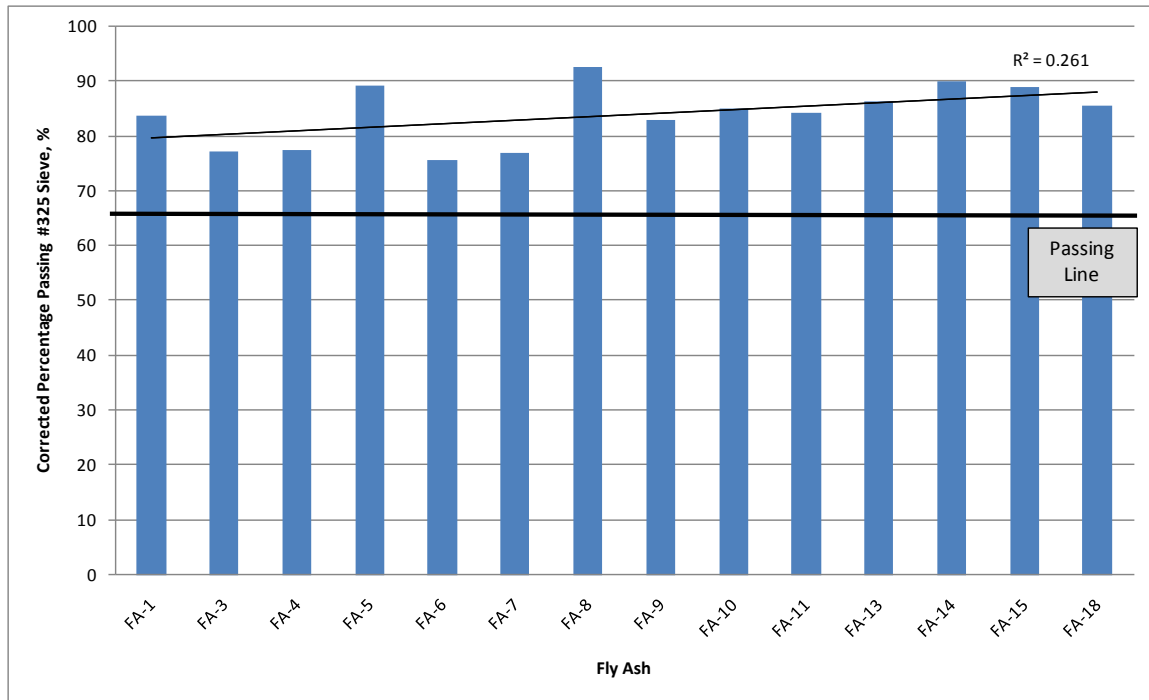


Figure 14: Percent Passing No. 325 Sieve

One can notice that the higher CaO fly ashes are finer in size and might conclude that they would be more effective for reducing ASR expansion. This is not the case for several reasons. The lower CaO fly ashes are already more pozzolanic because of their chemistry, not their particle size. When interpreting the results from particle size and relating them to ASR, only fly ashes with similar chemical compositions and different particle sizes should be compared. For example, when comparing two fly ashes with similar CaO and  $\text{Na}_2\text{O}_e$  contents and different particle sizes, the one with finer particles would be expecting to perform better.

#### 4.1.1.2 Laser Diffraction

Figure 15 shows the particle size distribution for all 18 fly ashes. The curves show a relatively even distribution of all sizes without any gaps. Figure 15 is divided into two groups, between Figure 16 and Figure 17, because of the large number of

samples. In order to more accurately understand the results the figures were divided by CaO content.

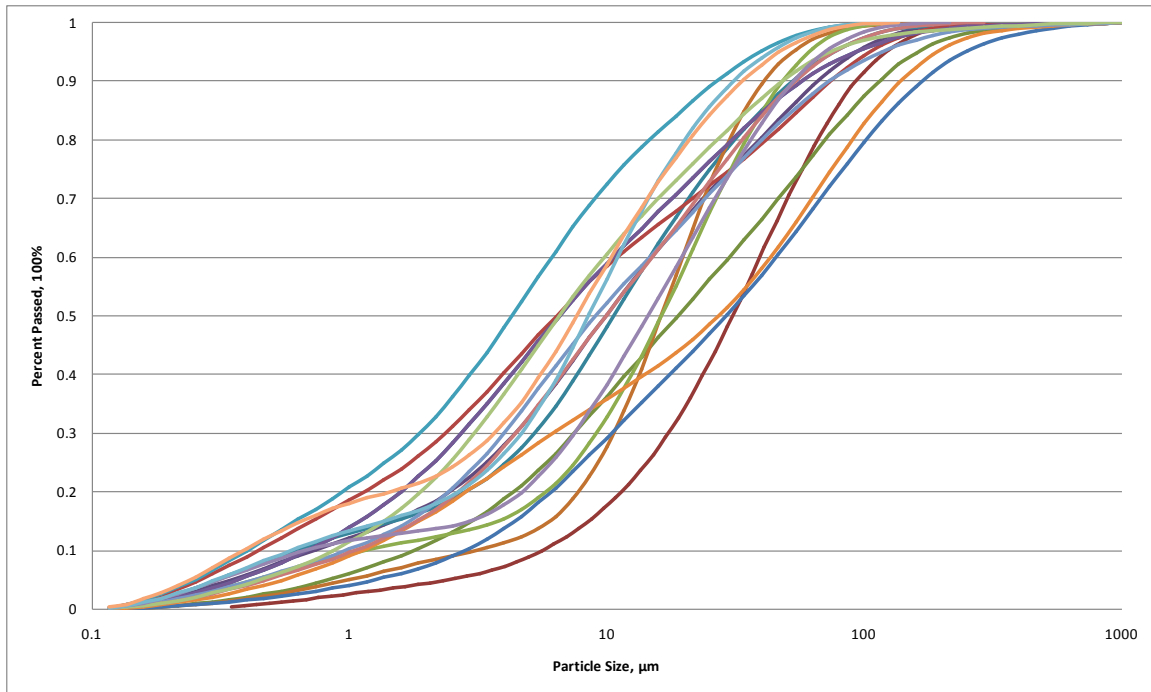


Figure 15: Fly Ash Particle Size Distribution

By studying the three figures, the higher CaO fly ashes again seem to have the smaller particle sizes. According to Roy et al. (1985), high calcium fly ashes have few cenospheres, generally have specific gravities of 2.3 to 2.8, and usually have finer particle sizes than low calcium fly ashes.

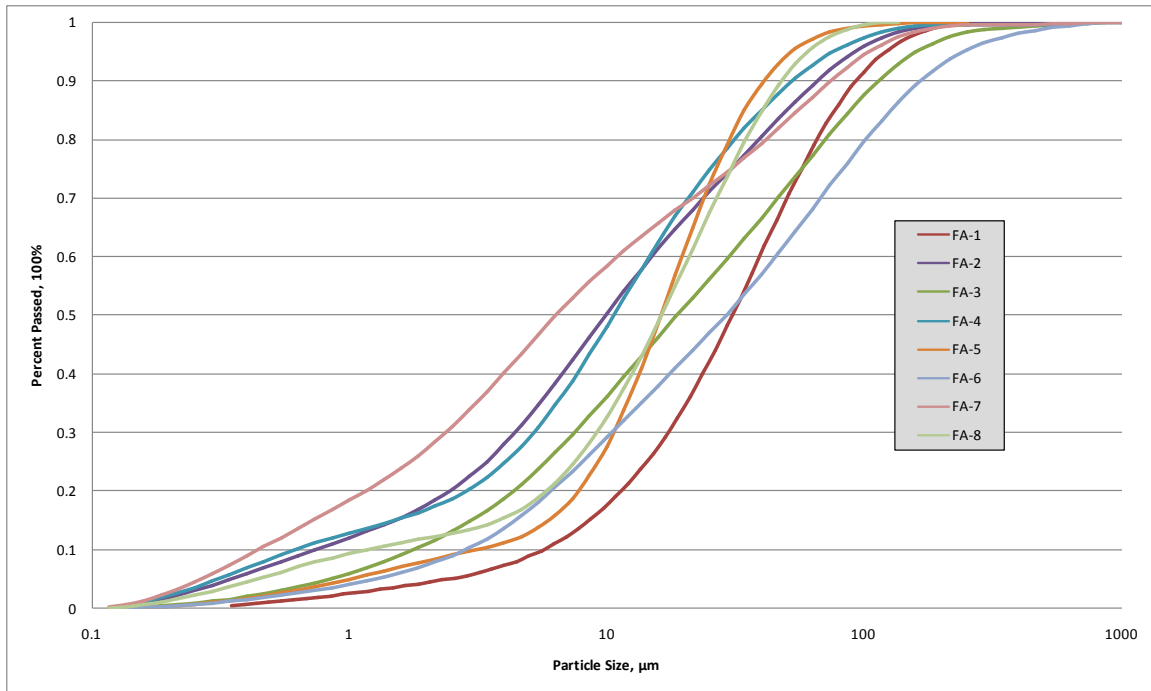


Figure 16: Particle Size Distribution (CaO<20%)

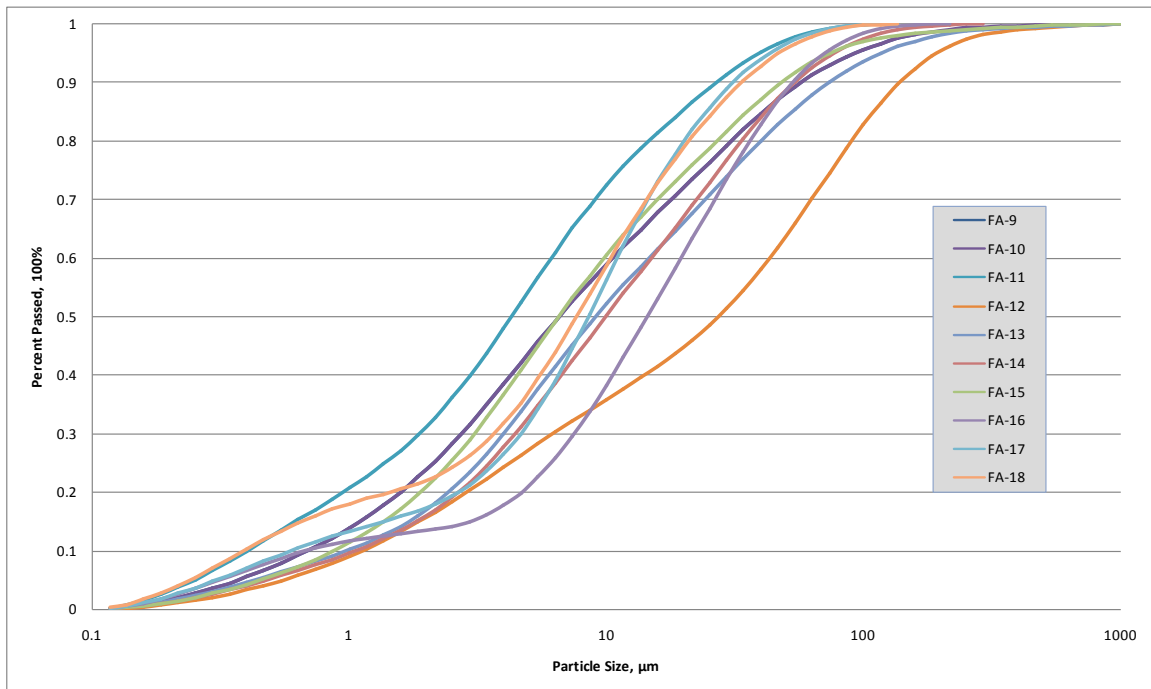


Figure 17: Particle Size Distribution (CaO>20%)



Figure 18 shows the  $D_{50}$  values (size below which 50 percent of the particles passed) for each of the fly ashes. In general, the higher CaO fly ashes appear to be finer than lower CaO fly ashes. The average  $D_{50}$  values for the Class C fly ash and Class F fly ash were,  $11.5\ \mu\text{m}$  and  $15.5\ \mu\text{m}$ , respectively.

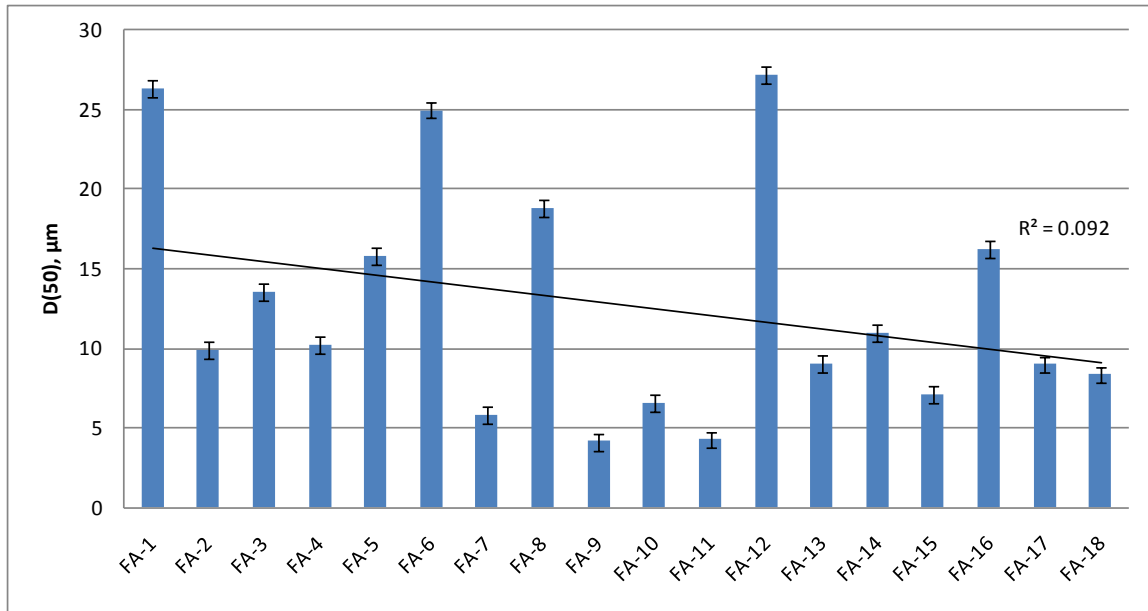


Figure 18: Average Particle Diameter by Mass

Lorenzo et al., (1994) conducted a study on two fly ashes with very similar calcium and alkali contents but different particle sizes. They studied alkali concentrations of pore solution of paste samples of these two fly ashes. They determined that the fly ash with the finer particles also had the paste samples with lower alkali concentrations in the pore solution.

If one closely studies Figure 17, one can see the particles of FA-15 are considerably smaller than those of FA-13. From Table 7, one can also see these two fly ashes have similar calcium and alkali contents with FA-15 having a slightly higher CaO

of 25.5 to 24.7 and higher  $\text{Na}_2\text{O}_e$  of 1.4 to 1.3. Results from two-year concrete prism testing show that F-15 expanded 0.009%, whereas F-13 expanded by 0.033%, approaching the 0.04 percent threshold for ASTM C 1293. It is quite possible that the increased fineness of F-15 was responsible for its superior performance with regard to suppressing ASR.

#### **4.1.2 X-Ray Fluorescence**

Table 7 and Table 8 show the XRF results for all fly ashes and cements, based on testing performed by TxDOT. The fly ashes were labeled and organized according to their CaO percentage. As one can see, the fly ashes are organized in an ascending manor with respect to the CaO percentage. Figure 19 shows the large ranges of CaO contents of the fly ashes chosen for this research along with the  $\text{Na}_2\text{O}_e$  percentages. The CaO contents range from 1 to almost 30%; while most of the  $\text{Na}_2\text{O}_e$  percentages are similar, there are two much higher at around 8%.

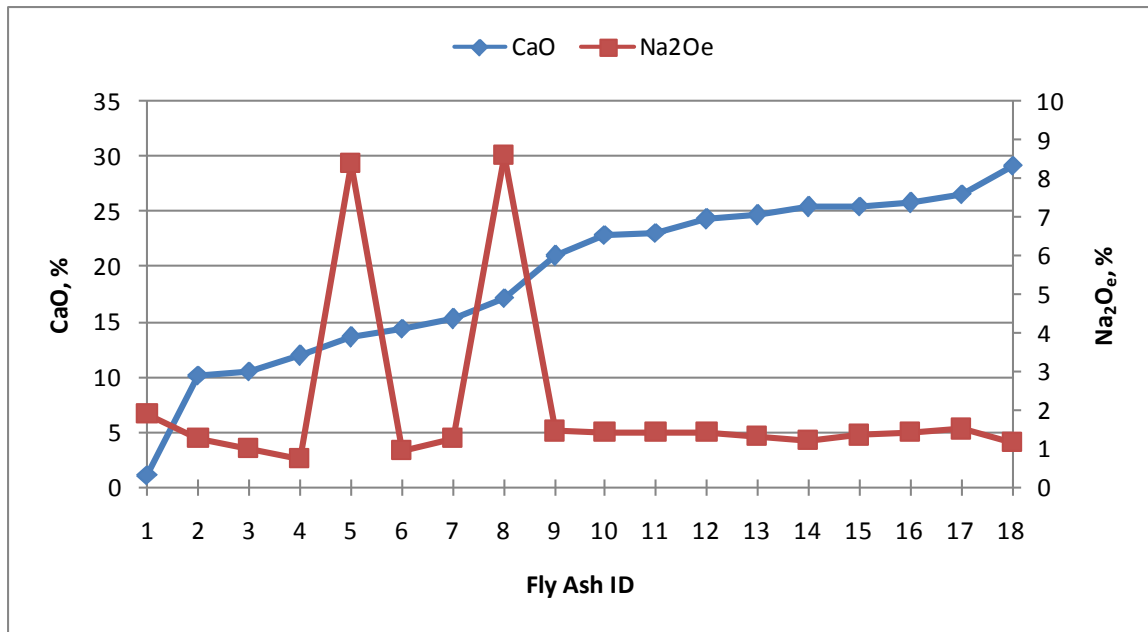


Figure 19: CaO and Na<sub>2</sub>O<sub>e</sub> Percentages

As mention previously in Table 2, the classification of fly ashes according to ASTM depends on the sum of three of the oxides. Any sum above 70% is a Class F fly ash and above 50% is a Class C ash. This attempt at classification is confusing since sum above 70% is also above 50% which means a Class F fly ash is also a Class C fly ash. The Canadian Standards Association (CSA) classifies fly ashes into three categories solely dependent on CaO content. Type F has CaO < 8%, Type CI has CaO 8-20%, and Type CH has CaO > 20%.

Table 7: Fly Ash XRF Results

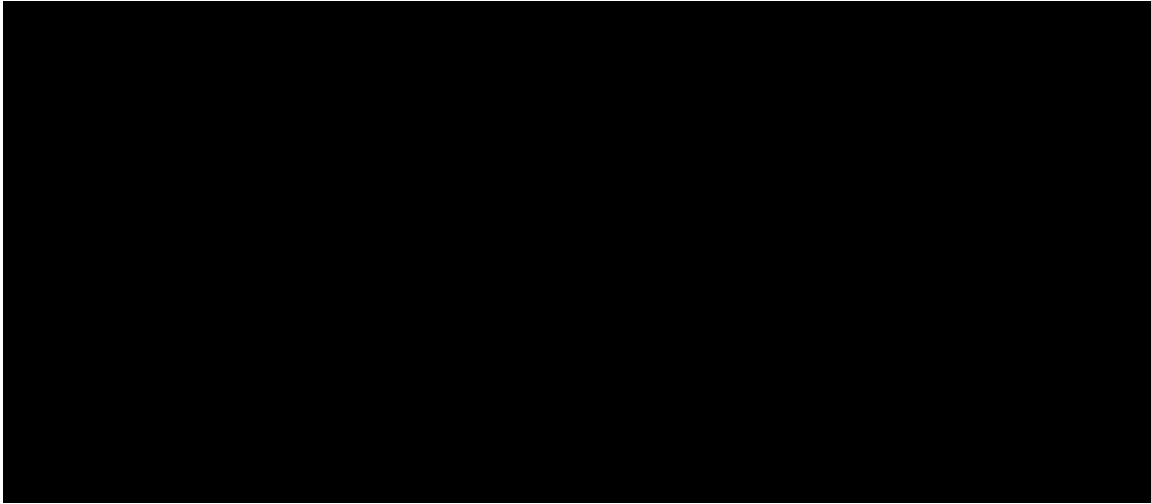
A large black rectangular box redacting the content of Table 7.

Table 8: Cement XRF

A black rectangular box redacting the content of Table 8.

Figure 20 shows the sum of oxides percentage on the left axis and the CaO percentage on the right axis. According to ASTM, there were a total of eight Class C fly ashes and 10 Class F fly ashes. According to CSA, there were FA 1-4 and FA 6-7 are Class F fly ashes and FA-5 and FA 8-18 are Class C fly ashes. According to CSA, there were a total of one Type F, seven Type CI, and 10 Type CH fly ashes.

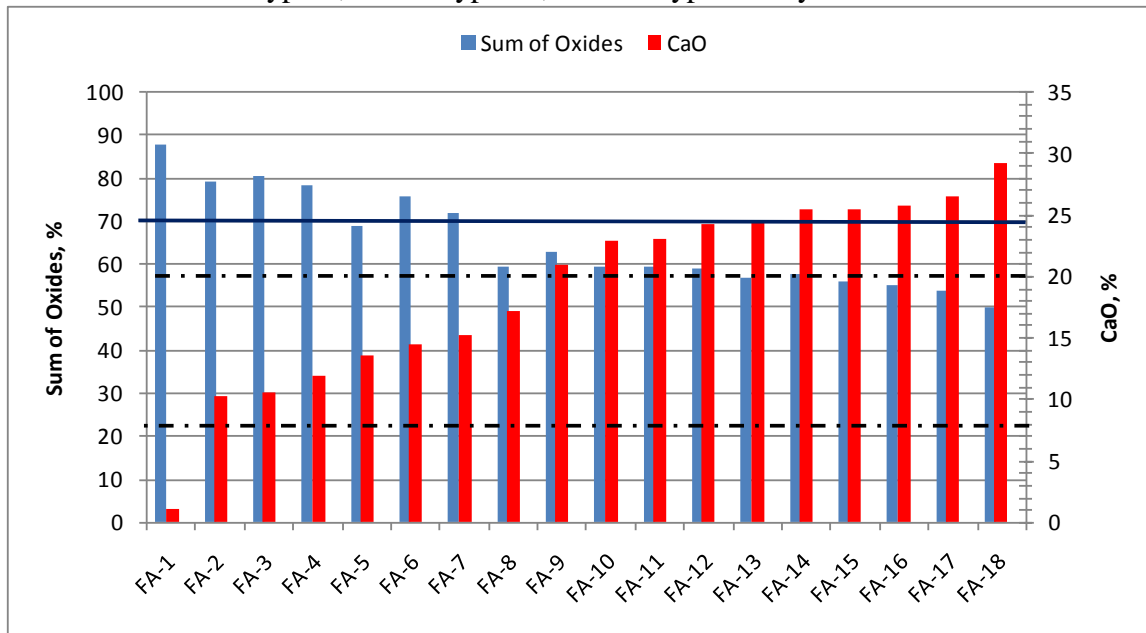


Figure 20: Sum of Oxides, CaO Percentages

Class C fly ashes are known to be less effective in reducing pore solution pH and require large dosages to control ASR induced expansion. Higher CaO fly ashes are less pozzolanic in nature which allows for more CH to remain in the system that assists at maintaining a high pH. This promotes dissolution of silica. The hydrates that are produced such as C-S-H when using a Class C fly ash tend to have a higher C/S ratio and lower potential for binding alkalis. The hydration products in Class F fly ashes tend to

have a lower C/S ratio and bind alkalis within thus removing them from availability for reaction.

#### **4.1.3 Total Alkalis (Acid-Soluble)**

This section presents the results and analysis of the Total Alkali test method from ASTM C 311 and ASTM C 114. The procedure is described in detail in Section 3.2.3. The standard states that this test method does not determine total alkalis of materials with large amount of acid-insoluble materials. In other words, this test method will only determine the acid-soluble alkalis in fly ash.

This procedure was implemented on 14 of the fly ashes. Figure 22, Figure 23, and Figure 25 display the results of the acid-soluble experiment. Figure 21 displays the results of the 14 fly ashes on a column chart with the  $\text{Na}_2\text{O}_e$  percentage by mass on the y-axis. Because the fly ashes are numbered from low to high calcium, from this figure it is already noticeable that the lower calcium fly ashes had considerably less acid-soluble alkalis. FA-5 and FA-8 are the high alkali fly ashes and as one can see they had more acid-soluble alkalis than others of similar calcium content. FA18 had the highest amount of acid-soluble alkalis, even higher than FA-5 and FA-8. In fact the majority of Class C fly ashes had higher amounts of acid-soluble alkalis than the fly ashes with high alkali contents.

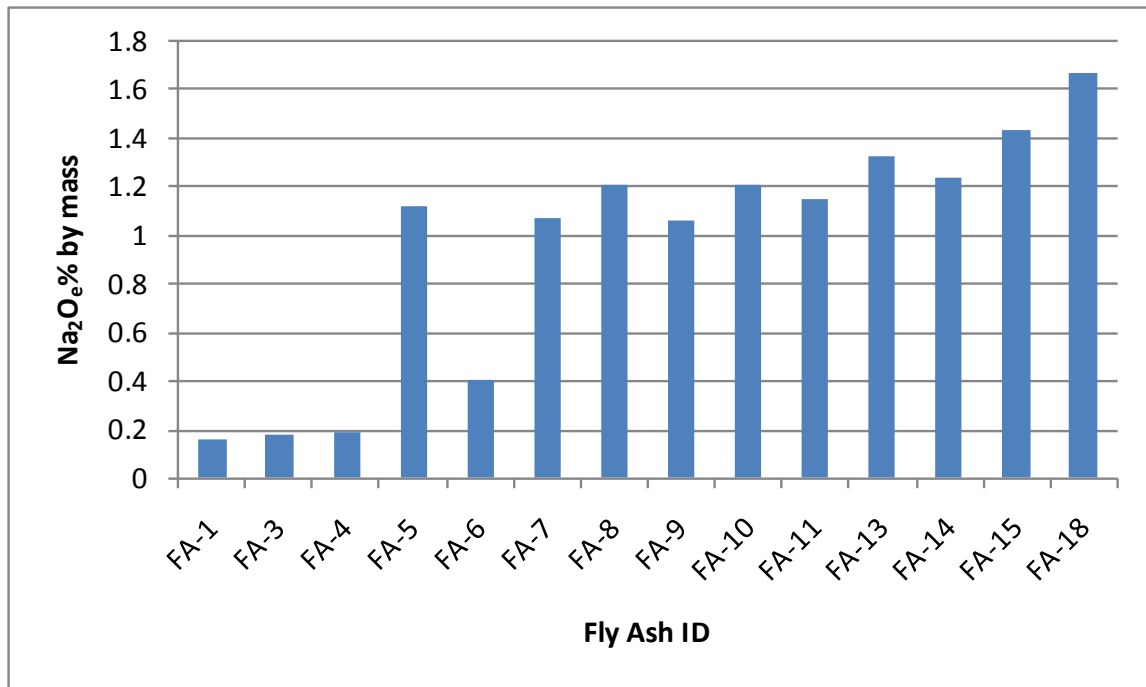


Figure 21: Acid-Soluble Results

Figure 22 has the same acid-soluble alkali results but plotted as CaO content increases. There is a general trend showing that as CaO content increases in the fly ash so does the amount of acid-soluble alkalis. The data points seem to be separated into groups and it is distinct which the Class C and Class F fly ashes are. The lower group of data points are Class F fly ashes and the higher group are the Class C fly ashes. There is a group of points in the middle of the chart, two of them are the high alkali fly ashes and the other is FA-7. FA-7 is Class F fly ash but has a rather high calcium content of 15.3%.

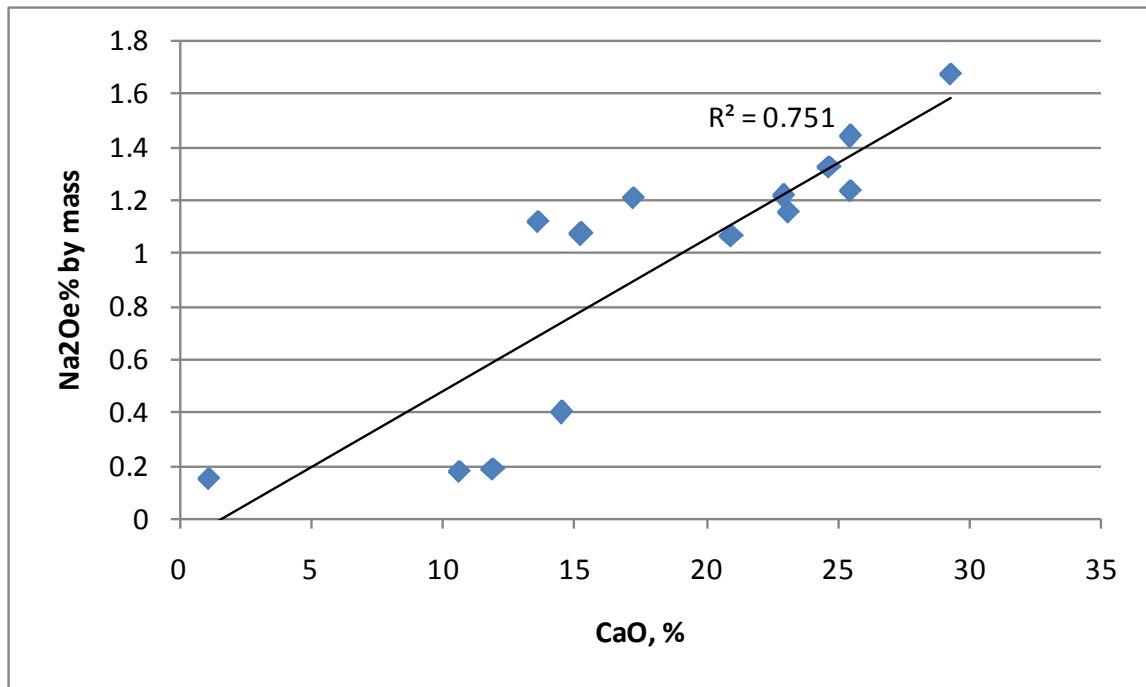


Figure 22: Acid-Soluble Alkalis (CaO)

Figure 23 displays the acid-soluble alkalis as a percentage of the amount of total amount of alkalis present in the fly ash. This again is plotted as CaO content increases. The trend line again fits the set data well and the r-squared value is higher than before at 0.763. What is noticeable here is that the two high alkali fly ashes only had a very small percentage of their alkalis acid-soluble. The only fly ash with a lower percentage was FA-1, the fly ash with the by far the lowest calcium content. From this figure, the two classes of fly ashes are again separated into two groups. The two groups are separated by the 60% line off of the y-axis. All of the Class C fly ashes have more than 60% of their alkalis acid-soluble and all the Class F fly ashes have less than 60%. The only exception was FA-7.



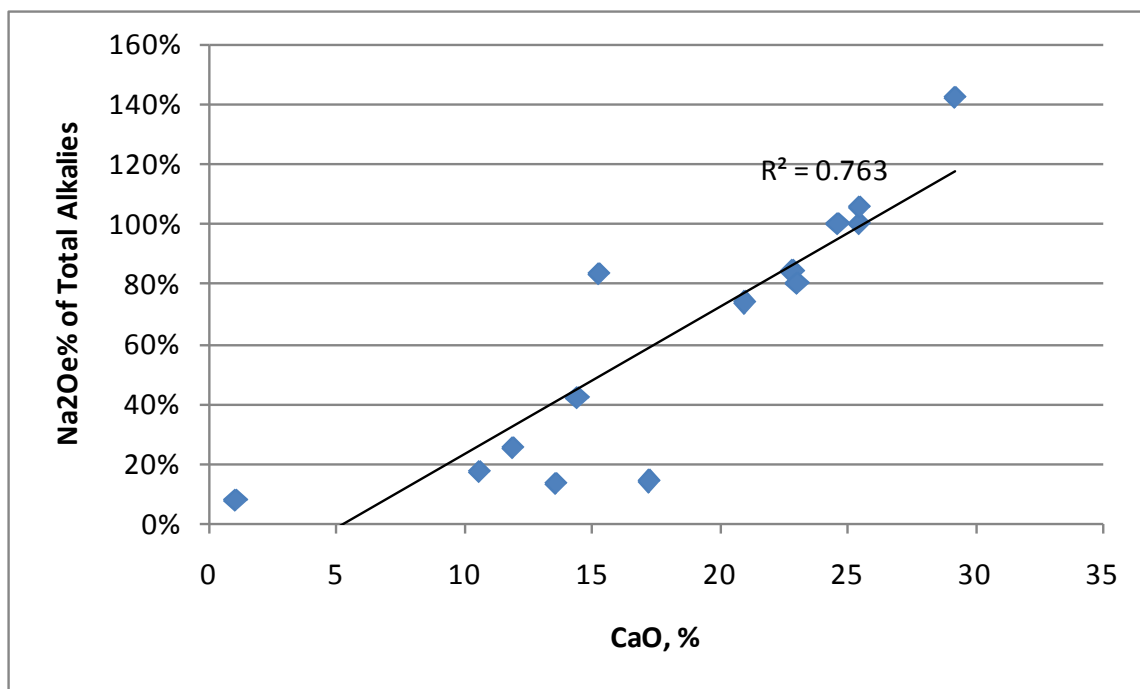


Figure 23: Acid-Soluble/Total Alkalies (CaO)

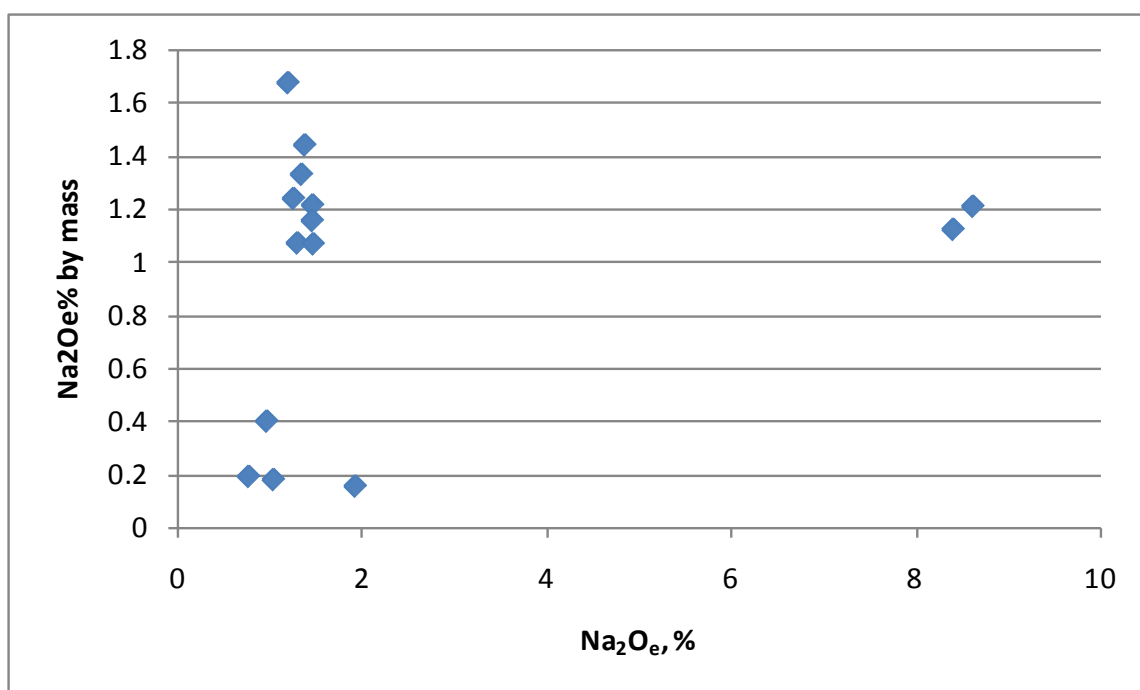


Figure 24: Acid-Soluble Alkalies (Na<sub>2</sub>O<sub>e</sub>)

Figure 24 shows the acid-soluble alkalis plotted with the total  $\text{Na}_2\text{O}_e$  on the x-axis. One would think that the amount of acid-soluble alkalis would relate to the amount of total alkalis. In fact, it seems that the CaO content of the fly ash has more effect on the amount of acid-soluble alkalis. Appendix C has more figures relating acid-soluble alkalis to the  $\text{SiO}_2$  content and other parameters. The  $\text{SiO}_2$  content of the fly ash appears to play a big role in acid-soluble alkalis, with the trend line having a r-squared value of 0.90. Figure 24 shows that there is a trend relating total alkalis to acid-soluble alkalis but the two high alkali fly ashes do not correspond greatly with the rest of the group. Also, a trend line was put on this set of data points but even with the exclusion of FA-5 and FA-8 the r-squared value was low.

Figure 25 plots the set of data against a compositional parameter that Professor M. Thomas of the University of New Brunswick has published on several of his papers. The x-axis is based off the chemical composition of the fly ashes  $[(\text{Na}_2\text{O}_e)^{0.33}\text{xCaO}]/\text{SiO}_2^2$  is what Dr. Thomas used to relate the chemical composition of a concrete binder to ASR induced expansion (Thomas, 2011). He has also concluded similar relationships with the  $\text{OH}^-$  concentration in pore solutions.

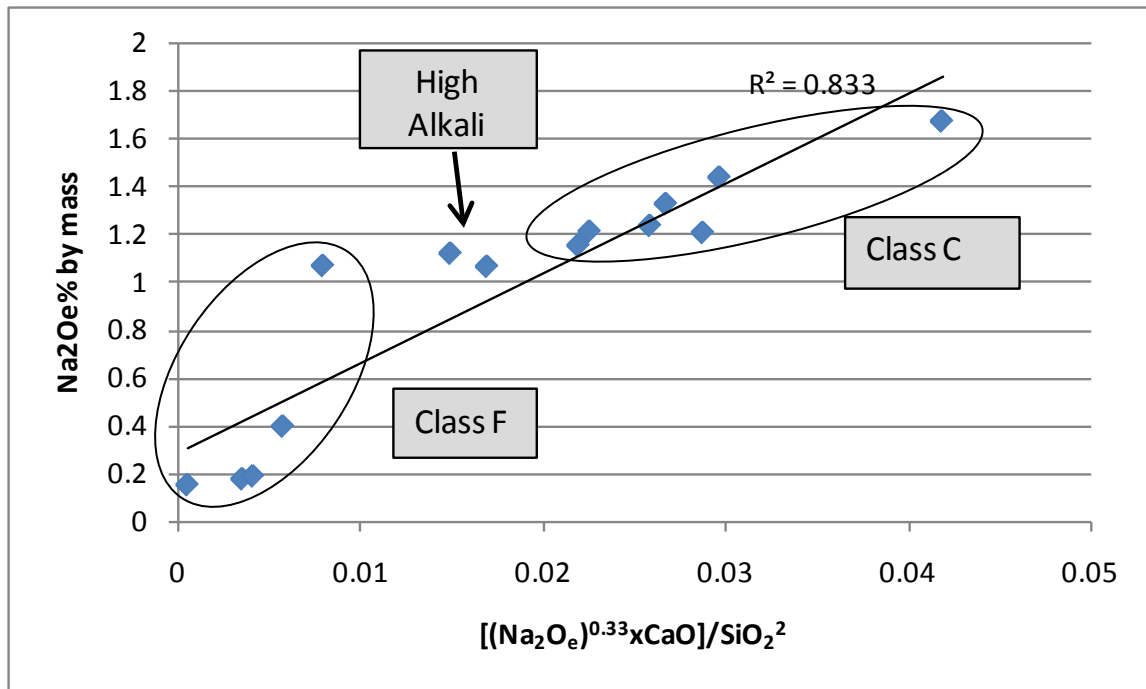


Figure 25: Acid-Soluble Compositional Parameter

$[(\text{Na}_2\text{O}_e)^{0.33} \times \text{CaO}] / \text{SiO}_2^2$  can also be used to relate the acid-soluble alkalis of fly ash. Figure 25 shows as the chemical ratio increases so does the amount of acid-soluble alkalis. This chemical index shows that acid-soluble alkalis are not just function of the amounts of  $\text{Na}_2\text{O}_e$ ,  $\text{CaO}$ , or  $\text{SiO}_2$  individually but a function of the three combined. All three factor into the amounts of acid-soluble alkalis that fly ash have.

#### 4.2 ASTM C 1260, 1567

ASTM C 1260 is the accelerated mortar bar test for reactive aggregates and ASTM C 1567 is the experiment for testing the effectiveness of pozzolans on preventing deleterious ASR expansion. As previously mentioned, expansion above 0.10% at 14 day measurements are indicative of potentially deleterious expansion. Expansions below 0.10% are likely to produce acceptable expansions when tested in concrete.

Six of fly ashes were chosen to be tested under ASTM C 1567 and the expansion results are located in Appendix A. These six fly ashes were tested because the project database did not contain ASTM C 1567 data on these six. The same reactive aggregate was used for all mixes. For the fly ashes chosen, testing was conducted at cement replacements of fly ash of 20, 30, and 40%. Further testing was conducted on FA-8 because of its failure to mitigate expansion and will be discussed later.

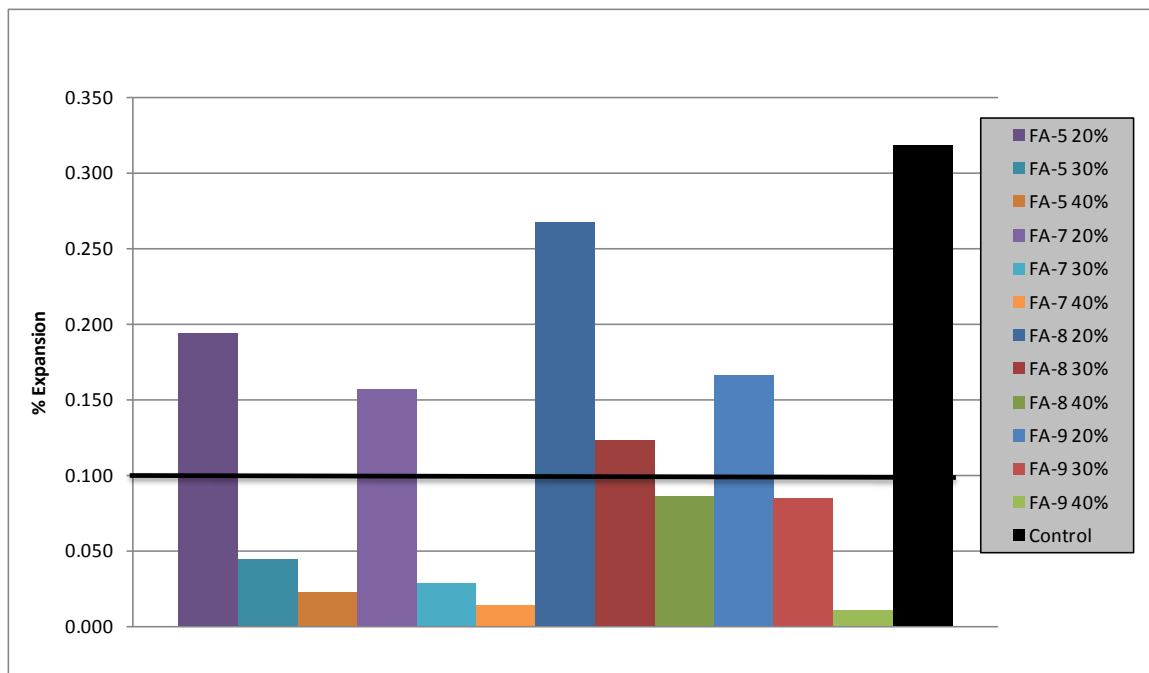


Figure 26: ASTM 1260 14 Day Similar Chemical Compositions

Figure 26 displays the 14 day expansion measurements for FA-5, 7, 8 and 9 for 20, 30, and 40% replacement levels. The black column is the control using C-1, the high alkali cement, and the black line coming across 0.1% expansion is the failure requirement. These four fly ashes were chosen because FA-5 and FA-8 have high alkali contents and the other two have similar chemical compositions to these two. One would

want to determine if the high alkali contents of the fly ashes affected the testing even though these mortar bars are exposed to essentially an infinity supply of alkalis from the 1 M NaOH host solution. By studying the results of FA-8, it appears the alkalis in the fly ash do play a role in the expansion. From Figure 30 it can be seen that expansion increases as the CaO of the mortar binder increases. Knowing this one would expect FA-9 to have higher expansions than FA-8 but the alkalis within the FA-8 affected the expansion of the mortar bars. In addition, FA-5 has slightly higher expansions than FA-7 with higher CaO content. Also, notice how all the fly ash samples performed better than the control using C-1. The control had a 14 day expansion greater than 0.30%, which is three times the limit for deleterious expansion. In this case, the replacement of high alkali cement with high alkali fly ash was an improvement and continued to improve as fly ash dosages increased. The same conclusions can be reached with Figure 27, the 28 day results. Also, from Figure 27, one can conclude that the rate of expansion after 14 days of FA-8 continued to increase.

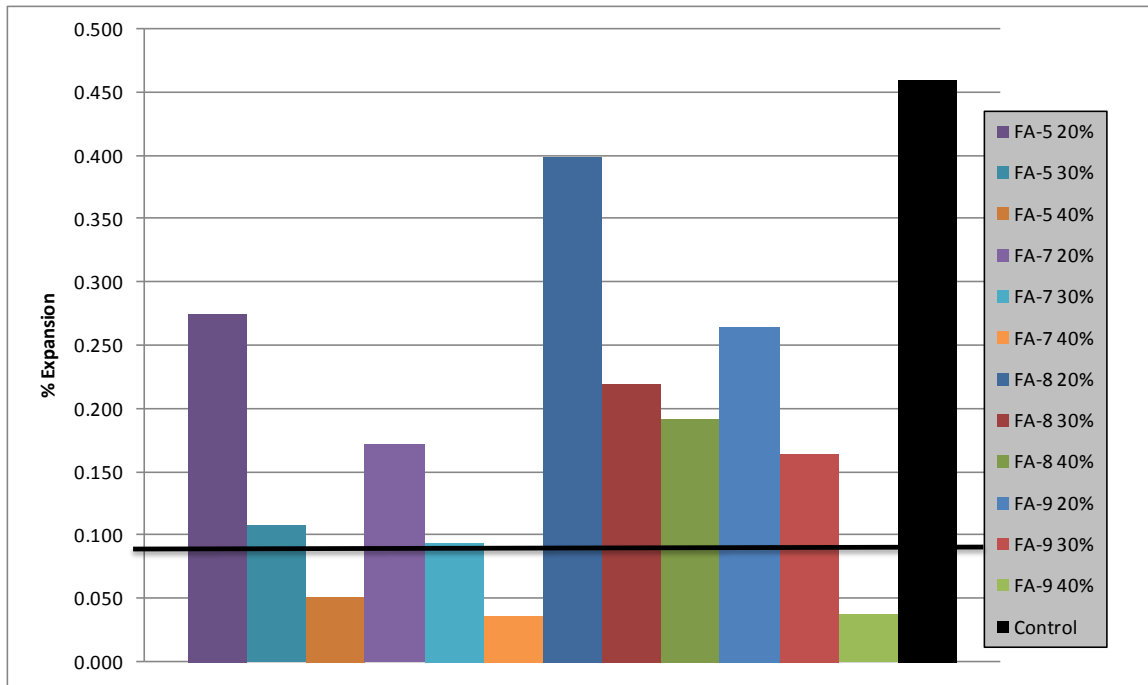


Figure 27: ASTM C 1260 28 Day Similar Chemical Compositions

Further testing was conducted on FA-8 because of its behavior. Even at 40% replacement, the expansion percentage was still way above the limit. Expansions close to 0.1% at 14 days and 0.2% at 28 days for 40% were noticed. Because of this, additional testing was conducted with higher replacement dosages. Results are located on Figure 28. From here we can see that increased dosages had adverse affects to some level. Expansions increase at dosages of 45 and 50%. The expansions at 45 and 50% are greater than those of 40%. Samples of replacement levels of 40, 45, and 50% were tested twice because of this behavior. The expansion began to decrease once again at a replacement of 55%.

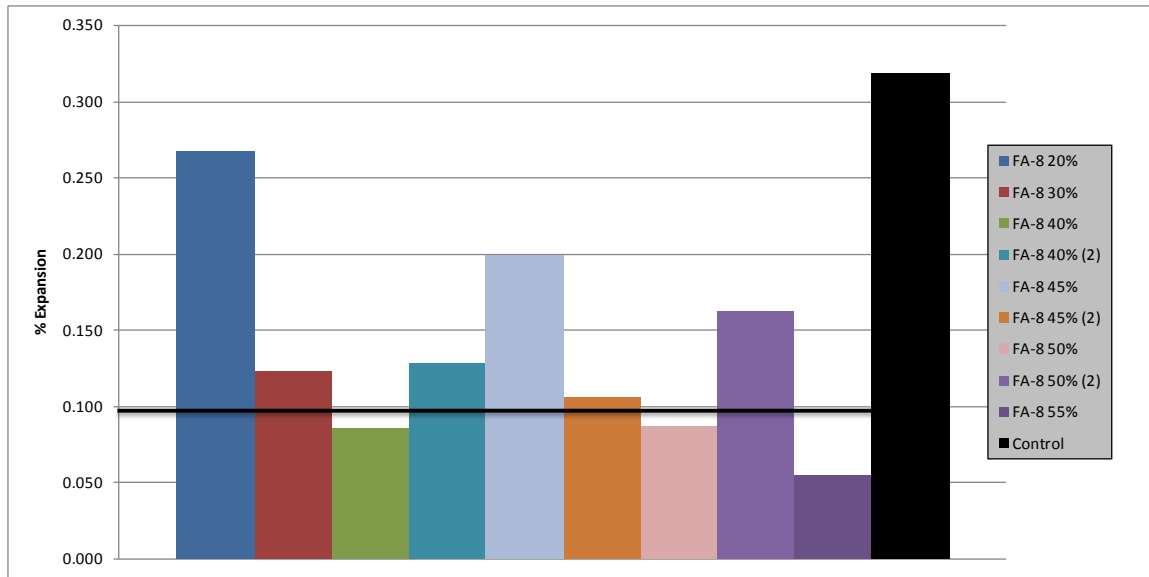


Figure 28: ASTM 14 Day FA-8

Figure 29 shows the results of FA-2, 8, 17 at 14 days using different replacement levels. FA-2 performed far better than FA-17, and even FA-8 performed better than FA-17. A replacement level of 20% percent of FA-2 was enough to keep expansions below 0.1% and 40% showed very small expansion. FA-17 is the fly ash with the second highest calcium content and showed very deleterious expansions at all replacement levels. It even performed worse than the high-alkali fly ash. The expansion with 40% replacement was still 0.20% at 14 days, not even slightly close to the limit. A mixture would require very large replacement levels to have the possibility of having acceptable expansions. FA-17 did however improve the performance over the control especially at 40% replacement.

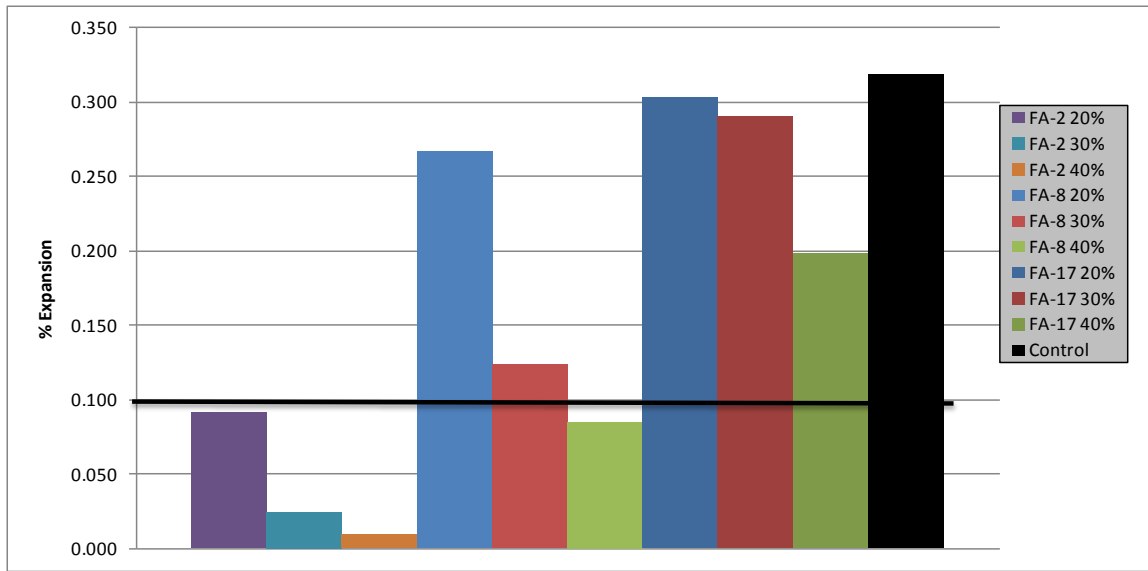


Figure 29: ASTM C 1260 14 Day Expansion - Wide Range of CaO

Figure 30 through Figure 33 contain the entire set of 1260 14 day expansion measurements conducted for this thesis. It contains readings from FA-2 to FA-17 with several in between and including the control. The exact fly ashes used can be seen on the plots in Appendix A.

As the acid-soluble alkalis were related to the chemical composition of the fly ash, the expansion results to the chemical composition of the mortar binder will now related. For example, the CaO content of the binder for the 20% FA-2 mix would be  $20\% \times \text{CaO}_{\text{FA-2}} + 80\% \times \text{CaO}_{\text{C-1}}$ . Figure 30 shows us the CaO content of the binder increases so generally does ASR induced expansion.



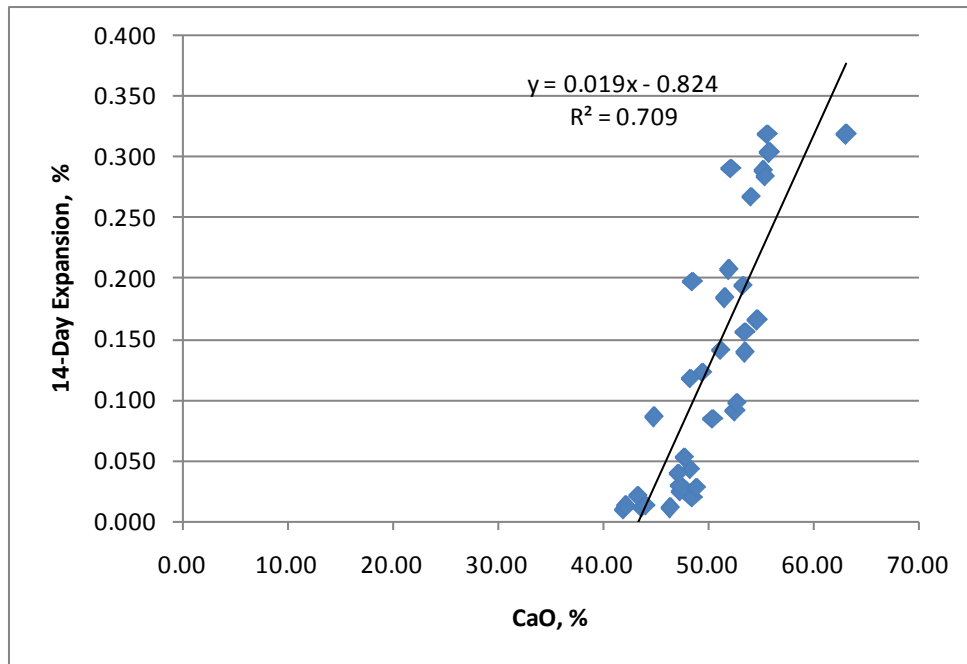


Figure 30: ASTM 1260 14 Day Expansion - CaO Relationship

Figure 31 relates expansion to the alkali content of the binder. The set of point far off to the right are the mixes involving high alkali fly ashes. Ignoring these points and adding a trend line to the rest of the set of data did not result in a high r-squared value. Although there was some correlation, it was not nearly as good as with CaO in Figure 30.

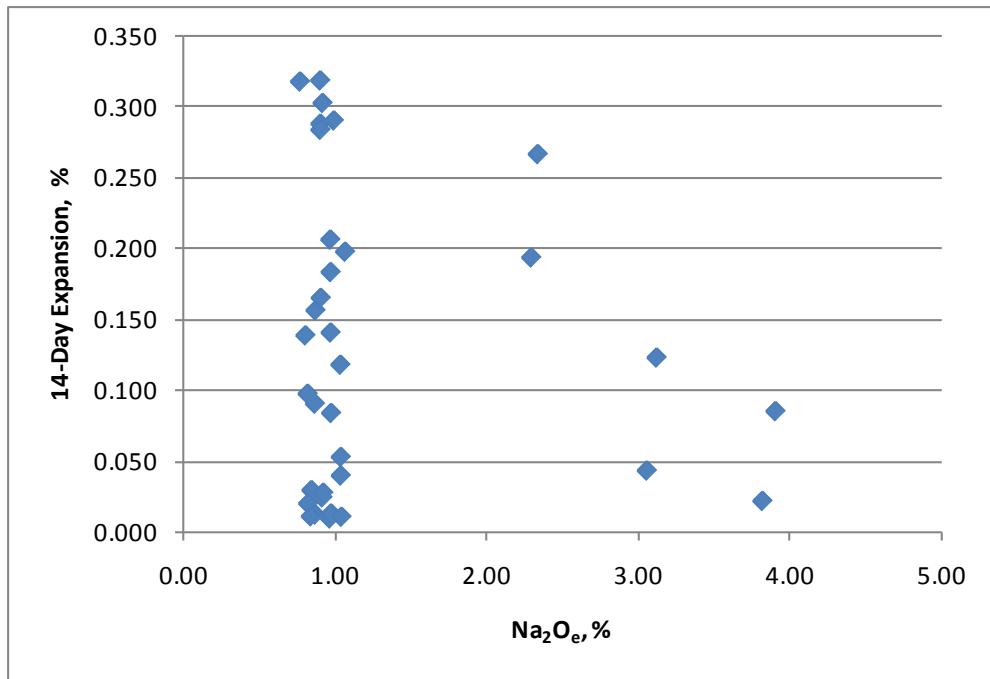


Figure 31: ASTM 1260 14 Day Expansion -  $\text{Na}_2\text{O}_e$  Relationship

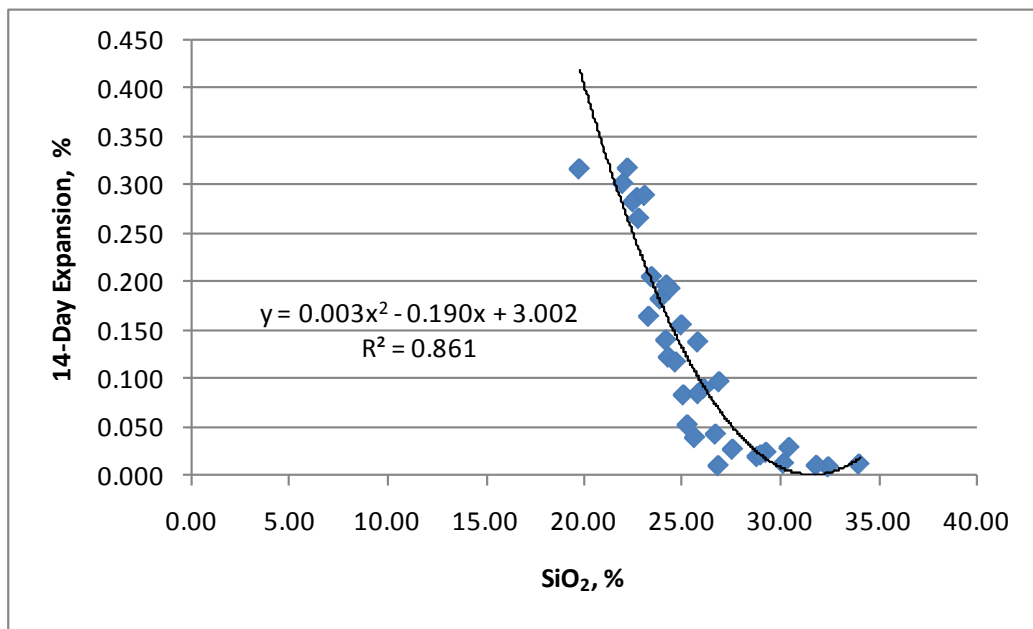


Figure 32: ASTM 1260 14 Day Expansion -  $\text{SiO}_2$  Relationship

Figure 32 illustrates the relationship between expansion and SiO<sub>2</sub> content of the binder. What is interesting about this set of data is that it follows the curve of a second order polynomial. It appears that as the SiO<sub>2</sub> content of the binder increase the expansion decreases linearly to about roughly 28% SiO<sub>2</sub>. After this point, there is hardly any expansion at all.

In Figure 33, the expansion data is related to the same chemical index used before. One can see that there is a trend, but it is not as strong as with the CaO and the SiO<sub>2</sub>. Despite this we can still notice that all three chemical parameters of the binder are affecting the expansion during the ASTM C 1260 experiment.

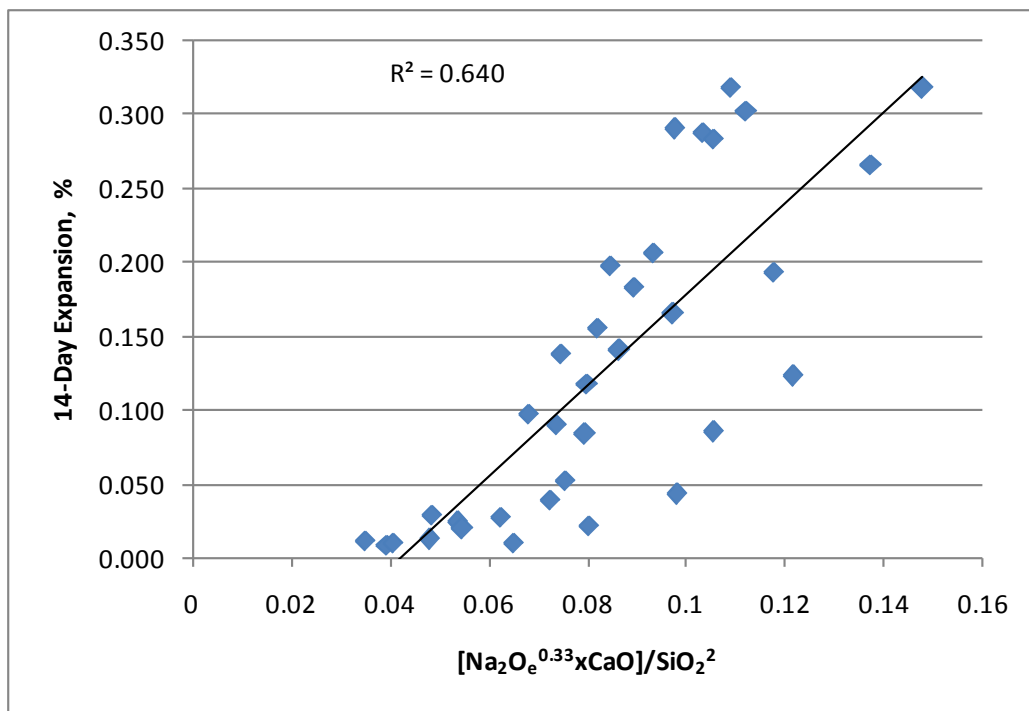


Figure 33: ASTM 1260 14 Day Expansion - Chemical Index

The same correlations from Figure 30 through Figure 33 were performed for 28 day expansion result and the plot are located in Appendix A. They again show strong trends relating the chemical parameters of the binder to the expansion results.

### **4.3 PASTE**

This following section discusses the results and analysis for the experiments involving paste samples. The pore solution extraction, available alkalis, and leaching experiments involved testing on paste samples with fly ash.

#### **4.3.1 Pore Solution Extraction**

The pore solution chemistry study was conducted on 15 mixes that were also used for the leaching experiment in the following section. The procedure for this experiment is described in section 3.2.5. 15 paste samples were created with 25% fly ashes replacement and a  $w/cm = 0.5$ . These sealed samples were allowed to cure over water at 100°F for 90 days.

Figure 34 displays the sum of the alkali concentrations in the pore solution after 90 days of curing. Hydroxide concentrations were not tested because of the small amount of pore solution extracted. Paste samples were only large enough to extract enough solution for alkali readings in the flame photometer.  $[Na^+ + K^+]$  should be very close to  $[OH^-]$  except if there are large amounts of other anions such as sulfate.

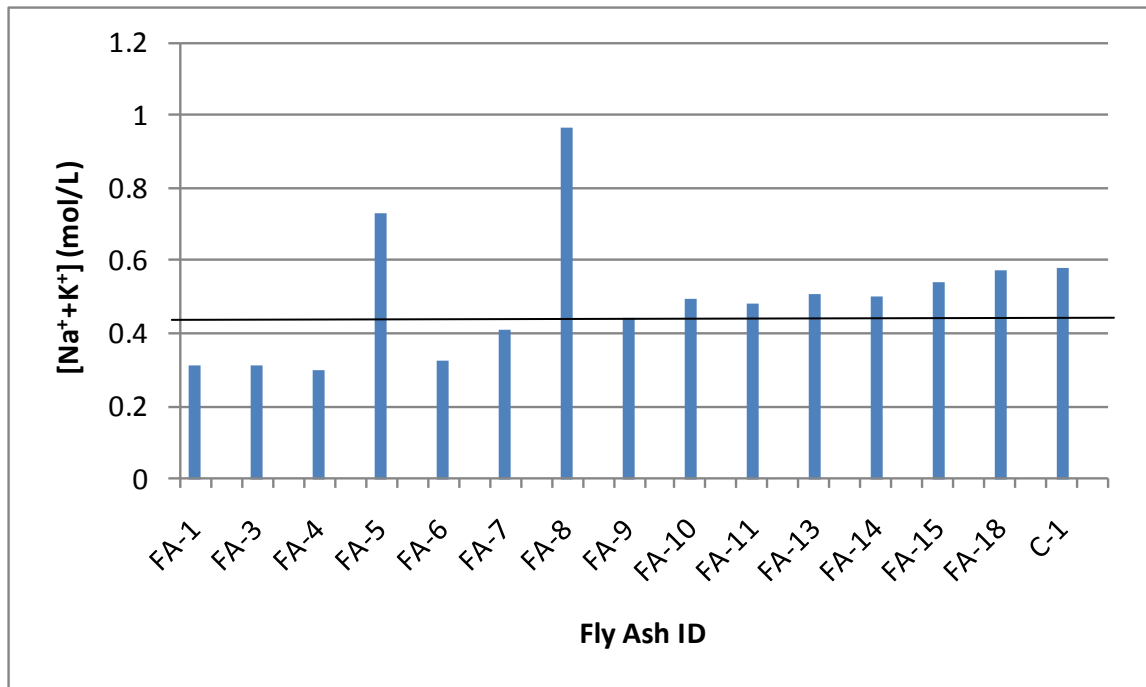


Figure 34: Pore Solution Alkali Concentrations

FA-5 and FA-8 have alkali concentrations significantly above any of the other fly ashes, and the effects of this are quite evident in the pore solution alkali concentrations. The horizontal line intersecting the y-axis at 0.44 represents what the theoretical pore solution concentration would be with a 25% inert diluent. All samples had a 25% cement replacement with fly ash except the control. Figure 34 shows that FA-9 acted as a diluent while the other Class F fly ashes (except FA-5 & FA-8) showed reduced the alkali concentration even more. This shows that these fly ashes are acting more than just a diluent but their hydration products are binding alkalis from the pore solution released by the cement.

By study the Class C fly ashes, one can notice that their concentrations are above that of theoretical inert diluent concentration. These fly ashes did not act as an inert dilute and did contribute alkalis into the pore solution. These fly ashes had no effect of

binding alkalis like the Class F fly ashes. More of their alkalis were available and went into solution.

Figure 35 through Figure 40 relate the chemical composition of the paste binder to the alkali concentration in the pore solution. All but three samples followed the same trend, the high alkali fly ashes (HA and FA) and control (C-1). Figure 35 illustrates that as the CaO content of the binder increases so does the alkali concentration of the pore solution. Figure 36 shows that as the SiO<sub>2</sub> content of the binder increases the pore solution concentration decreases. The trend lines fit the data very well with r-squared values of 0.839 and 0.958. Figure 37 shows the relationship with the amount of alkalis in the binder to the alkali pore solution concentration. There is noticeable but weak trend showing that as the alkali content in the binder increases so does the alkali pore solution concentration. The trend is not as strong here because many of the Class F and C fly ashes have similar alkali contents but it is clear that lower calcium fly ashes have more impact on reducing alkali pore solution concentrations.

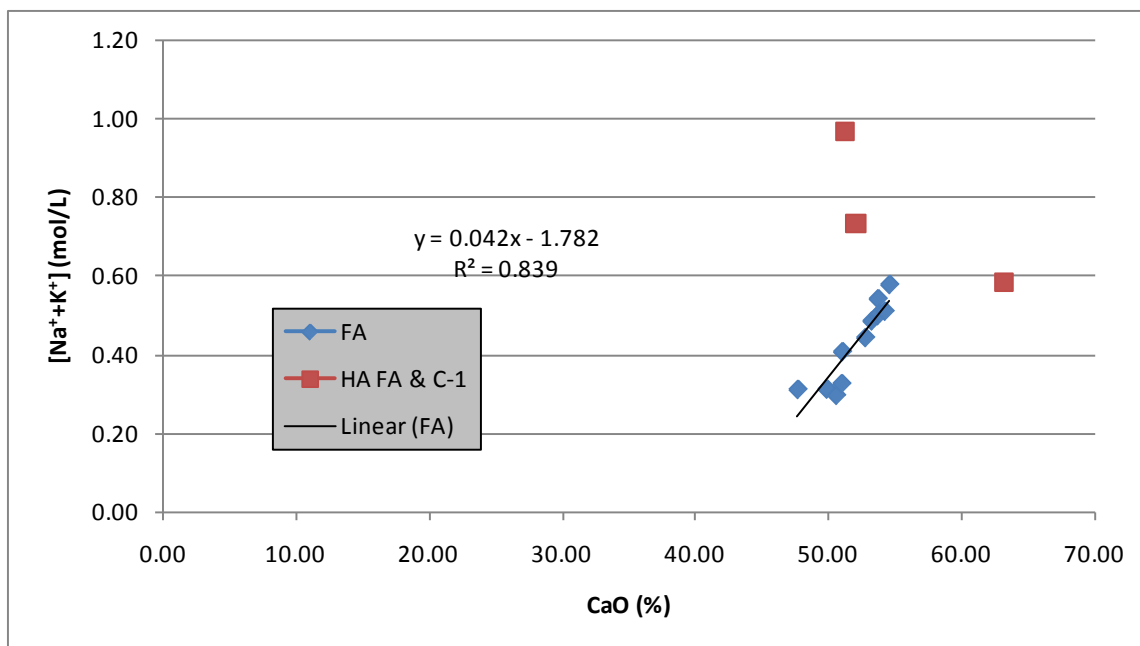


Figure 35: Pore Solution Concentration (CaO)

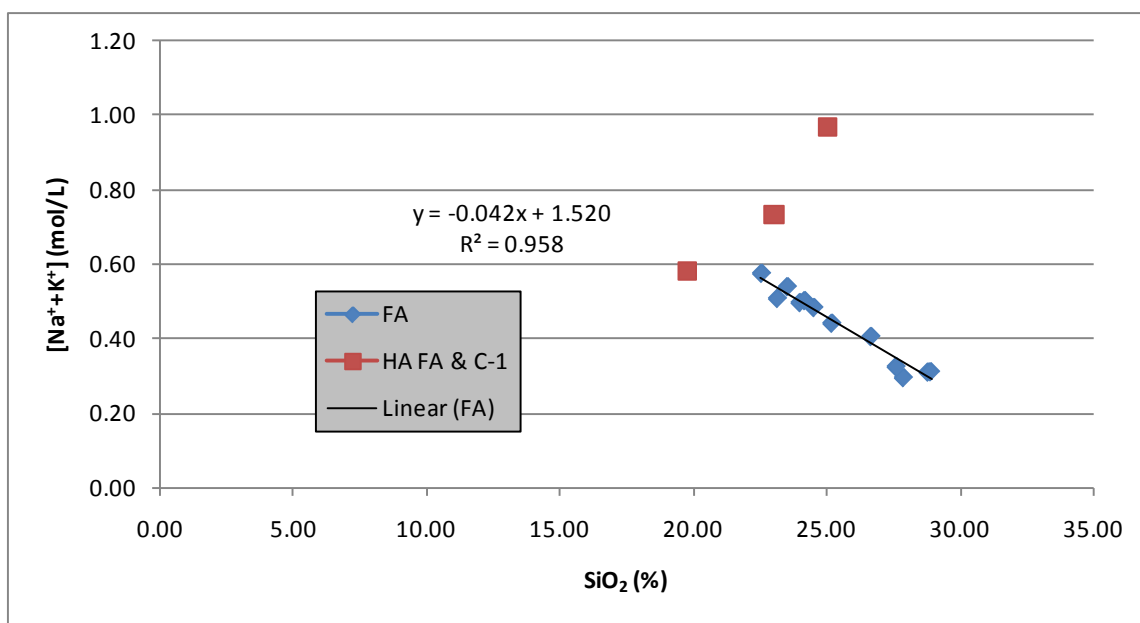


Figure 36: Pore Solution Concentration ( $\text{SiO}_2$ )

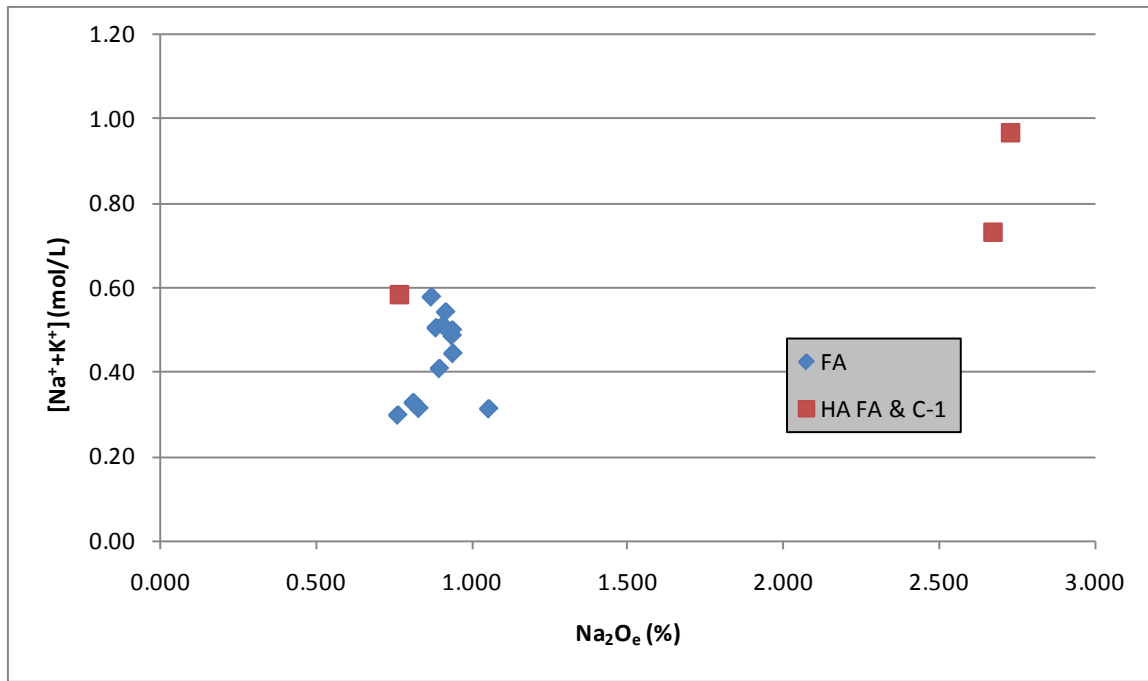


Figure 37: Pore Solution Concentration ( $\text{Na}_2\text{O}_e$ )

Many researchers believe that the  $\text{CaO}/\text{SiO}_2$  of the binder greatly factors into the amount of alkalis present in the pore solution. This can be seen in Figure 38. Others (Thomas, Shehata, 2006) propose that the  $\text{Na}_2\text{O}_e$  of the binder also plays a role. Figure 39 shows the contribution of all three being combined.



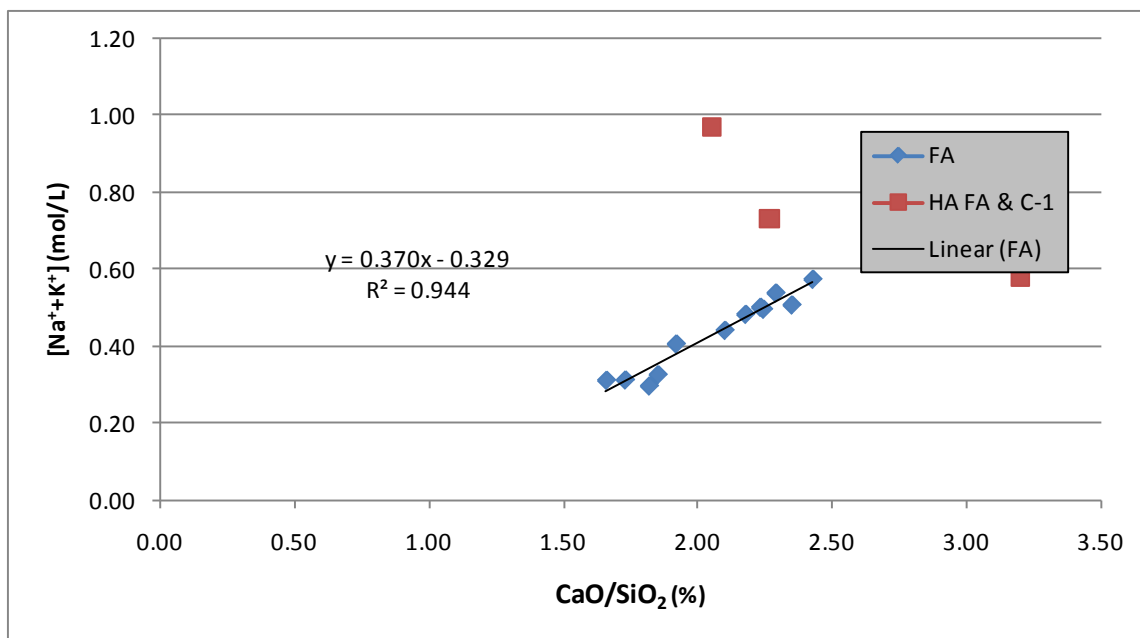


Figure 38: Pore Solution Concentration ( $\text{CaO/SiO}_2$ )

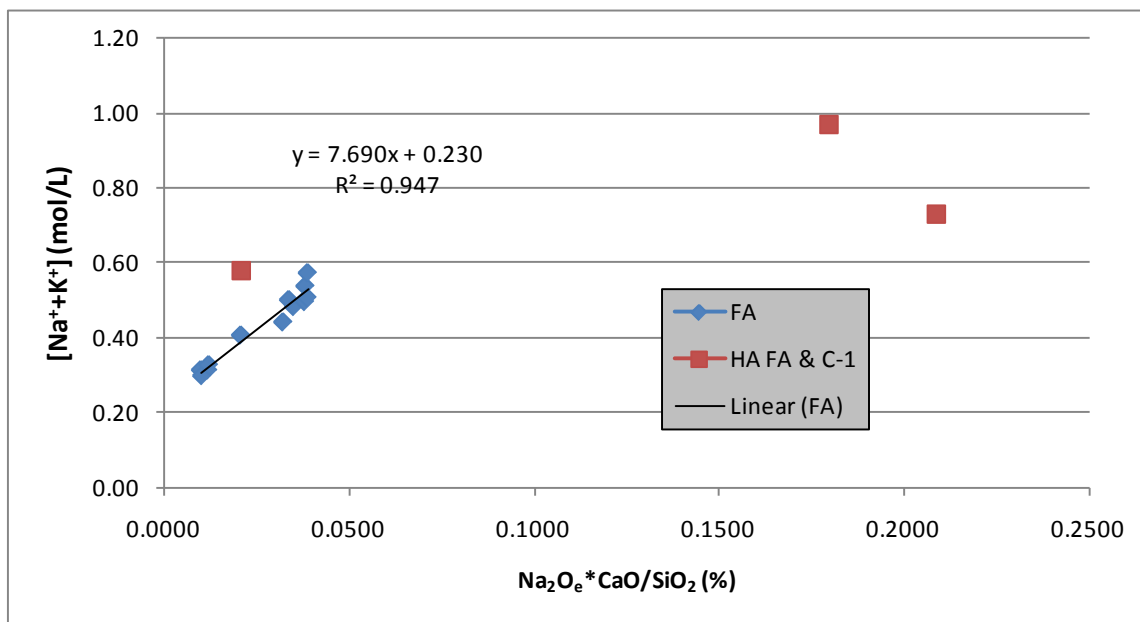


Figure 39: Pore Solution Concentration ( $\text{Na}_2\text{O}_e * \text{CaO/SiO}_2$ )

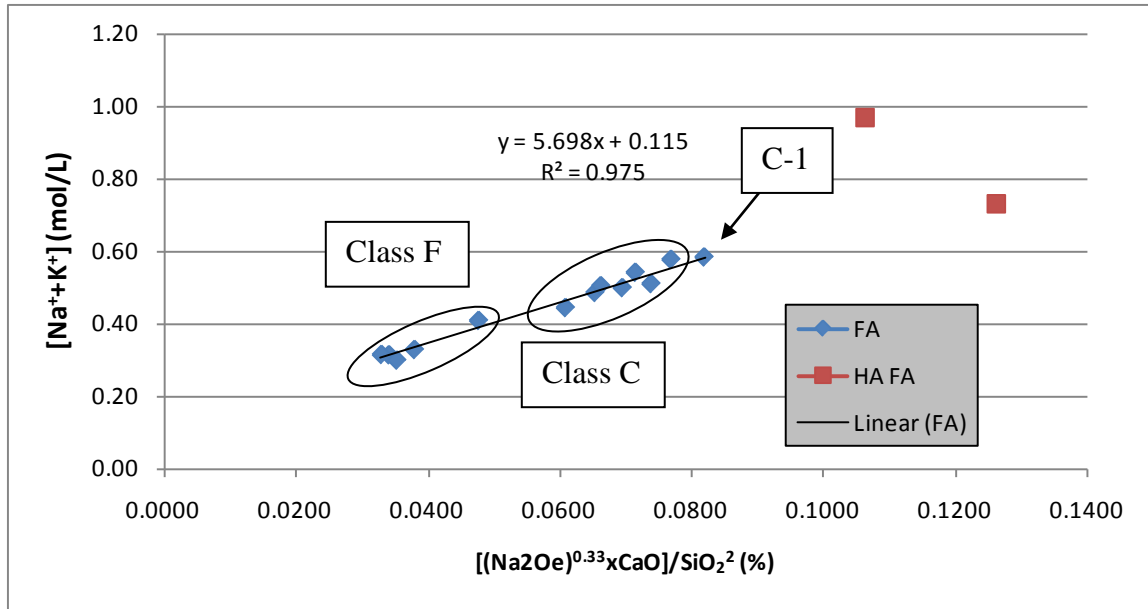


Figure 40: Pore Solution Concentration (Chemical Index)

None of the previous figures accounted for the absence of fly ash or the high alkali mixes. Using the chemical index in Figure 40, developed by Dr. Thomas, the control mixture is included in the trend line. As this chemical index of the binder increases so does the alkali pore solution concentration and the figure also distinguishes the two classes of fly ashes. The r-squared value here is the highest of all the previous figures, although it is not a good indicator for high-alkali fly ashes.

### 4.3.2 Leaching

This leaching experiment was conducted to investigate the amounts of alkali that can be leached from paste samples into simulated pores solutions of different alkali concentrations. The solutions were created with the same  $K_2O/Na_2O$  ratio as the paste binder to be placed in it. The procedure is described in detail in section 3.2.7. The same paste samples used for the pore solution extraction were used for this experiment.

Figure 41 displays the results of the leaching experiment at 0 M OH<sup>-</sup> with the available alkalis expressed on the y-axis. The term available alkalis refers to the amount of alkalis that were released from the paste into the simulated pore solutions. They are expressed as Na<sub>2</sub>O<sub>e</sub>% of the mass of the binder of the cementing materials. The mass of the cementing materials was corrected for evaporable and bound water with a correction for LOI. The concentrations of the alkalis were also corrected for the small amounts of pore fluid contributed by the paste when soaked into the solution.

Figure 41 illustrates that the higher calcium and higher alkali fly ashes released more alkalis into solution than the low calcium fly ashes. Similar relationships can be noticed on the figures at different OH<sup>-</sup> concentrations in Appendix C. The two classes of fly ashes appear to be separated by the 1% available Na<sub>2</sub>O<sub>e</sub> line off of the y-axis.

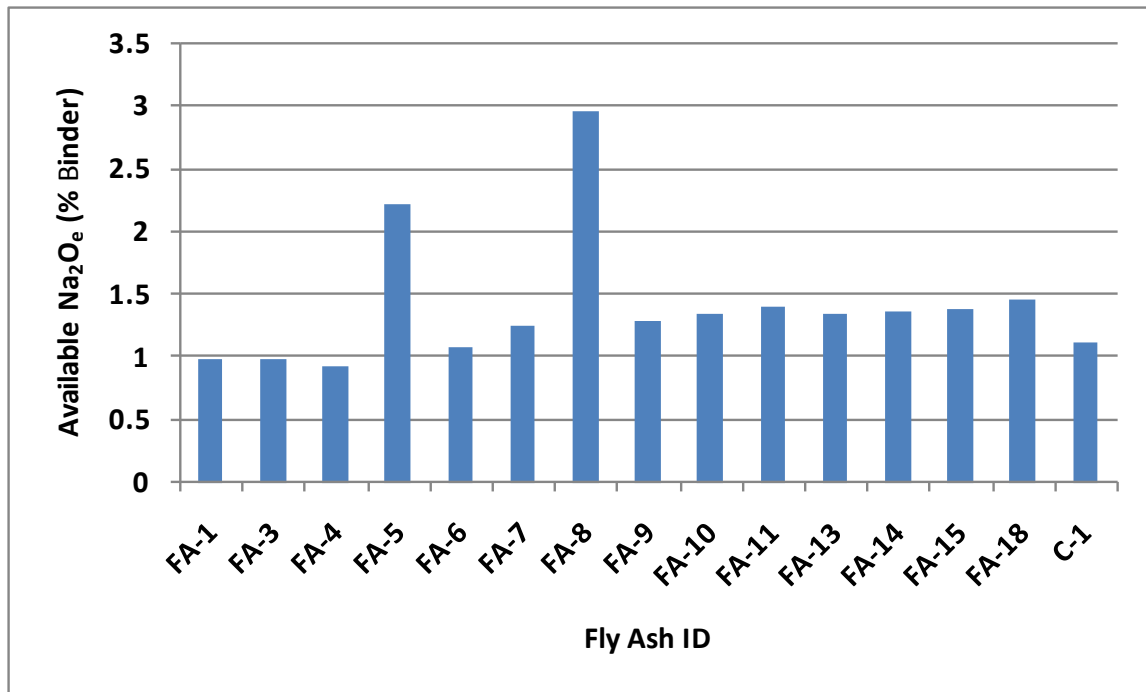


Figure 41: Leaching at 0 M OH<sup>-</sup>

Figure 42 through Figure 45 show how the chemical compositions of the paste binder factor into the amount of available alkalis when placed in distilled water. Again here one notices a positive correlation as CaO increases and a negative correlation as SiO<sub>2</sub> increases. The two high alkali fly ashes and C-1 do not fit the trend that the others follow. Figure 44 illustrates that the amount of alkalis present in the binder does not affect the amount of available alkalis as much as CaO and SiO<sub>2</sub> do. The trend for this set of data is not as strong.

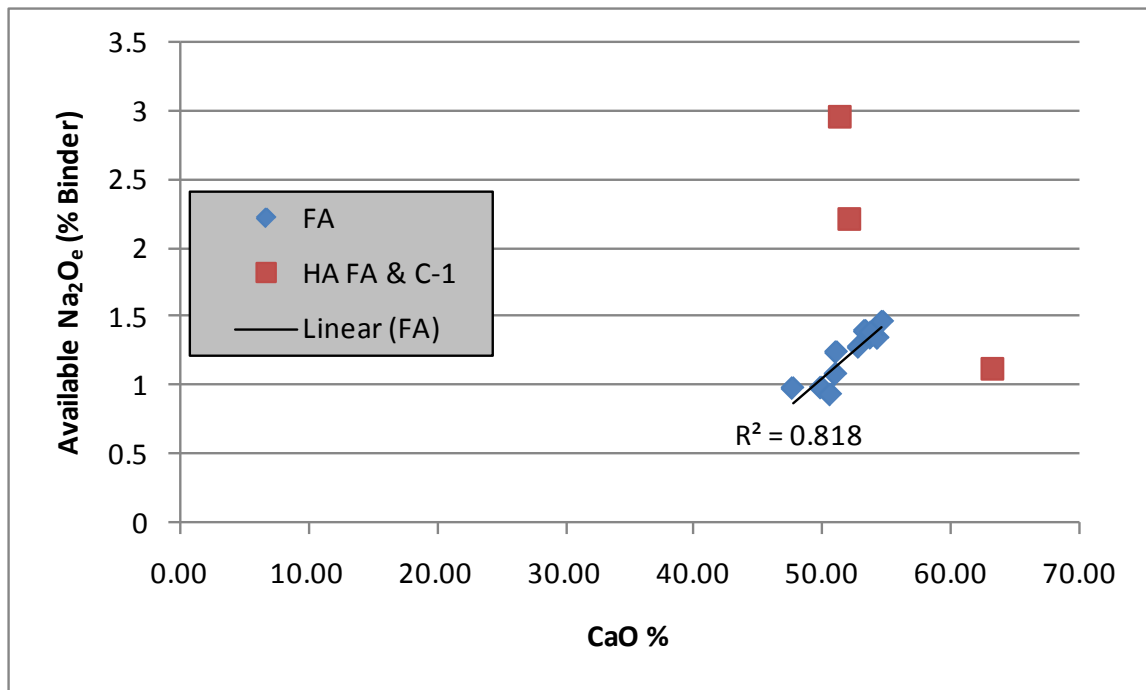


Figure 42: Leaching at 0 M OH<sup>-</sup> (CaO)

When combining the three chemical parameters into the chemical index described before, one can again see a positive correlation. Figure 45 shows that as this chemical index increase so does the amount of available alkalis. This figure is displaying only the results from the paste placed in distilled water.

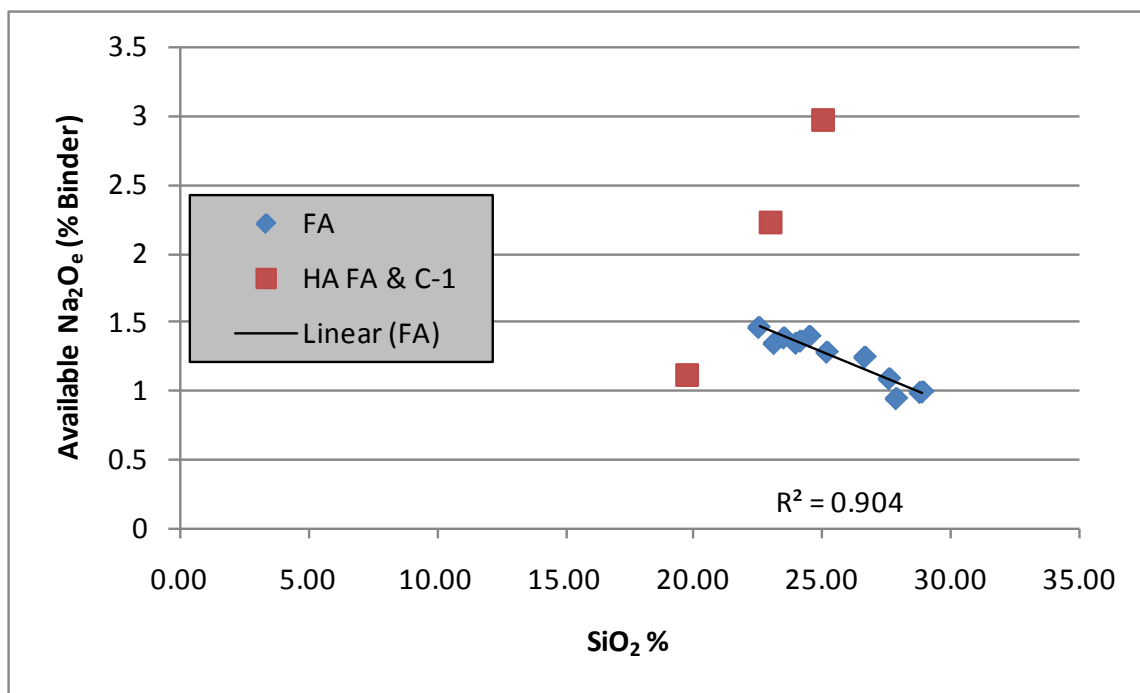


Figure 43: Leaching at 0 M  $\text{OH}^-$  ( $\text{SiO}_2$ )

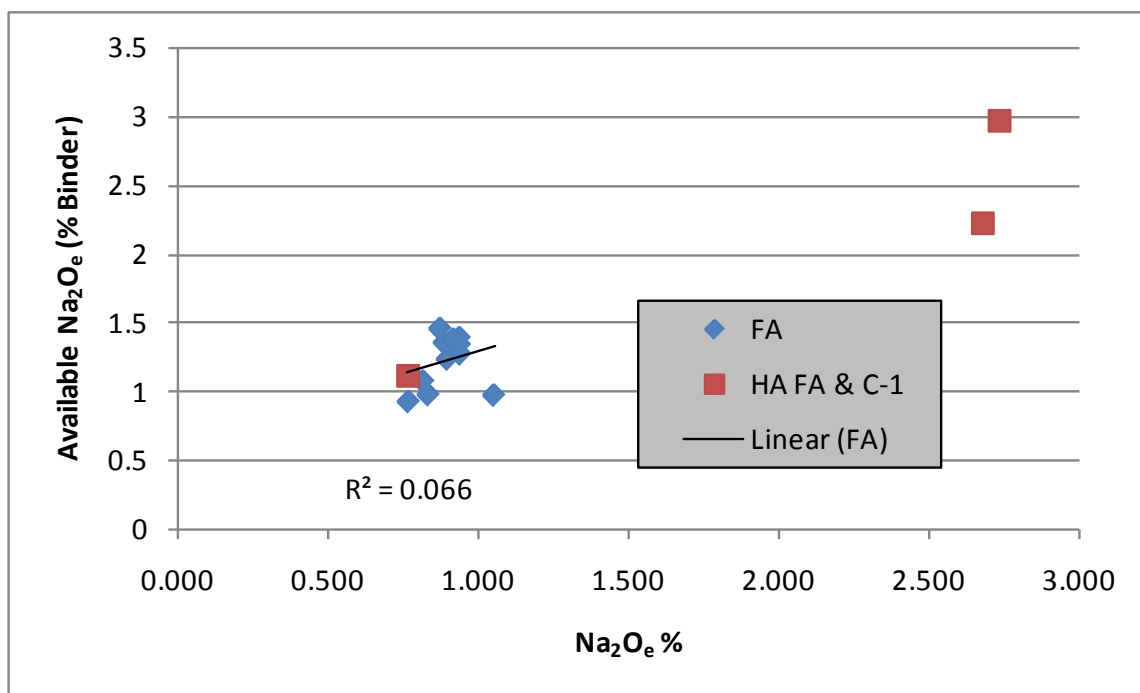


Figure 44: Leaching at 0 M  $\text{OH}^-$  ( $\text{Na}_2\text{O}_e$ )

Figure 45 through Figure 49 show the chemical index being linked to the available alkalis when the paste was place in solutions of different alkalinity. Notice in Figure 45 how the majority of the data set is between 1.5% and 1.0% alkalis except for FA-5 and FA-8. Now, in Figure 46 one can see this same group migrated between roughly 1.5% and 0.5%. This figure is displaying the results for a simulated pore solution of 0.1 M OH-. Figure 47 displays the results of concentrations at 0.2 M OH-. The same thing occurs as the concentration increased. The data set moved the available alkali range of 1.0 to 0%. In this figure one can see a data point in the negative region. This means that the paste did not release any alkalis but it instead absorbed or bound alkalis.

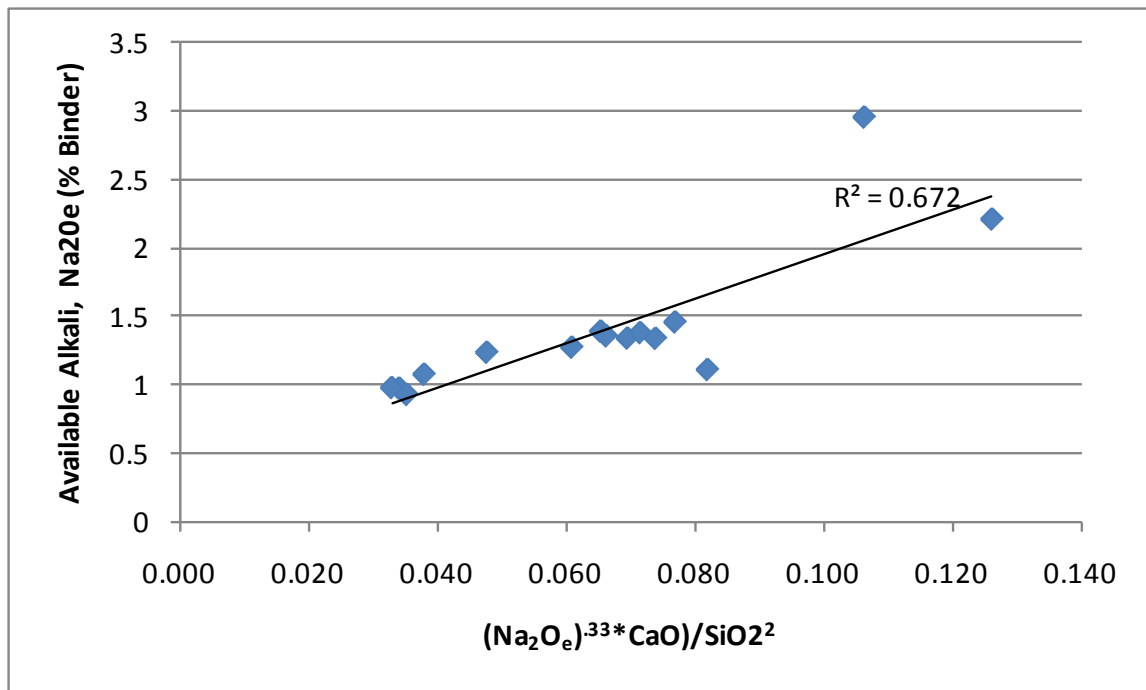


Figure 45: Leaching at 0 M OH- (Chemical Index)

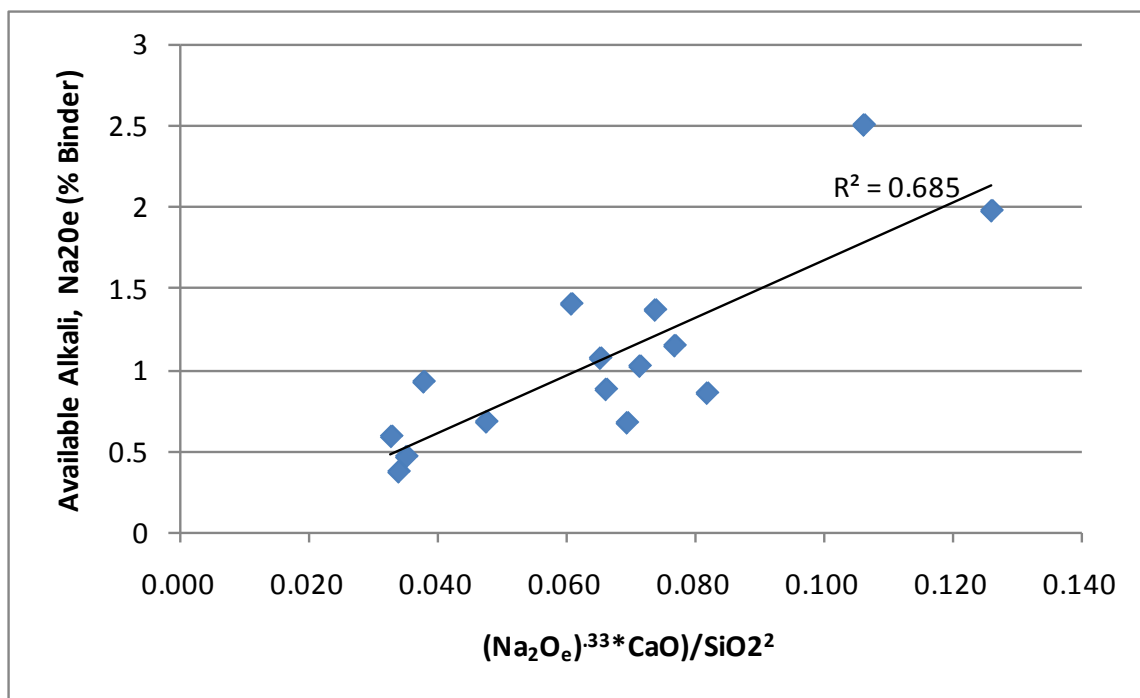


Figure 46: Leaching at 0.1 M OH<sup>-</sup> (Chemical Index)

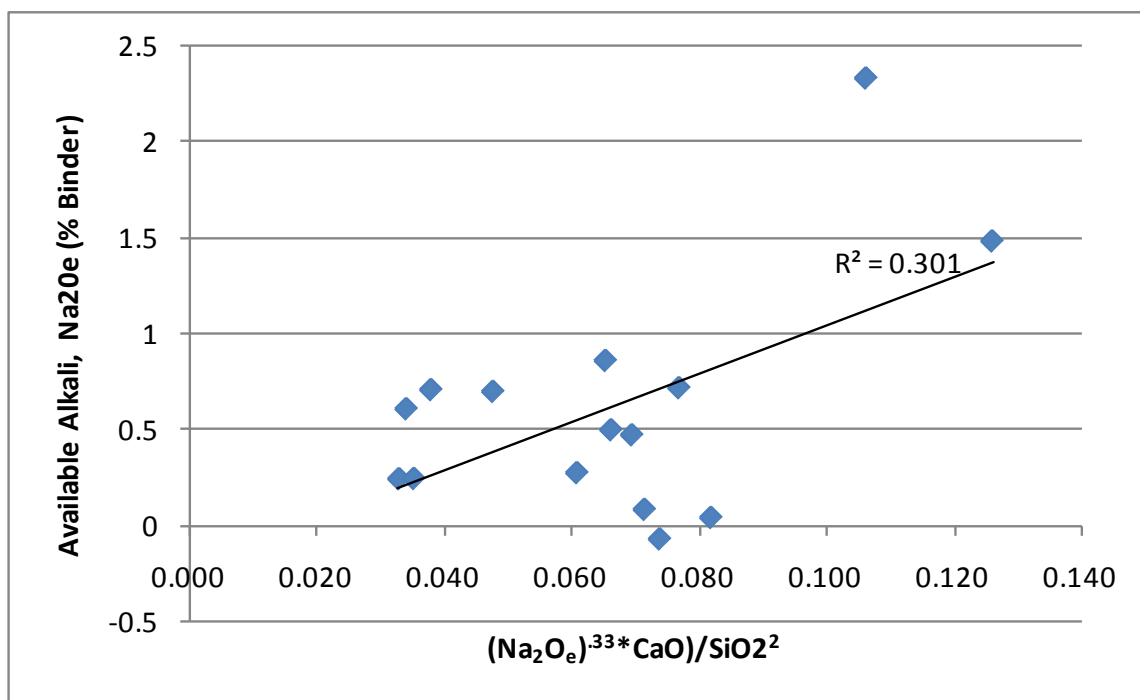


Figure 47: Leaching at 0.2 M OH<sup>-</sup> (Chemical Index)

This trend discontinues in Figure 48 as the concentration is increased to 0.3 M OH<sup>-</sup>. The set of data is spread out linearly between 0.5 and 2.5%. The slope of the trend line is greater it also fits the data set well. In this figure one can make the distinction between the two fly ashes as the upper right group are Class C and the lower left group are Class F. This figure however did not accommodate the results for the high alkali fly ashes as the previous figures did.

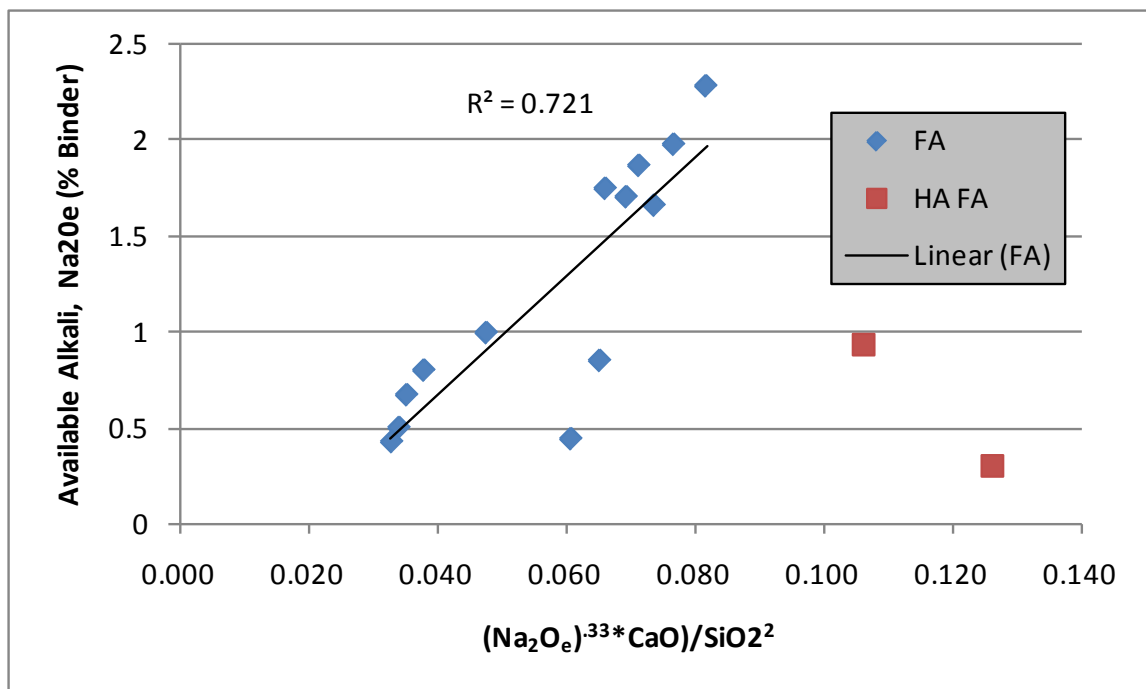


Figure 48: Leaching at 0.3 M OH<sup>-</sup> (Chemical Index)

Figure 49 shows the results for the paste samples placed in 0.6 M OH<sup>-</sup> solutions. The results for this test were completely different from the others. At this concentration the data set displayed a negative correlation as the chemical index increased. Several of the data points are in the negative range meaning the samples absorbed alkalis. This is unusual because the points that absorbed alkalis are the fly ashes with high alkalis.



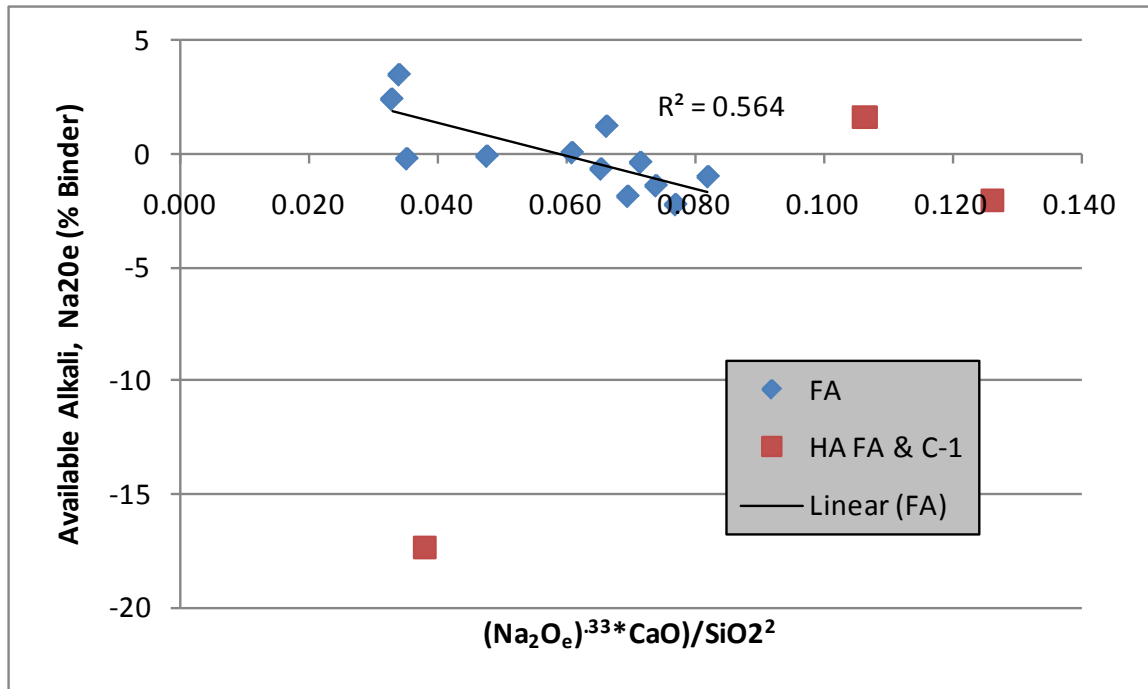


Figure 49: Leaching at 0.6 M OH<sup>-</sup> (Chemical Index)

Figure 50 illustrates the entire data set for this leaching experiment. The plot is congested with the large amount of data but the overall trend can be seen. The majority of the fly ashes follow this trend. The amount of available alkalis decrease as the simulated pore solution concentration goes from 0 to 0.2 M. From 0.2 to 0.3 M there is a significant increase in the available alkalis but it goes down again from 0.3 M to 0.6 M.

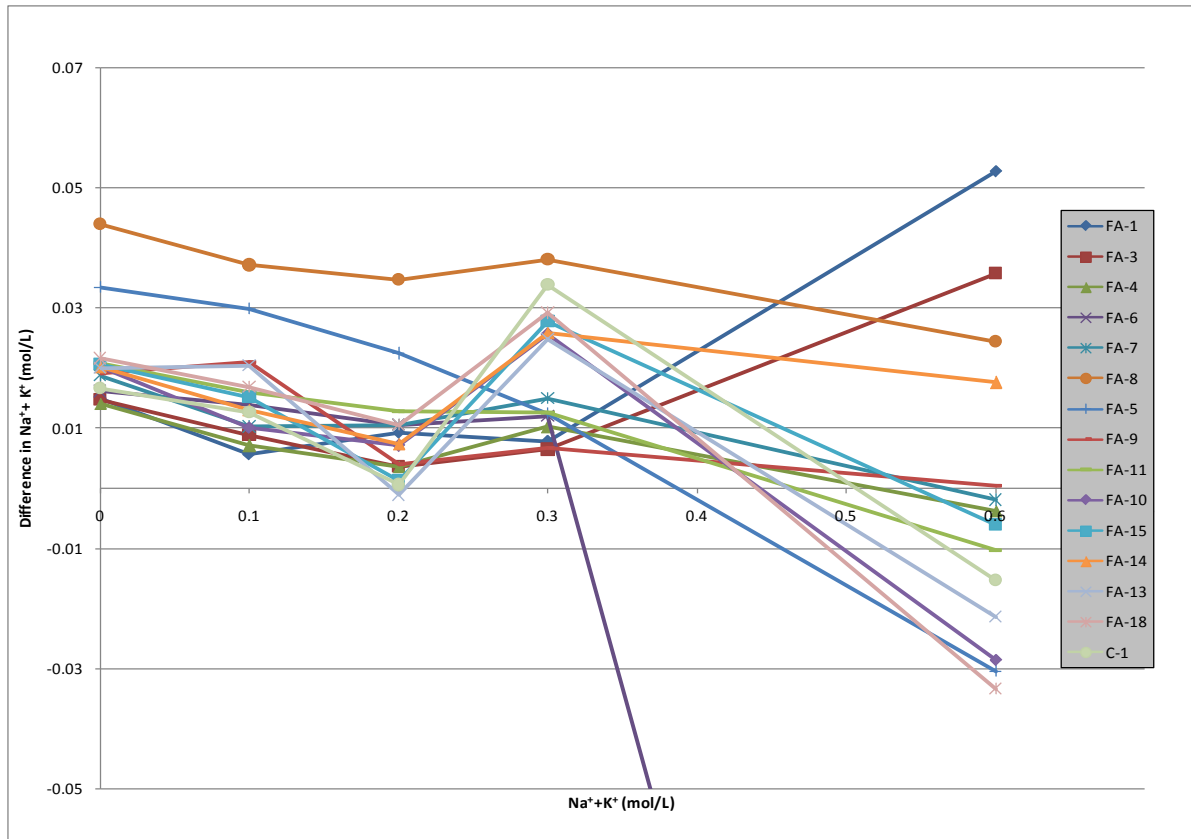


Figure 50: Overall Data Set for Leaching Experiment

### 4.3.3 Available Alkalis

This section discusses the results of the available alkali experiment from ASTM C 311. The procedure is explained in detail in section 3.2.4. The purpose of this experiment is to determine the amount of alkalis that are available from fly ashes for reaction with aggregates. Because some of the fly ash alkalis can be tied up in crystalline phases, this experiment attempts to determine how much are not.

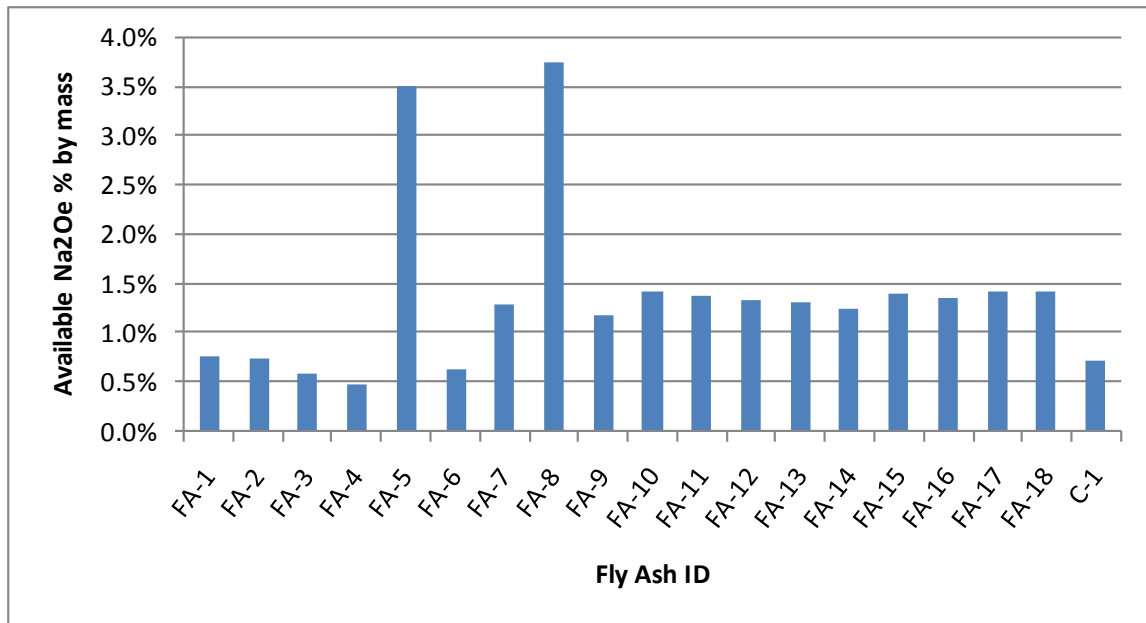


Figure 51: Available Alkalis

Figure 51 shows the results for this experiment performed on all 18 fly ashes. Here one can see the two high alkalis had a large amount of alkalis available. The Class F fly ashes had significantly less alkalis available than the Class C fly ashes. FA-7 had a large amount of its alkalis present especially for a Class F ash but it does have a high amount of CaO relatively speaking. It appears as if the 1.0% available alkalis is a reasonable distinction between Class C and F fly ashes. All Class C fly ashes have above 1.0% available alkalis and Class F fly ashes are below.

Figure 52 through Figure 54 relate the available alkalis to the chemical composition of the fly ash to the amount of available alkalis. Relationships between CaO and available alkalis were not performed because of the addition of hydrated lime to the fly ashes during the experiment.

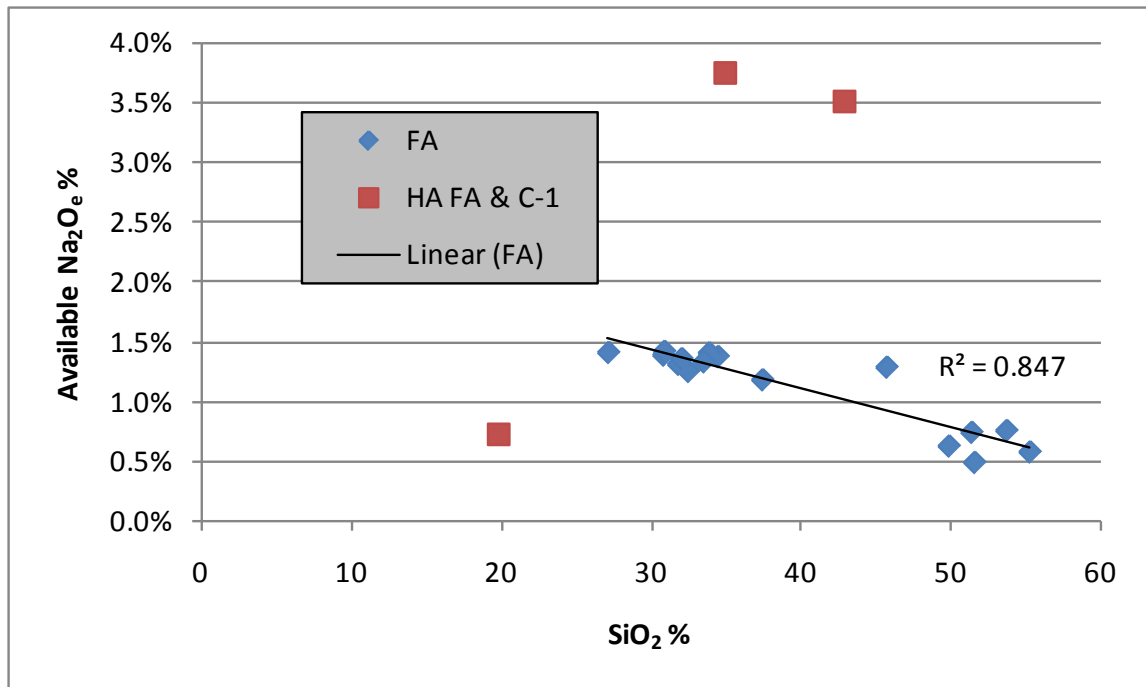


Figure 52: Available Alkalis (SiO<sub>2</sub>)

Figure 52 relates the available alkalis to the SiO<sub>2</sub> content of the fly ash. As SiO<sub>2</sub> increases, the amount of available alkalis decreases. The high alkali fly ashes and cement again did not fit the trend but the rest of the group had a r-squared value of 0.847. Here one can also see the distinction between both classes of fly ash with Class F being cluster on the right and Class C being the group on the left.

Figure 53 shows this relationship with SiO<sub>2</sub> but the y-axis expresses the available alkalis as a percentage of the total alkalis. Now here one can see that some fly ashes showed over a hundred percent of their alkalis being available. This is probably due to some error but what can still be noticed here is that the higher SiO<sub>2</sub> fly ashes had significantly less percentages of their alkalis available.

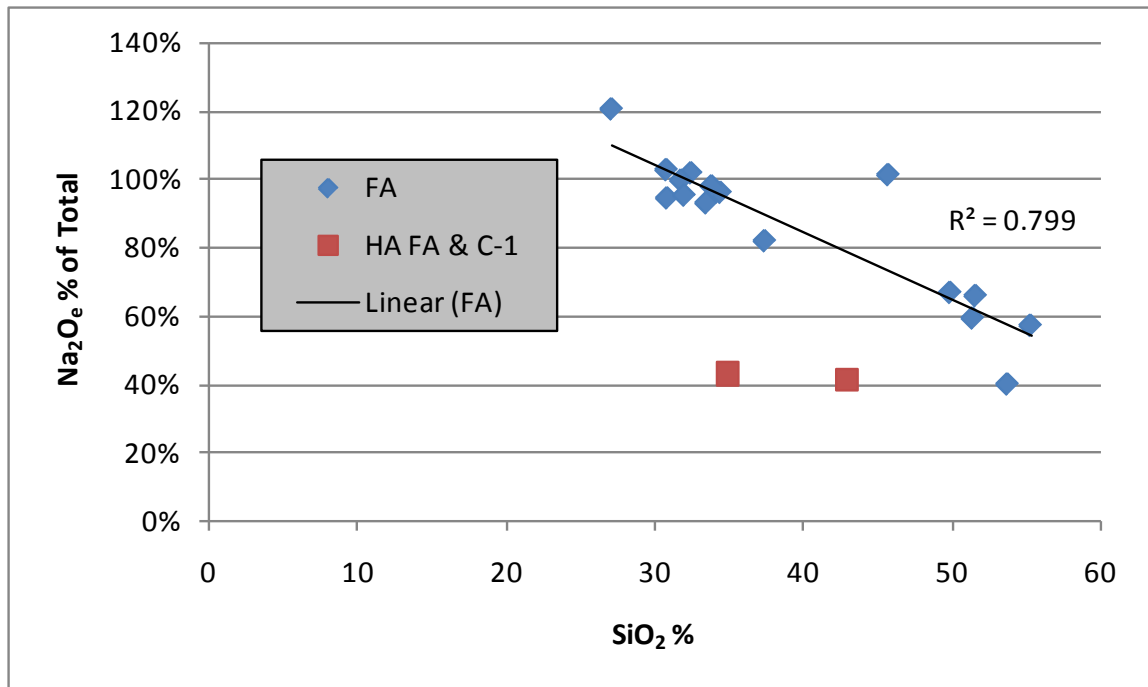


Figure 53: Available Alkalis/Total (SiO<sub>2</sub>)

Figure 54 shows the relationship between available alkalis and alkali contents of the fly ashes. A weak trend can be noticed, as alkali content increase so does the amount of available alkalis for ASR reaction. The high alkali fly ashes followed this trend as well with their large Na<sub>2</sub>O<sub>e</sub> percent resulting in high amounts of available alkalis.

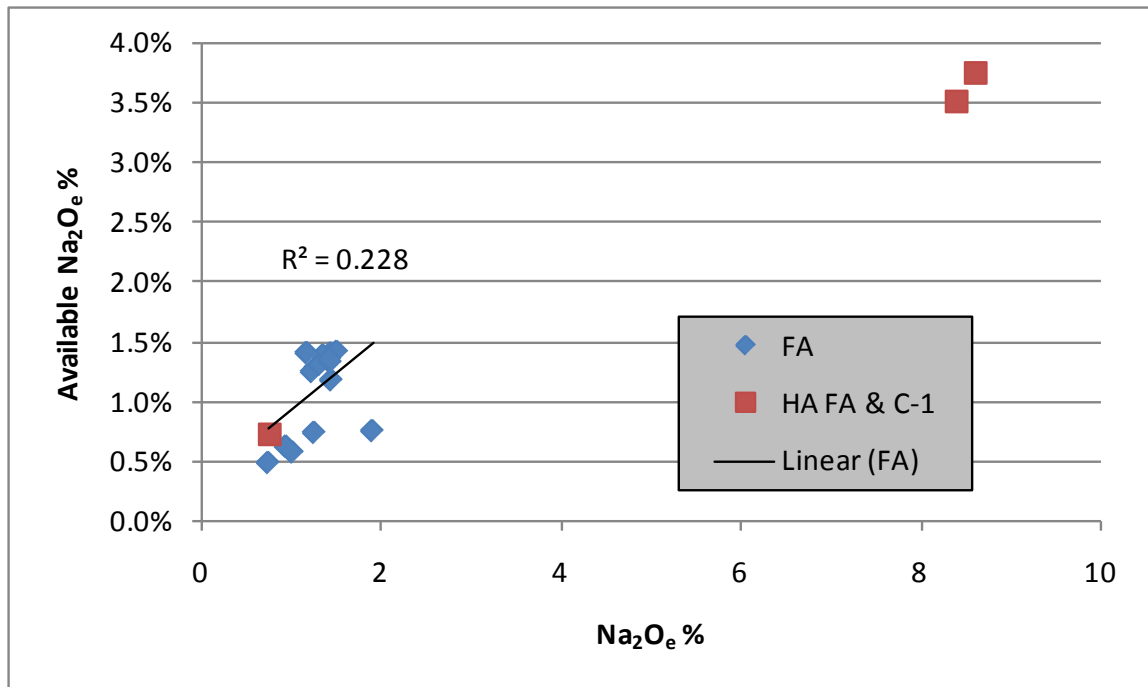


Figure 54: Available Alkalis (Na<sub>2</sub>O<sub>e</sub>)

## Chapter 5: Discussion

The experiments conducted in this project were aimed at generating data that would hopefully by itself, or in combination with other tests, act as a reasonable predictor of the efficacy of a given fly ash to suppress ASR. In this section, some of the key data will be compared with long-term data from previous ASR studies.

The following three figures contain expansion results from ASTM C 1260 & 1293, and outdoor exposure blocks. Figure 55 has 2-year expansion data from ASTM C 1293 concrete prisms with 35% fly ash replacement. The x-axis has the corresponding results from the paste pore solution study with 25% fly ash replacement. There had not been any 1293 testing performed with 25 % fly ash replacement so the data for 35% was used. Despite this fact, there appears to be a linear relationship between the paste pore solution alkali concentration and concrete expansion. As the pore solution increases, the ASR expansion percentage increases. This figure illustrates how the pozzolanic activity of fly ash reduces pore solution alkalis thus reducing ASR induced expansion. Notice the differences between FA-7 and FA-10. This is the fly ash that changed from a Class F to Class C fly ash due to a change in the source of coal used at the power plant. This difference in the chemical composition resulted in these differences on the plot. FA-10 had an increase 0.1 M in the pore solution and this also resulted in an increase of expansion by more than 0.025%. The highest data point on the plot is FA-18. This fly ash had the highest calcium content, the highest pore solution concentration, and this highest concrete expansion.

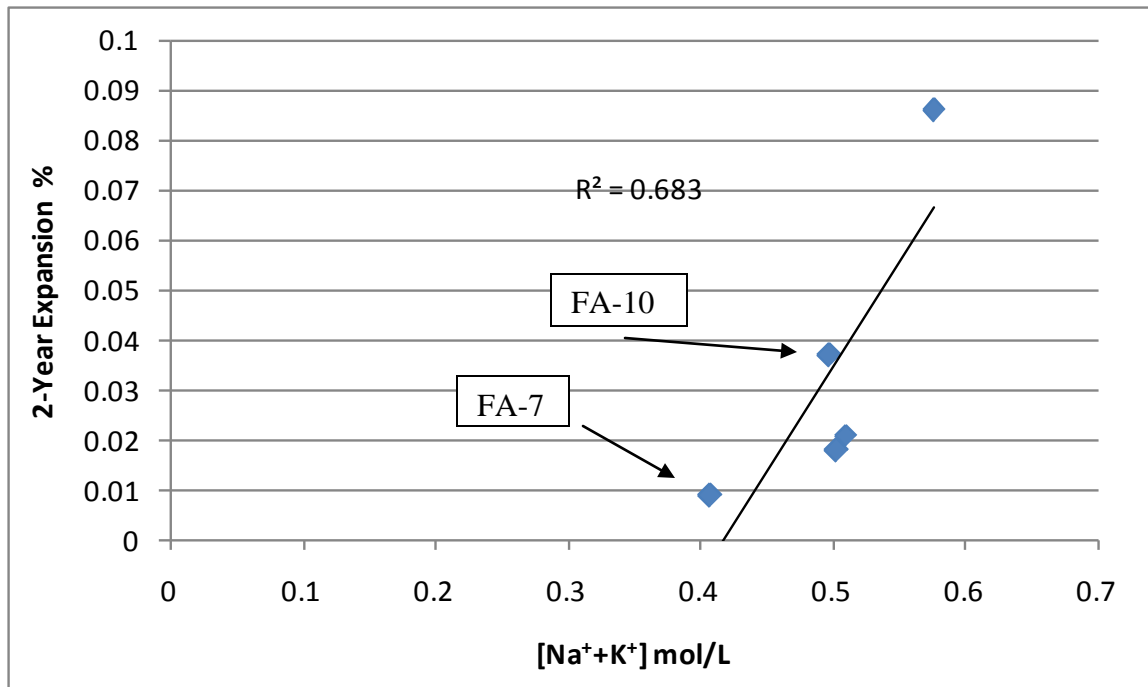


Figure 55: ASTM C 1293 35% Fly Ash Expansion with Pore Solution Study

Figure 56 illustrates similar relationships but with ASTM 1260 results with 30% fly ash replacement. There is a linear relationship between the paste pore solution and mortar expansion. As the pore solution increases, so does the expansion of the mortar bar. The lowest data point is FA-3 and the highest point is FA-11. The points in between also have calcium contents that are in between FA-3 & 11. There are significant differences in pore solution concentrations and expansion.



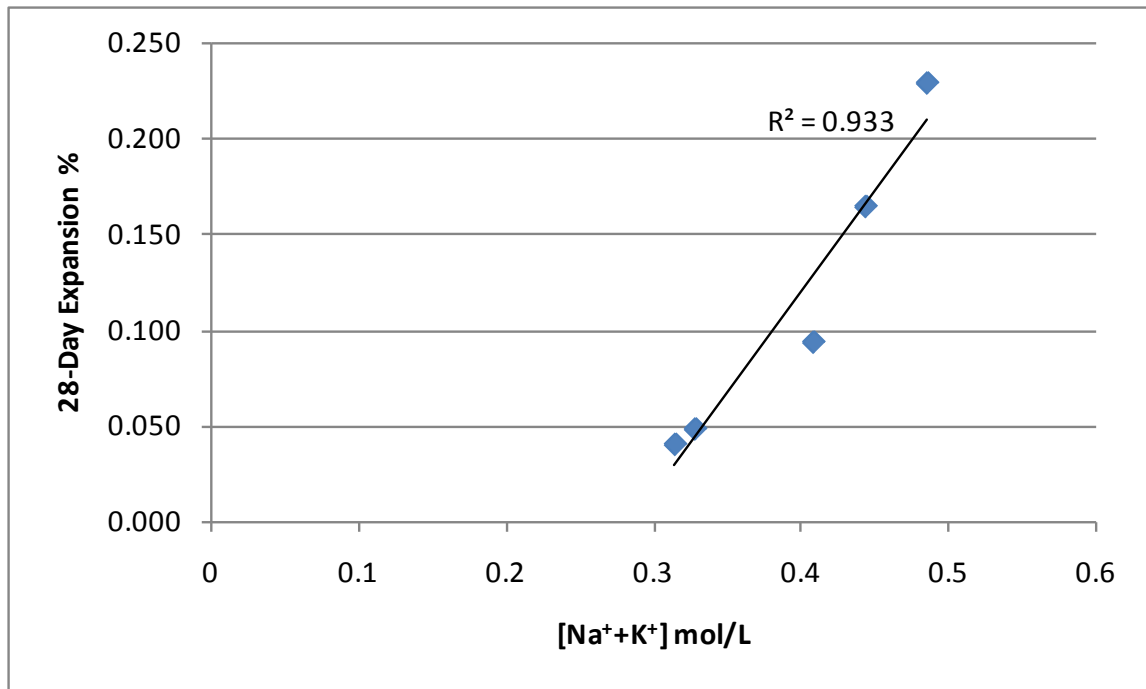


Figure 56: ASTM C 1260 Expansion with Pore Solution Study

Figure 57 illustrates between the chemical index and the outdoor exposure block expansion. This figure has four different sets of plots because of the differences of age and aggregate type. This set of data consists of three different aggregates but aggregate WR has two sets because they are of different ages. This set of data consists of several different fly ashes used at different replacement levels. The chemical index corresponds greatly with the expansion data. This index creates a great trend but it is high dependent on the aggregate used and age of the specimen. Notice the high r-squared value of aggregate WR. This fine aggregate has an almost perfect relationship between the data points and the trend line. The other aggregates showed similar trends but not nearly as strong. The points that are on the far right of each set are the control mixes. These mixes have no fly ash in them and have large differences in chemical index and expansion data. For example, the red squares represent FA-13 at 30, 35, and 40% replacement and its

control mix. Notice the large difference between 30% replacement and its control mix. The difference is large even with the use of a high calcium fly ash. The PL mixes had Class F fly ashes used and notice how almost the entire located on the bottom left corner of the chart. The only data point on the right side is the control. These mixes have replacement levels between 20 and 30% while the Class C mixes had higher replacement levels and did not perform as well. Lower replacement levels of Class F fly ash outperformed the higher replacement levels of Class C mixes.

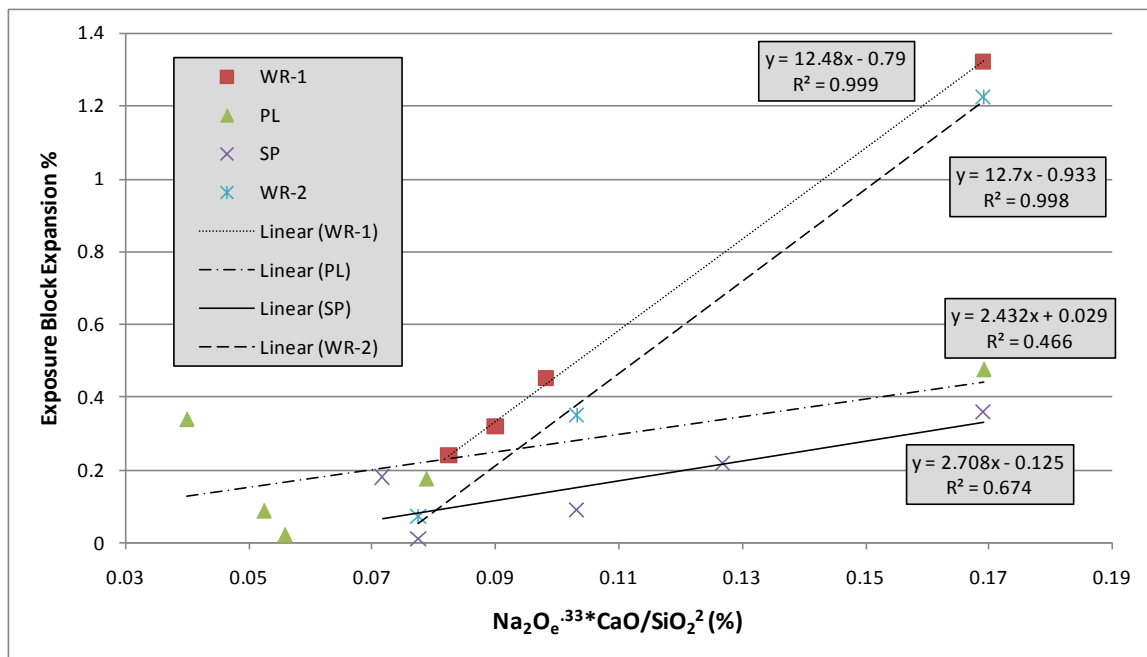


Figure 57: Exposure Block Data with Chemical Index

Figure 59 is the same as the figure in the pore solution section but illustrates the difference between FA-7 and FA-10. Recently this fly ash underwent a change in its chemical composition. The chemical compositions for these two fly ashes are located in Table 9. This change from Class F to Class C resulted in an increase of the paste pore solution concentration from 0.40 to 0.50 with a 25% replacement level. The chemical

index relates the change in chemical composition to the change in pore solution alkali content. The alkali content did not change very much but the CaO and SiO<sub>2</sub> did and this result in the fly ash not being as effective in lowering pore solution alkalis.

Table 9: Chemical Composition of FA-7 & 10

--	--

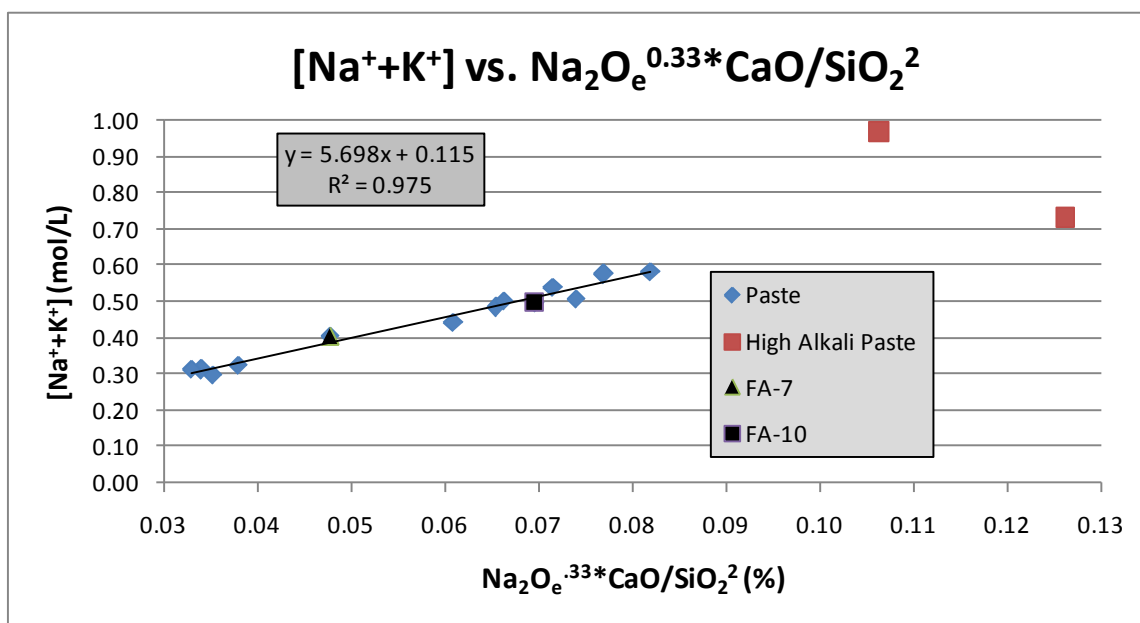


Figure 58: Pore Solution Study with Chemical Composition Change of Fly Ash

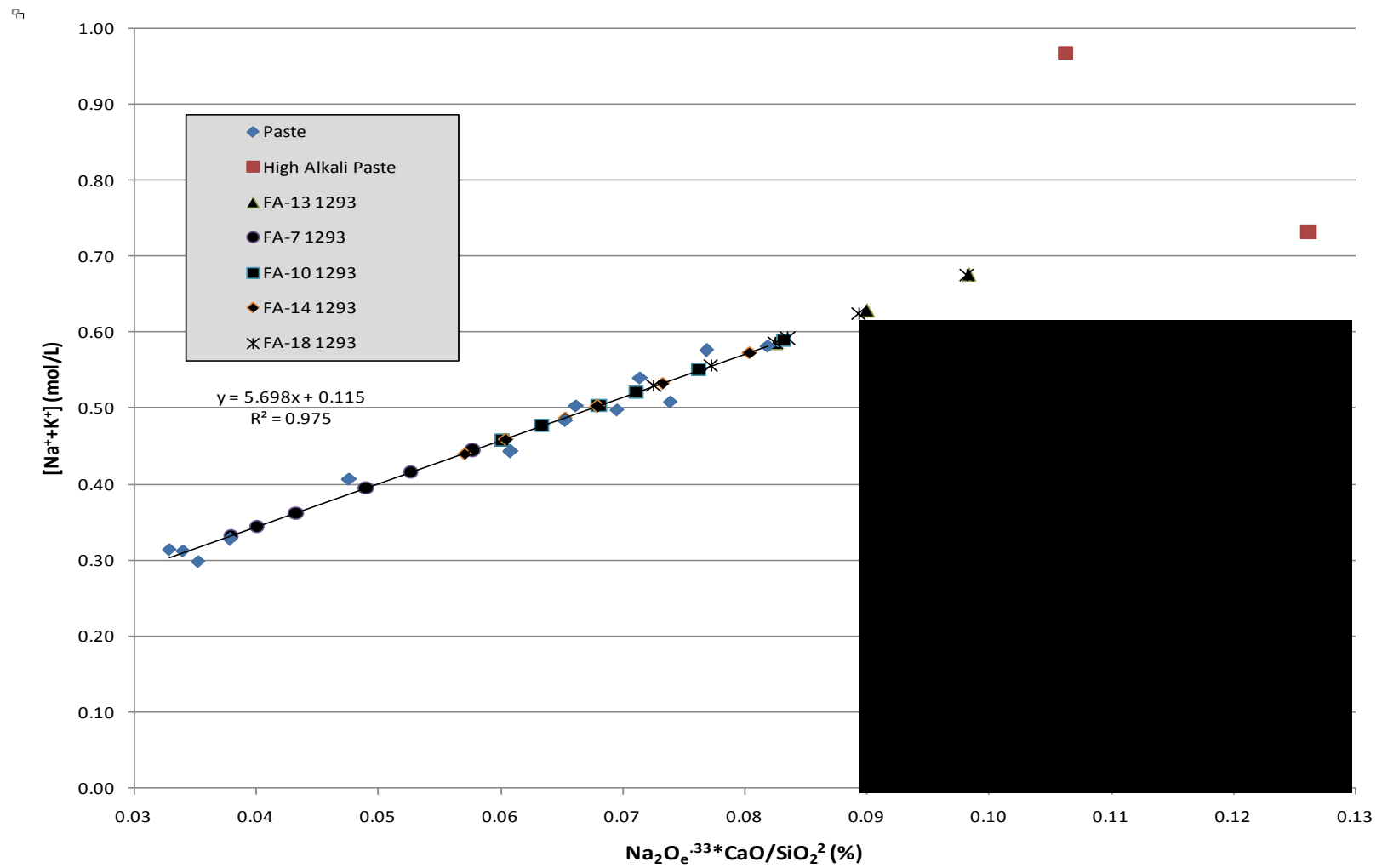


Figure 59: Comparison of ASTM C 1293 Pore Solution

The chemical index will not work completely in predicting pore solution alkali concentration because the pore solution is dependent on many parameters other than the chemical composition of the binder. Aggregates and fineness of the fly ash can also effect pore solution concentrations. The chemical index can however be used to roughly estimate what the pore solution can be. The equation from the trend line from the pore solution data using the chemical index was used on ASTM C 1293 specimens. Figure 59 used the equation  $y = 5.698x + 0.115$  to estimate the pore solution concentration of concrete prisms with four different fly ashes with different alkali dosages. This plot shows how the Class F fly ash is predicted to have a lower pore solution than the Class C fly ashes according to the chemical index.

## Chapter 6: Conclusion

### 6.1 SUMMARY

Fly ash is used very often in concrete because of its many technical benefits including improved ASR resistance. Some fly ashes provide better resistance to ASR than others. There are several factors, including the mineralogical, chemical, and physical composition of the fly ash that plays a role in the effectiveness of fly ash to controlling ASR. This project aimed at the characterization of fly ash while relating these findings to fresh, hardened, and durability properties of concrete with respect to ASR.

### 6.2 CONCLUSIONS

For the materials and testing investigated during this research, the following conclusions are drawn:

- From the data collected from the laser diffraction testing, it was shown that finer fly ashes performed better than coarser fly ashes. Fly ashes with similar chemical compositions but smaller particle sizes showed lower percentage ASR expansion.
- The acid-soluble results did not correspond with the actual total alkalis in the fly ash but did show other trends. Class F fly ashes showed lower percentages of acid-soluble alkalis when compared to Class C fly ashes despite the fact that some Class F fly ashes had the same or larger percentages of alkalis present. Also, the chemical index,  $[(\text{Na}_2\text{O}_e)^{0.33} \times \text{CaO}] / \text{SiO}_2^2$  relates the chemical composition to the acid-soluble alkalis; as the chemical index increases the amount of acid-soluble alkalis increase as well.
- ASTM C 1260 data showed how low CaO fly ashes performed better than fly ashes with high CaO and alkali contents. Also, the performances improved as fly

ash replacement levels increased. This was true for all fly ashes except the high alkali ashes. The chemical index also related the chemical composition of the mortar binder to the 14-day expansion results.

- Pore solution studies demonstrated that Class F fly ashes removed alkalis from the paste pore solution. These fly ashes had lower pore solutions concentrations than what a paste mix with an inert diluent used instead of fly ash. The hydration products of Class F fly ashes bind alkalis preventing from reaction. Class C fly ashes provided more alkalis to the system instead of binding them. Furthermore, the chemical index related the chemical composition of the paste binder to pore solution concentrations.
- The leaching experiment showed how available alkalis increase as the simulated pore solution  $\text{OH}^-$  concentration increased up to a certain point. Higher CaO fly ashes had more available alkalis according to this study. The trend with chemical index was also followed with this data. As the chemical index of the paste binder increased so did the percent of available alkalis. The trend was followed by all mixes including the control except for the two high alkali fly ashes.
- The available alkalis test illustrated that Class C fly ashes have a greater percentage of their alkalis available. Also, the majority of fly ashes with percentages great than 1.0% available alkalis were Class C fly ashes. This 1.0% appeared to be a distinction between Class C and F fly ashes.
- When relating the pore solution data to ASTM C 1293 expansion data, it was shown that as pore solution alkalinity increased so did the percent expansion. This was also the case for the ASTM C 1260 testing.

- Data collected from outdoor exposure block demonstrated that its expansion can be related to the chemical index. The trends created depend greatly on the source of reactive aggregate used.
- The testing conducted during this project showed that pore solution alkalis and ASR are greatly related to chemical composition of the fly ash and the binder of the mix. The CaO, SiO<sub>2</sub>, and the Na<sub>2</sub>O<sub>e</sub> percentages of the fly ashes all contribute to its ASR resistance. It appears the chemical index  $[(Na_2O_e)^{0.33} \times CaO] / SiO_2^2$  can create good quality trends with the data from several of the testing conducted during this project.

### **6.3 RECOMMENDATIONS FOR FURTHER STUDY**

The following work is recommended to further increase the knowledge on fly ash behavior in ASR resistance:

- Use more fly ashes with high alkali content especially with low and high CaO content. This would create a large data base with more variety. It would be interesting to see how low CaO fly ashes with high alkali contents would perform in ASR.
- Create ASTM C 1293 concrete prisms with 25% replacement levels to run pore solution extraction with and compare leaching results.
- Create exposure outdoor exposure blocks with 25% replacement levels to run pore solution extraction and compare leaching results.
- Perform ASTM C 1260 on the entire set of fly ashes with a variety of replacement levels to gain better knowledge in the how performance differs with fly ash and dosages.



- Create more paste samples with a variety of replacement levels to determine how the pore solution concentration is effected with fly ash dosage.
- Run the leaching experiment with intermediate simulated pore solutions between 0.20 M and 0.30 M to further understand the increase of available alkalis in this range. Also, samples should be created to run at 0.40 M and 0.50 M.
- Investigate the hydration products of the fly ash paste samples with SEM to determine if changes in the hydration composition is related to the fly ash composition. This will investigate whether the pore solution alkalinity can be explained with the amount of alkalis bound by the hydration products.

## Appendix A: ASTM C 1260 Testing Results

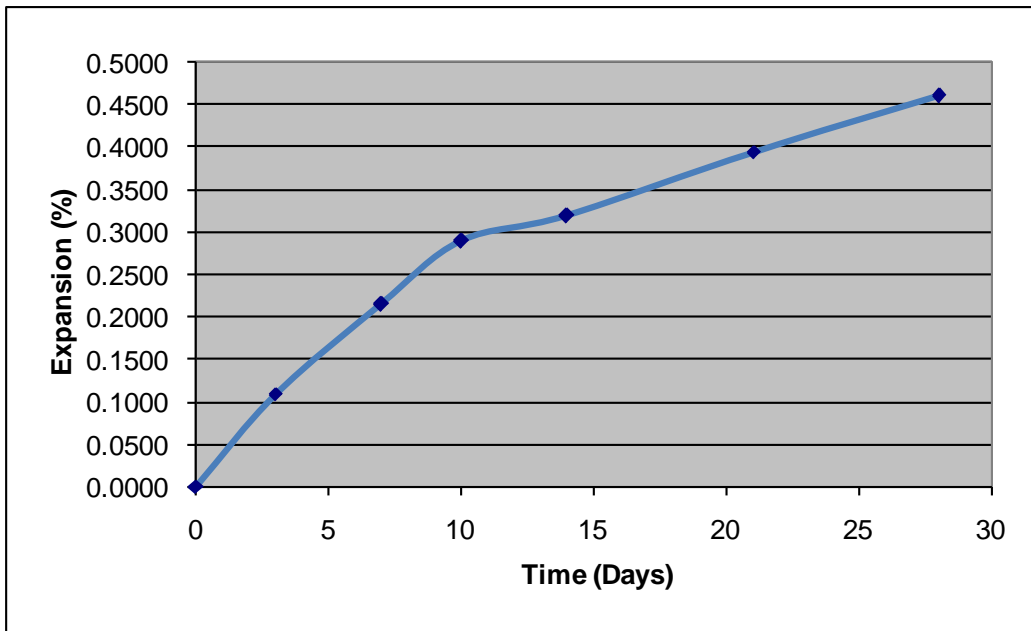


Figure A - 1: C-1 (Control)

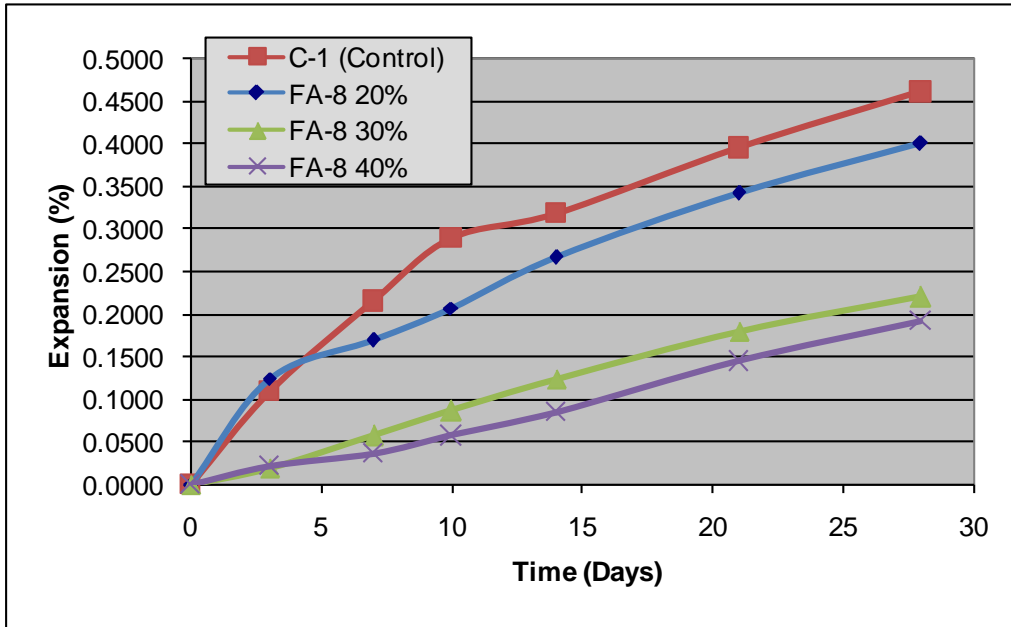


Figure A - 2: FA-8 (1)

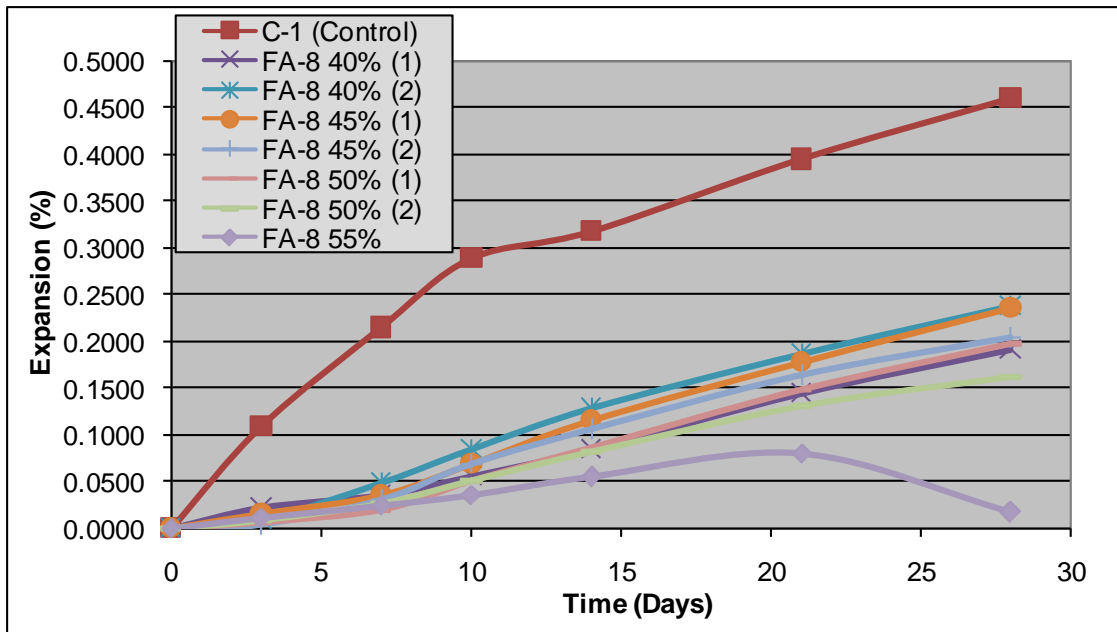


Figure A - 3: FA-8 (2)

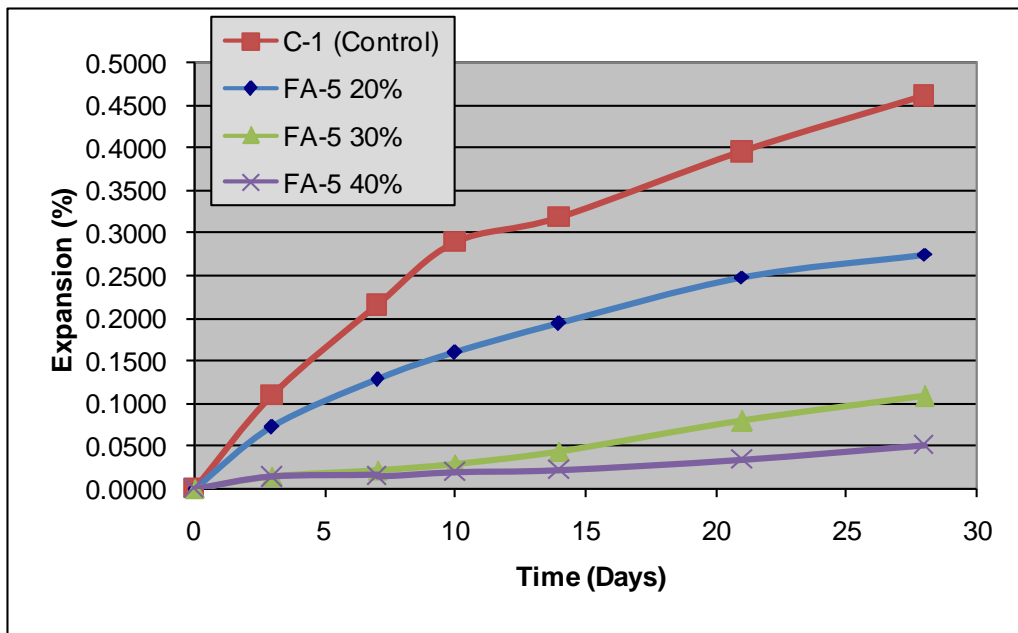


Figure A - 4: FA-5

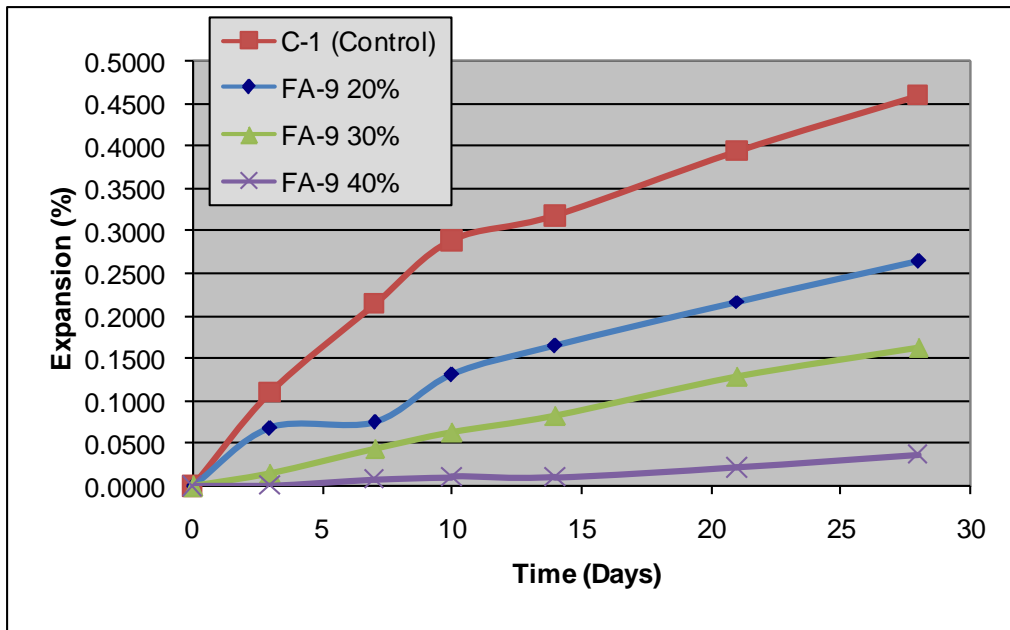


Figure A - 5: FA-9

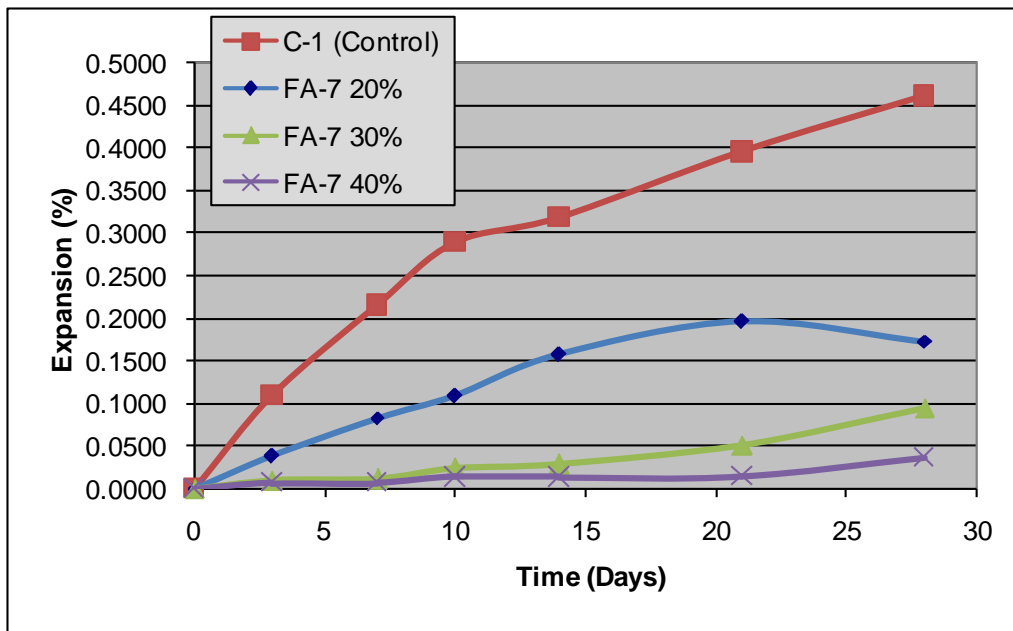


Figure A - 6: FA-7

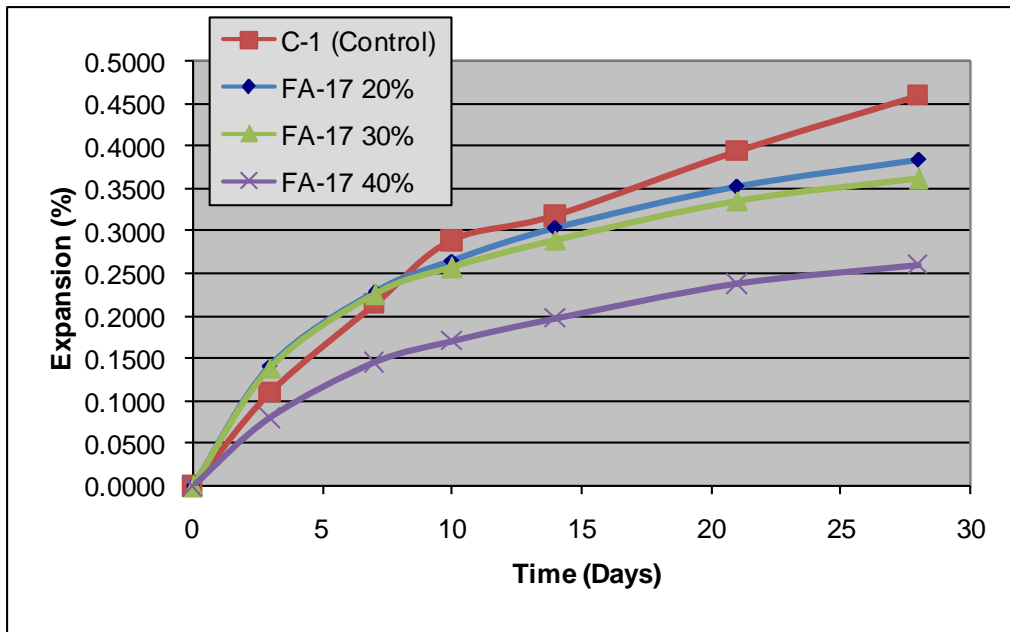


Figure A - 7: FA-17

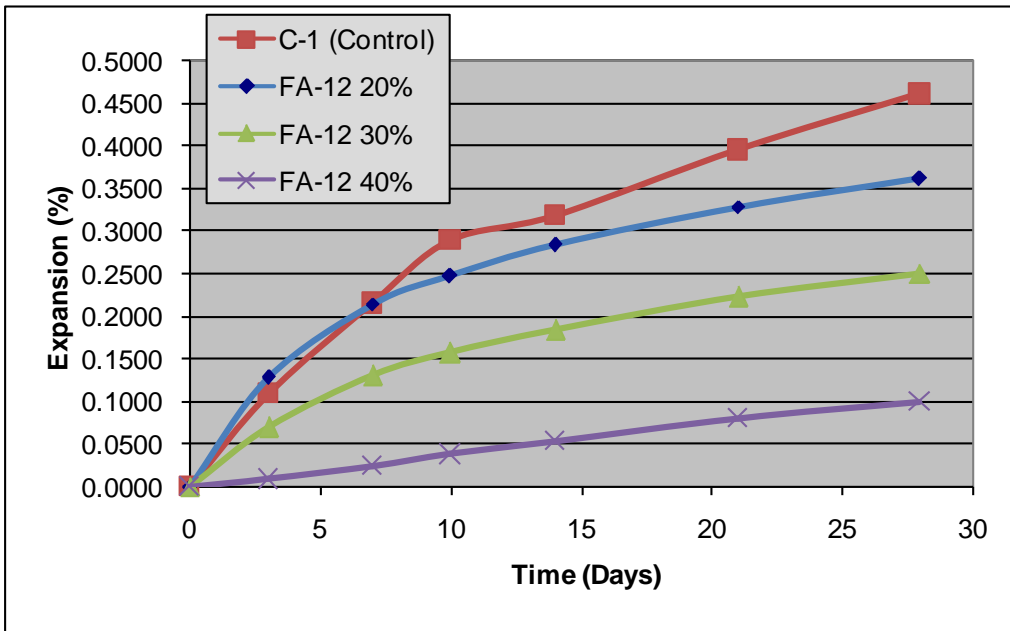


Figure A - 8: FA-12

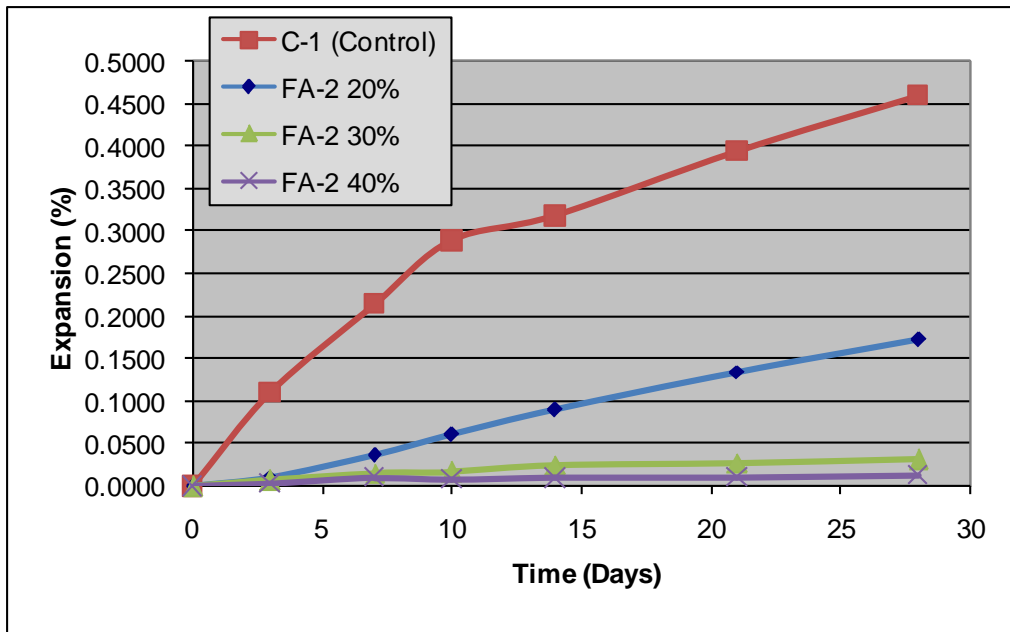


Figure A - 9: FA-2

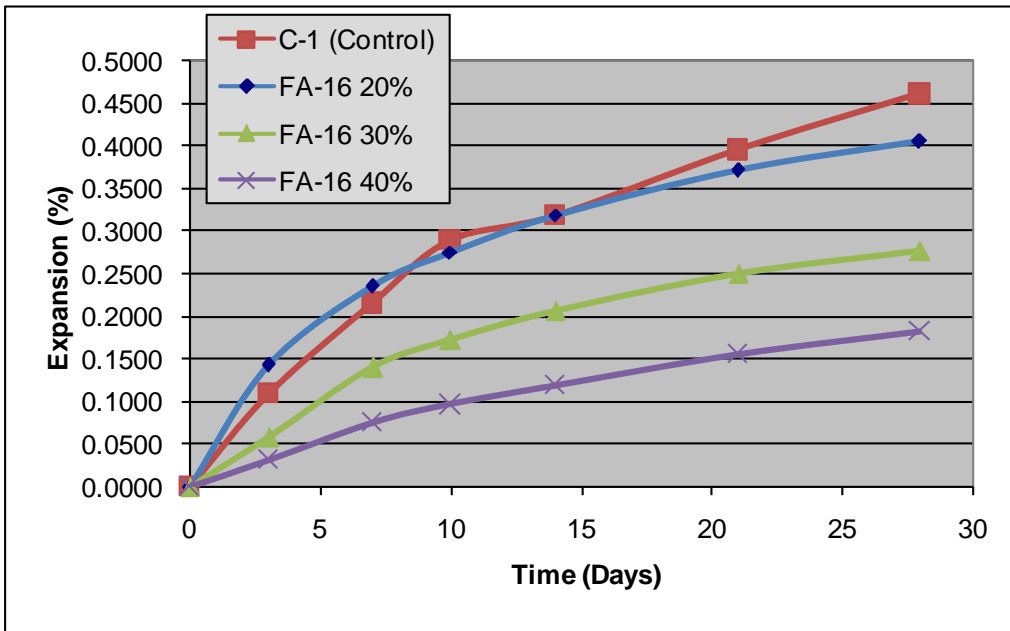


Figure A - 10: FA-16

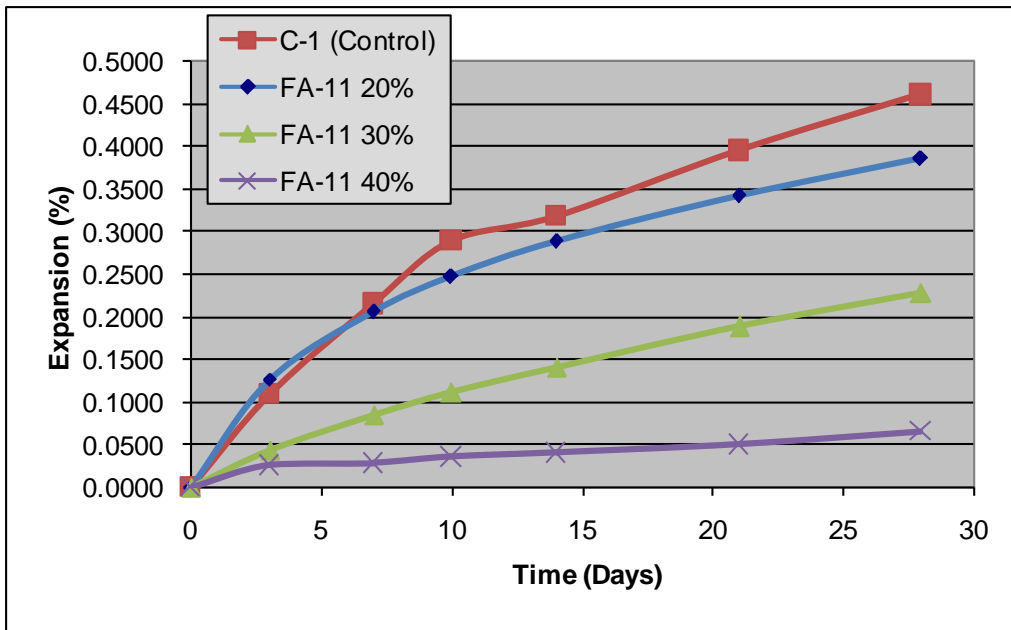


Figure A - 11: FA-11

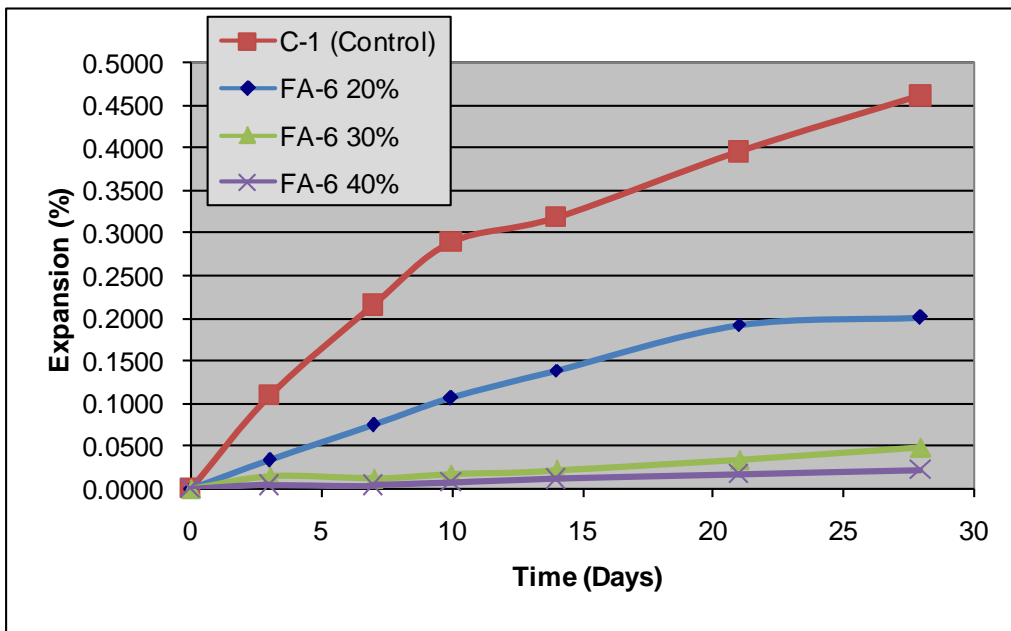


Figure A - 12: FA-6

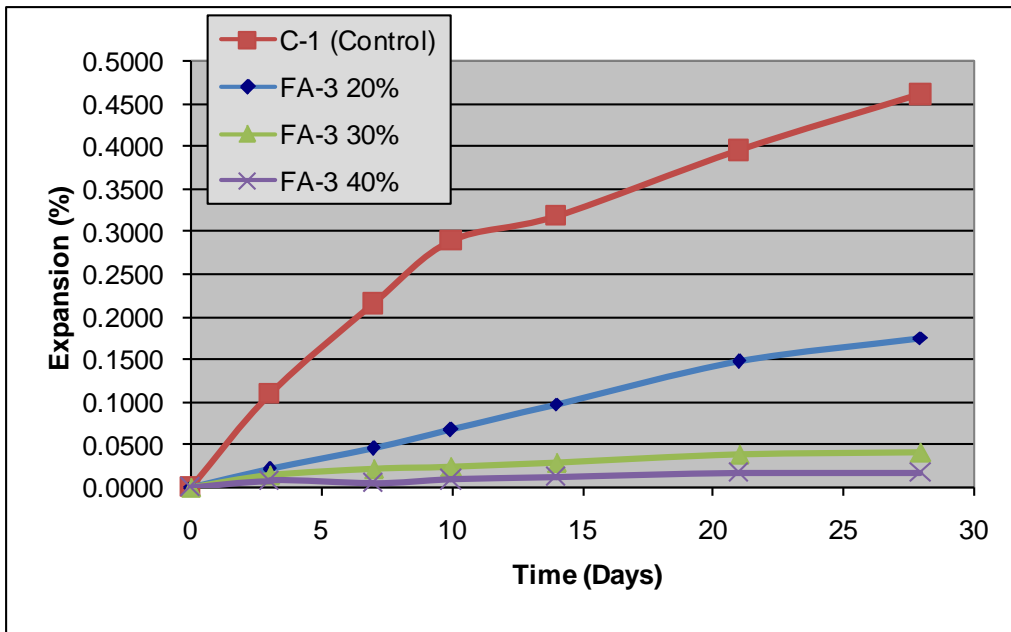


Figure A - 13: FA-3

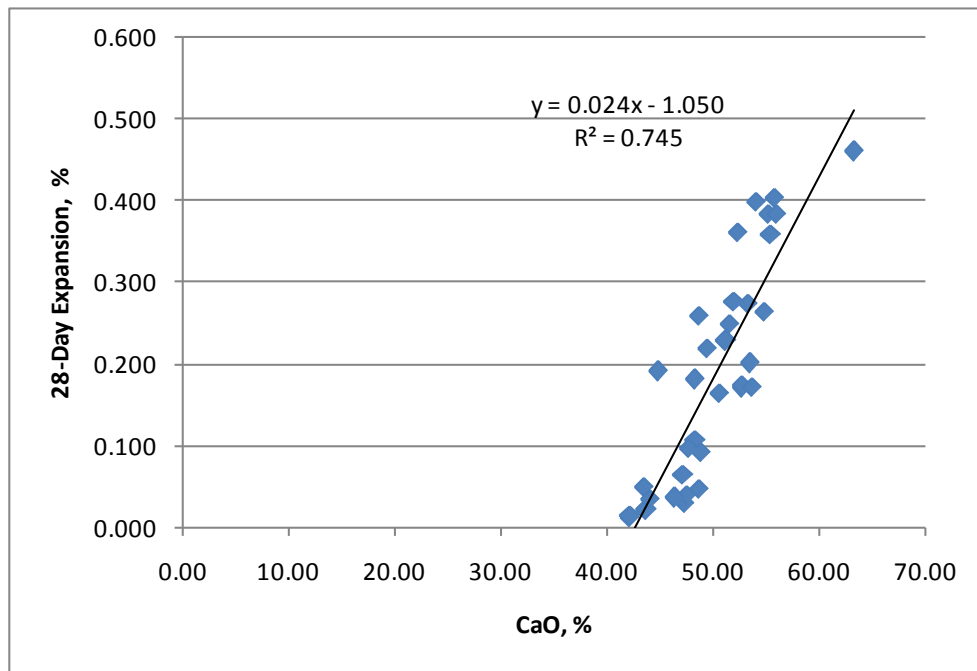


Figure A - 14: ASTM C 1260 28 Day (CaO)



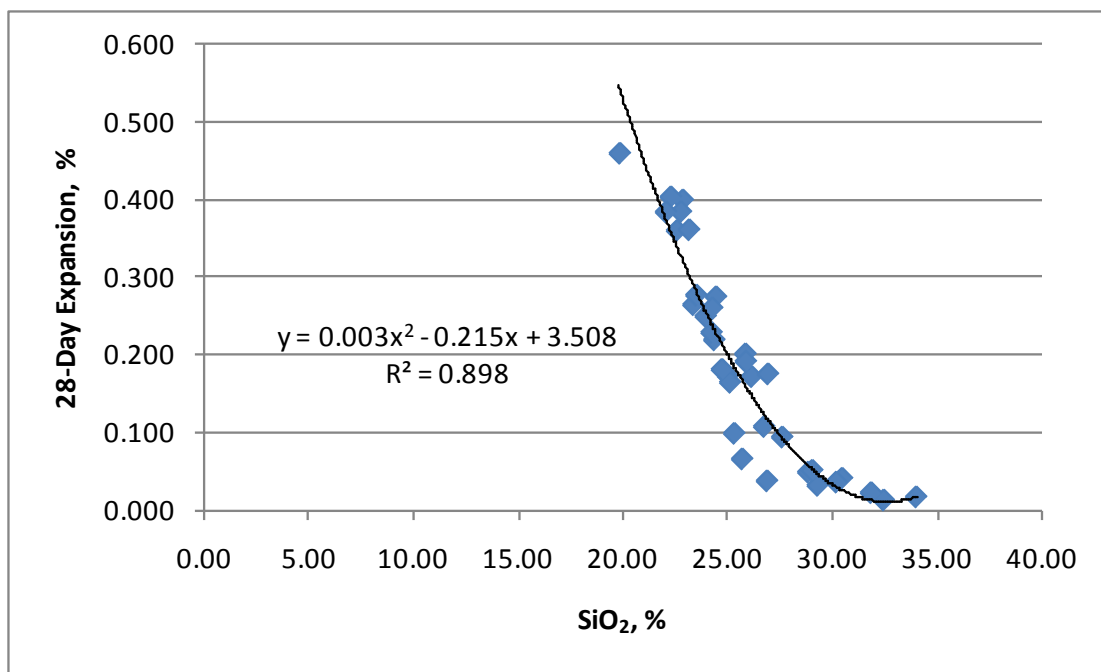


Figure A - 15: ASTM C 1260 28 Day (SiO<sub>2</sub>)

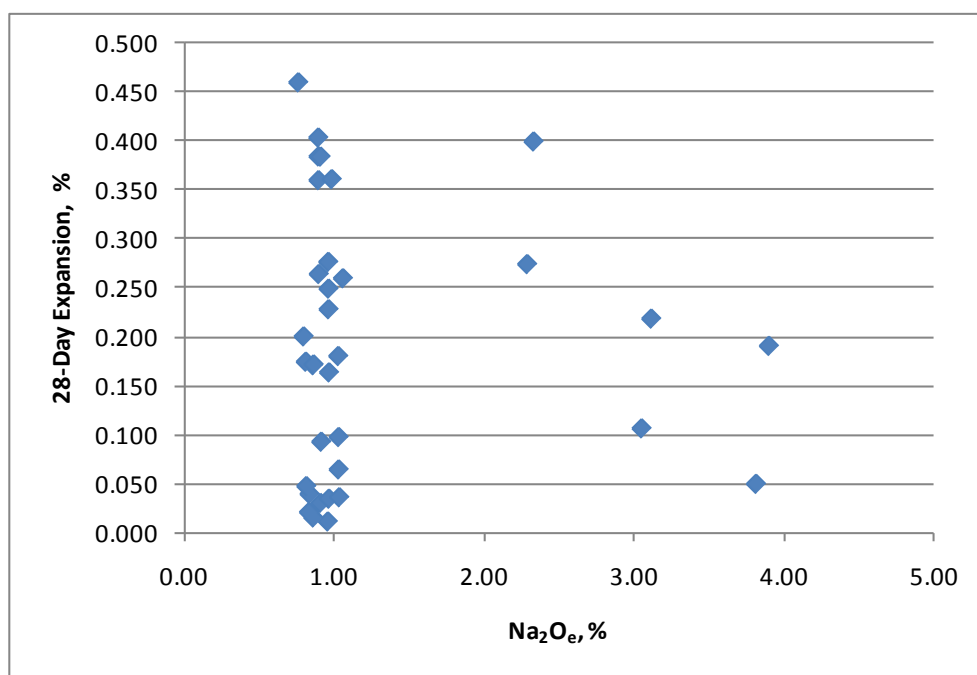


Figure A - 16: ASTM C 1260 28 Day (Na<sub>2</sub>O<sub>e</sub>)

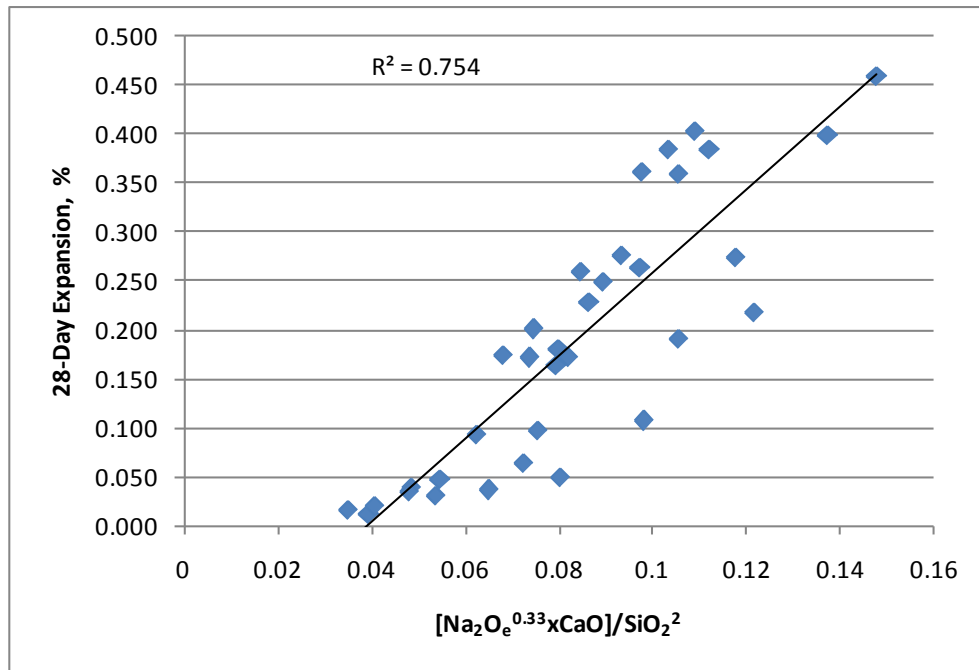


Figure A - 17: ASTM C 1260 28 Day Chemical Index

## Appendix B: XRF Trends

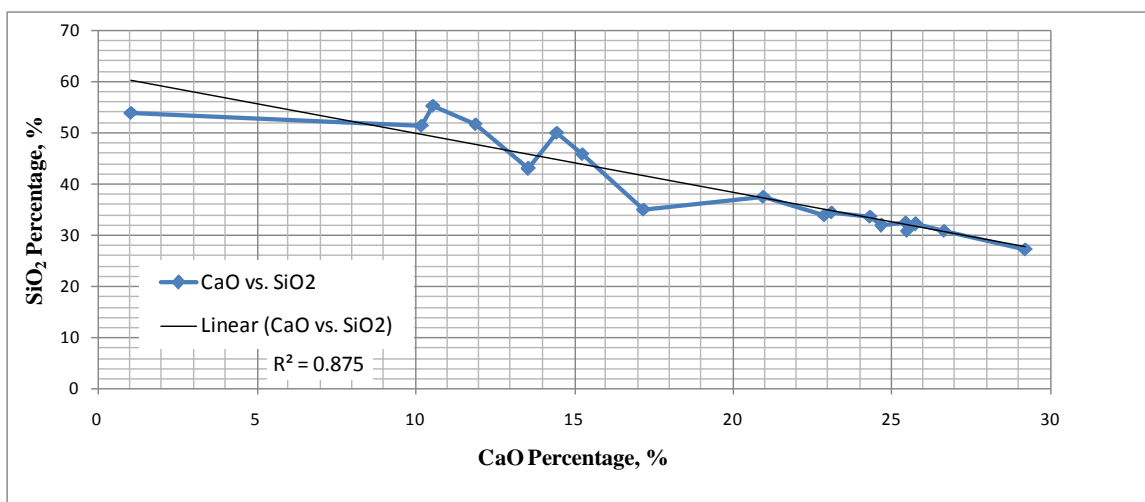


Figure B - 1: CaO vs. SiO<sub>2</sub>

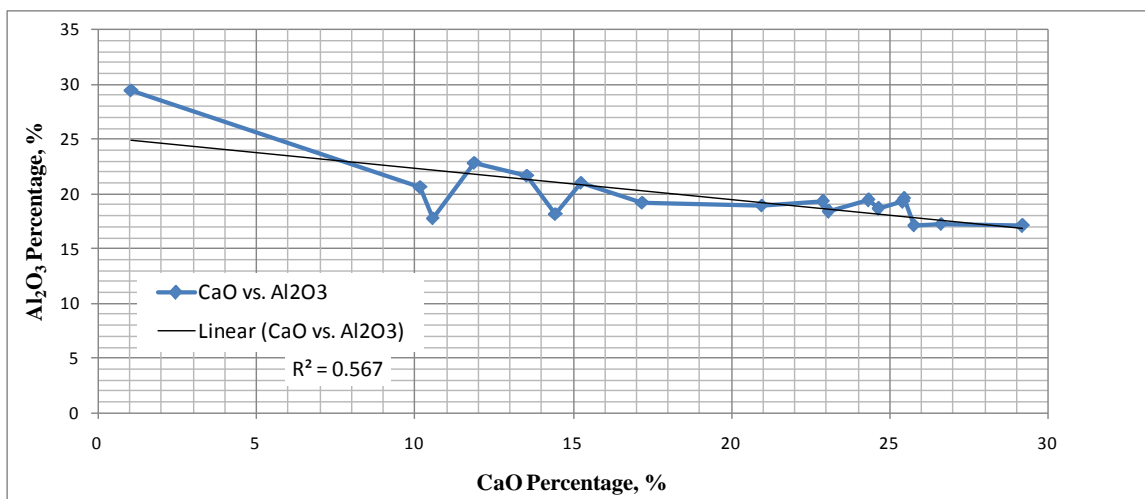


Figure B - 2: CaO vs. Al<sub>2</sub>O<sub>3</sub>

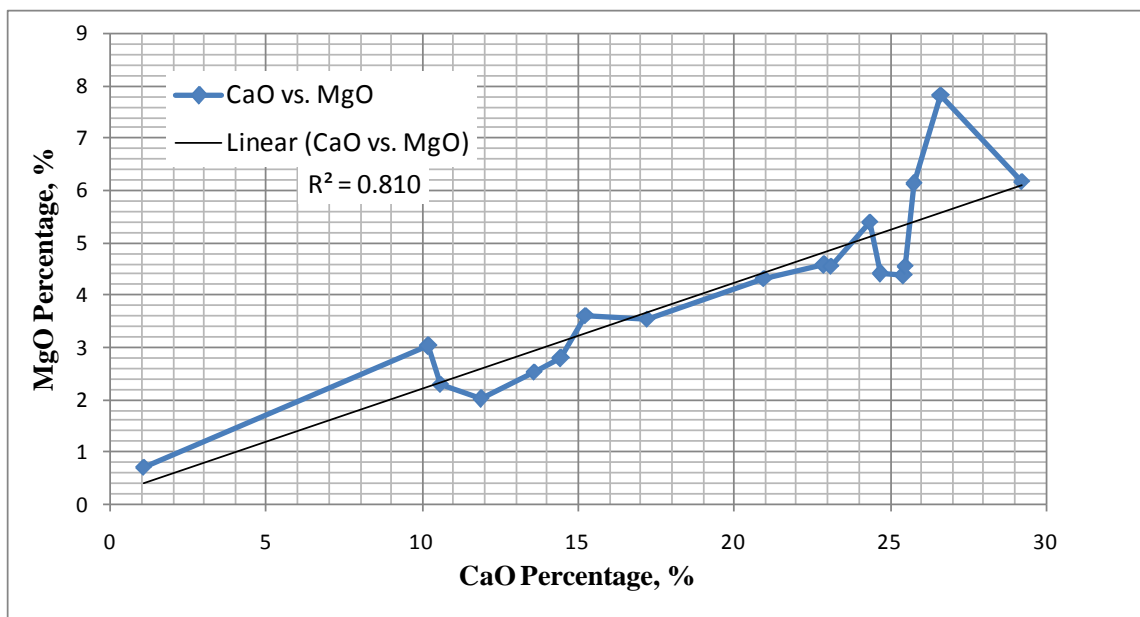


Figure B - 3: CaO vs. MgO

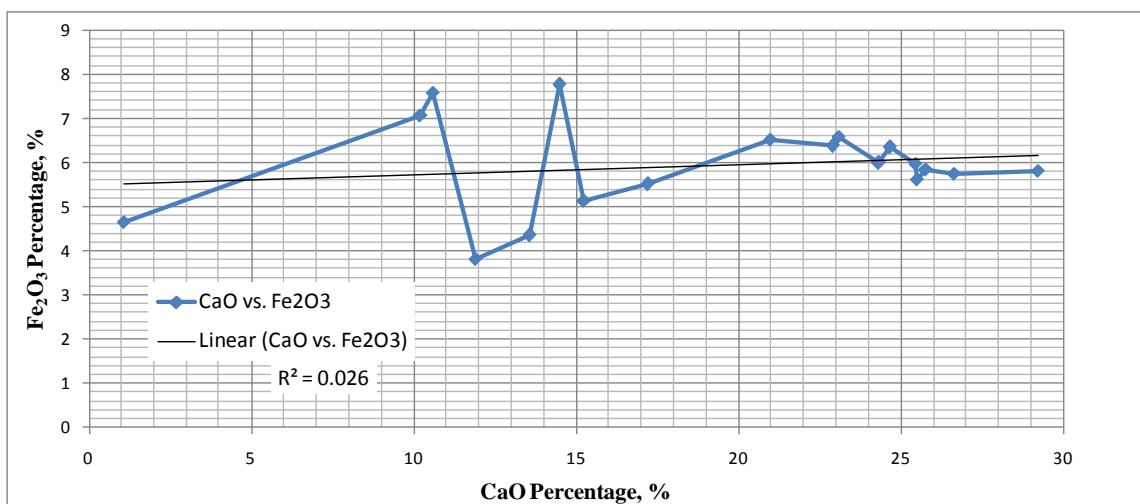


Figure B - 4: CaO vs. Fe<sub>2</sub>O<sub>3</sub>

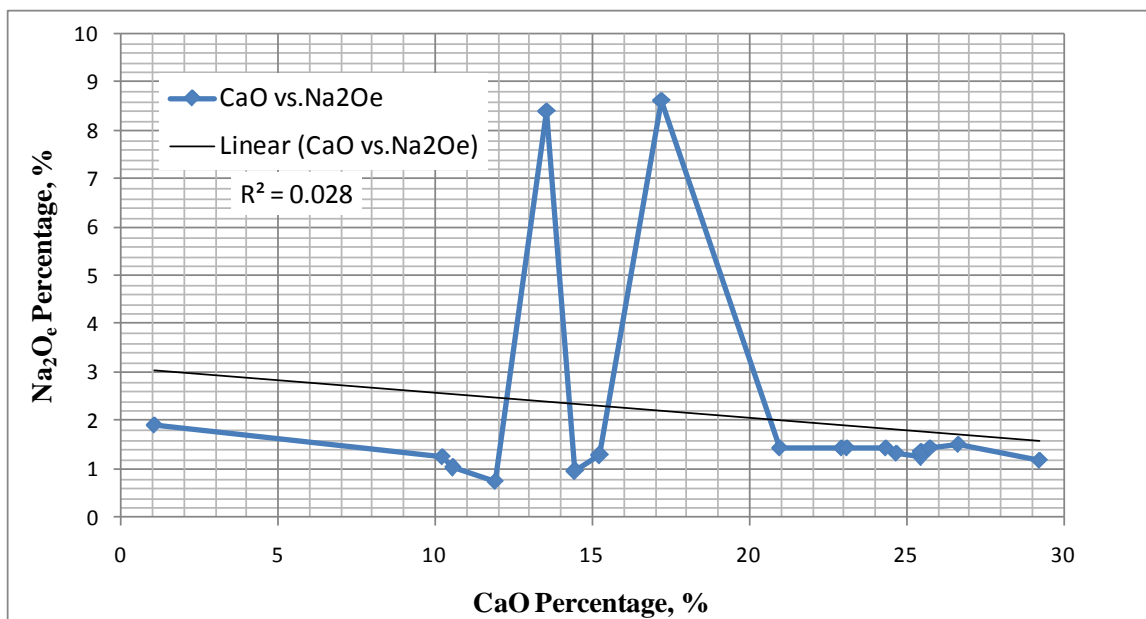


Figure B - 5: CaO vs. Na<sub>2</sub>O<sub>e</sub>

## Appendix C: Trends for Total Alkalis, Available Alkalis, Pore Solution, and Leaching

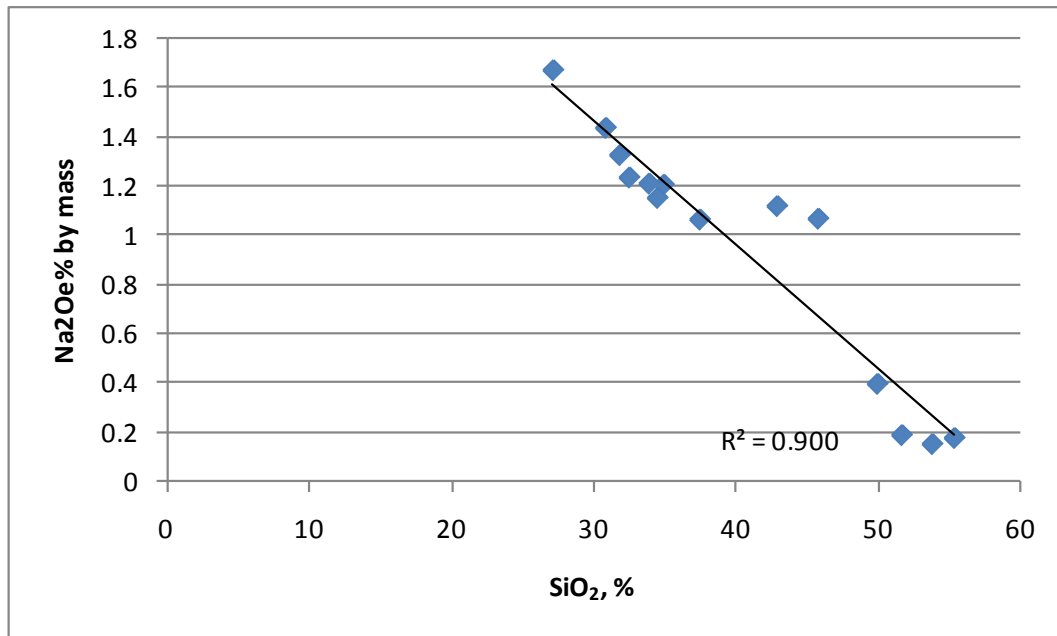


Figure C - 1: Acid-Soluble Alkalis ( $\text{SiO}_2$ )

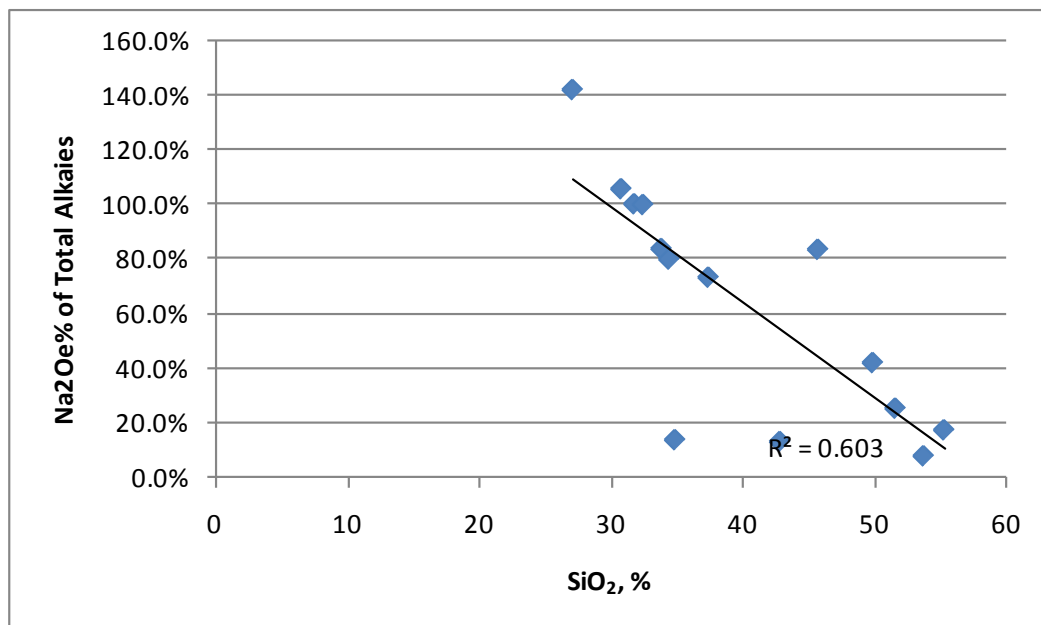


Figure C - 2: Acid-Soluble/Total Alkalis ( $\text{SiO}_2$ )

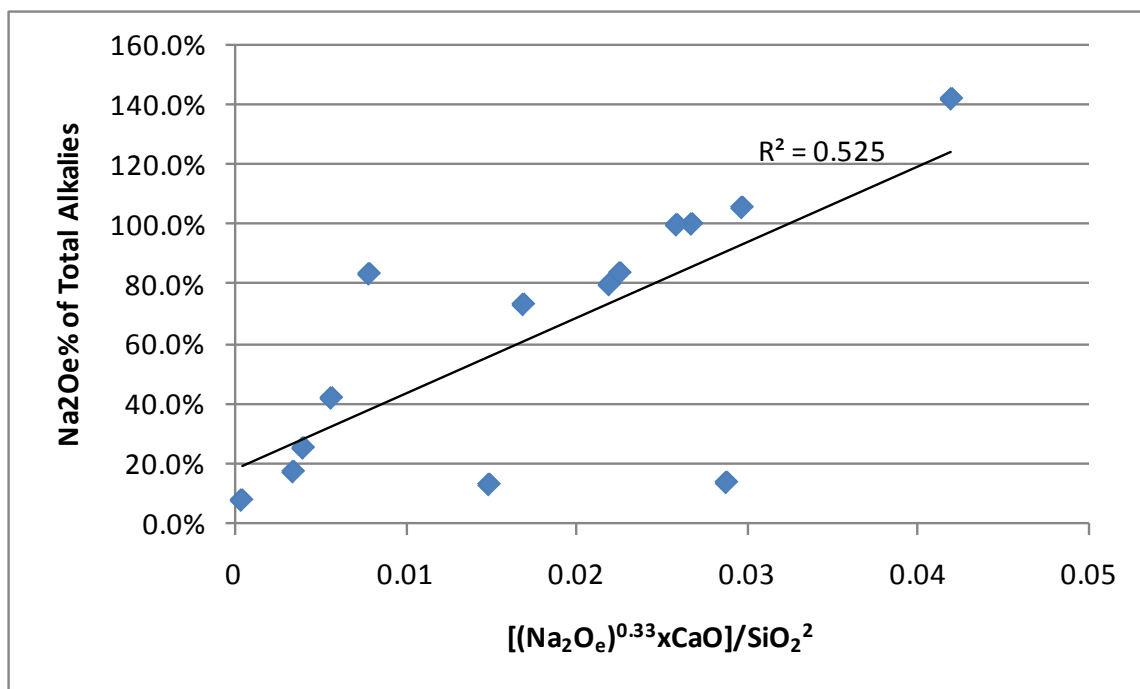


Figure C - 3: Acid-Soluble/Total Alkalies (Chemical Index)

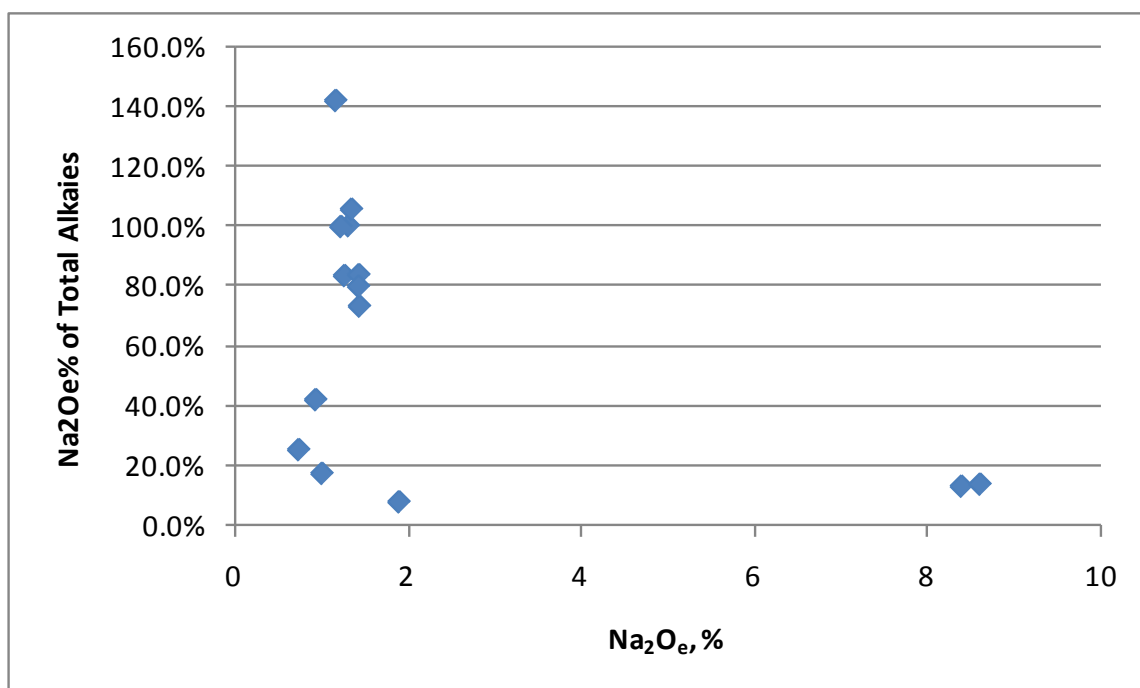


Figure C - 4: Acid-Soluble/Total Alkalies (Na<sub>2</sub>O<sub>e</sub>)

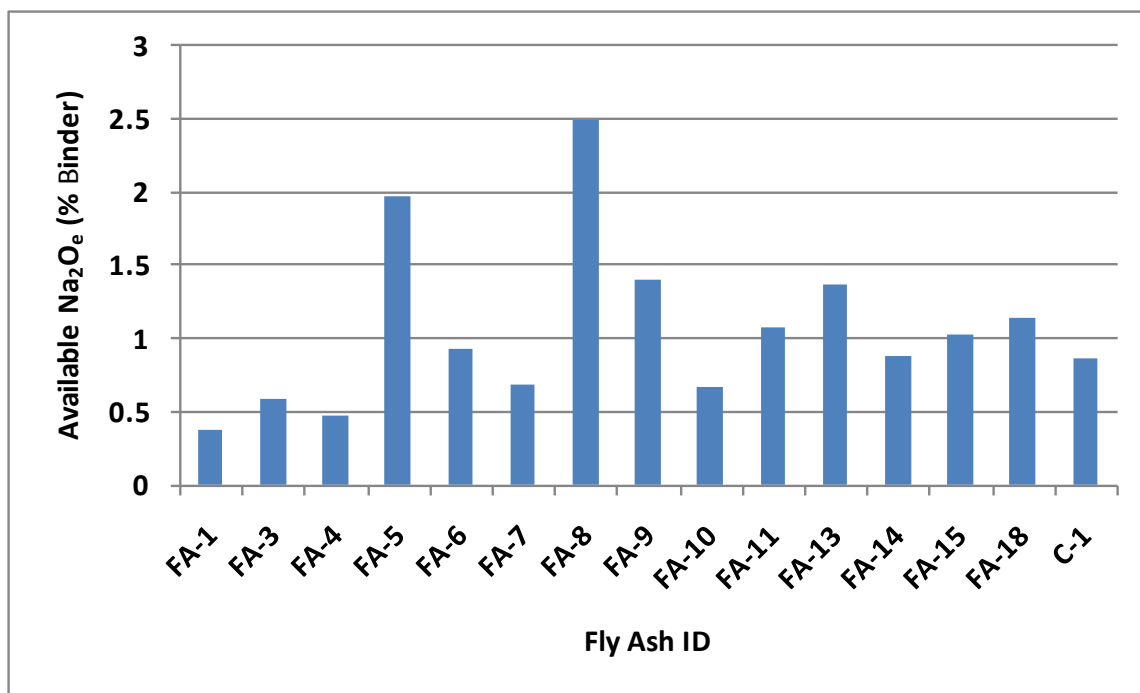


Figure C - 5: Leaching at 0.1 M  $\text{OH}^-$

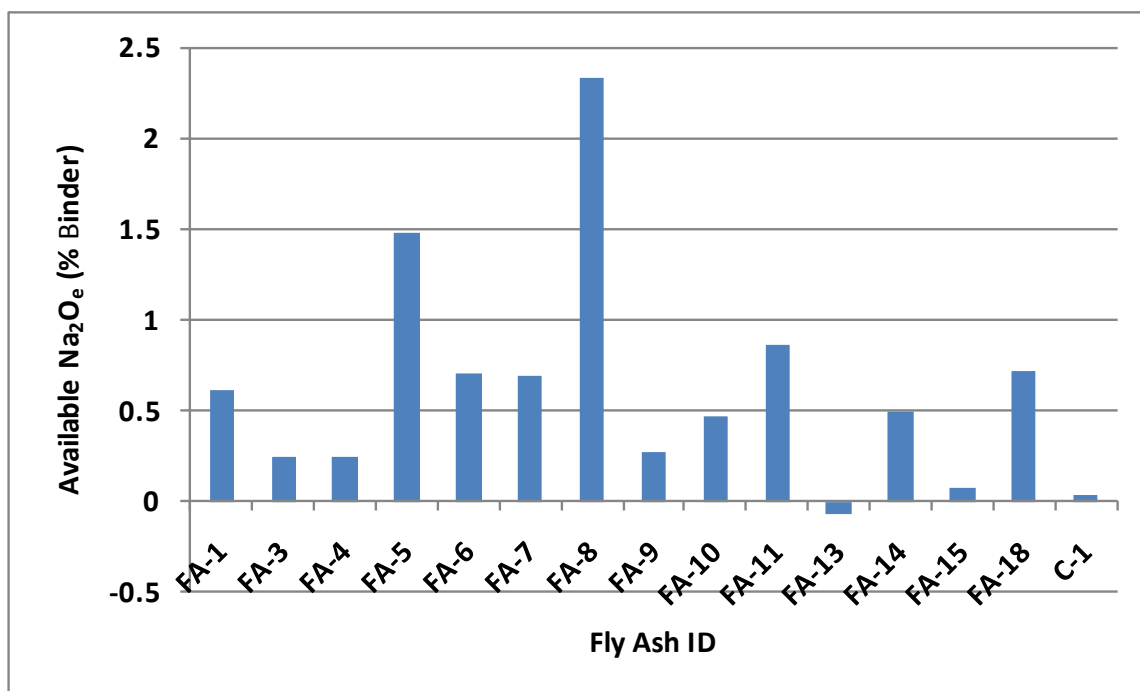


Figure C - 6: Leaching at 0.2 M  $\text{OH}^-$



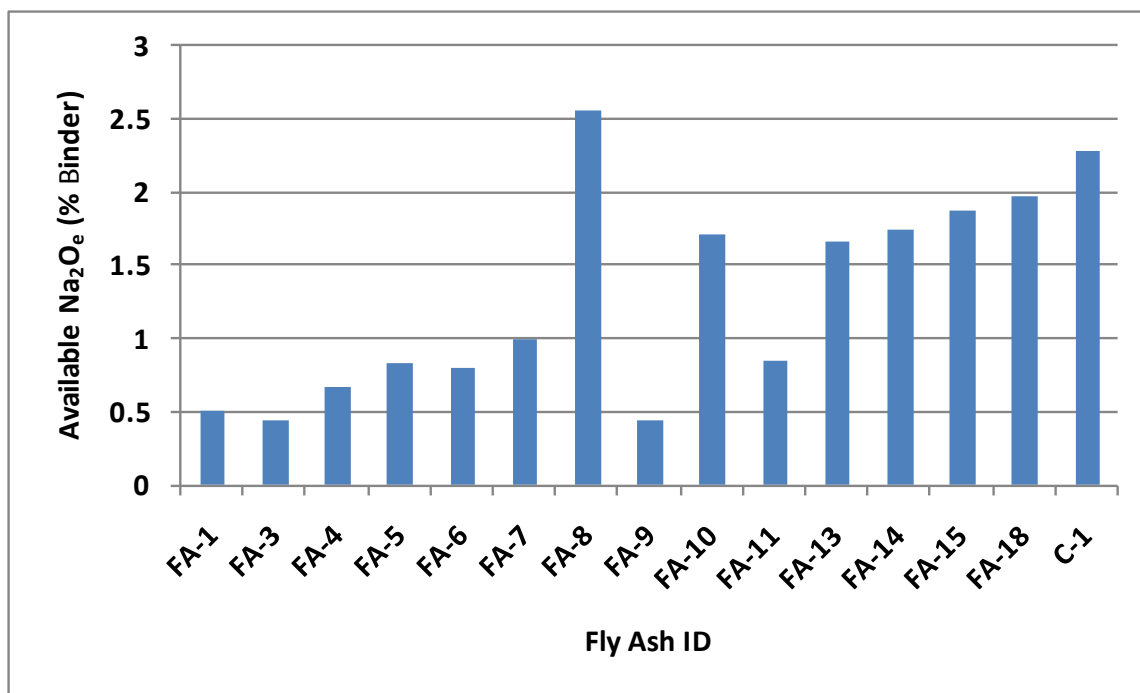


Figure C - 7: Leaching at 0.3 M  $\text{OH}^-$

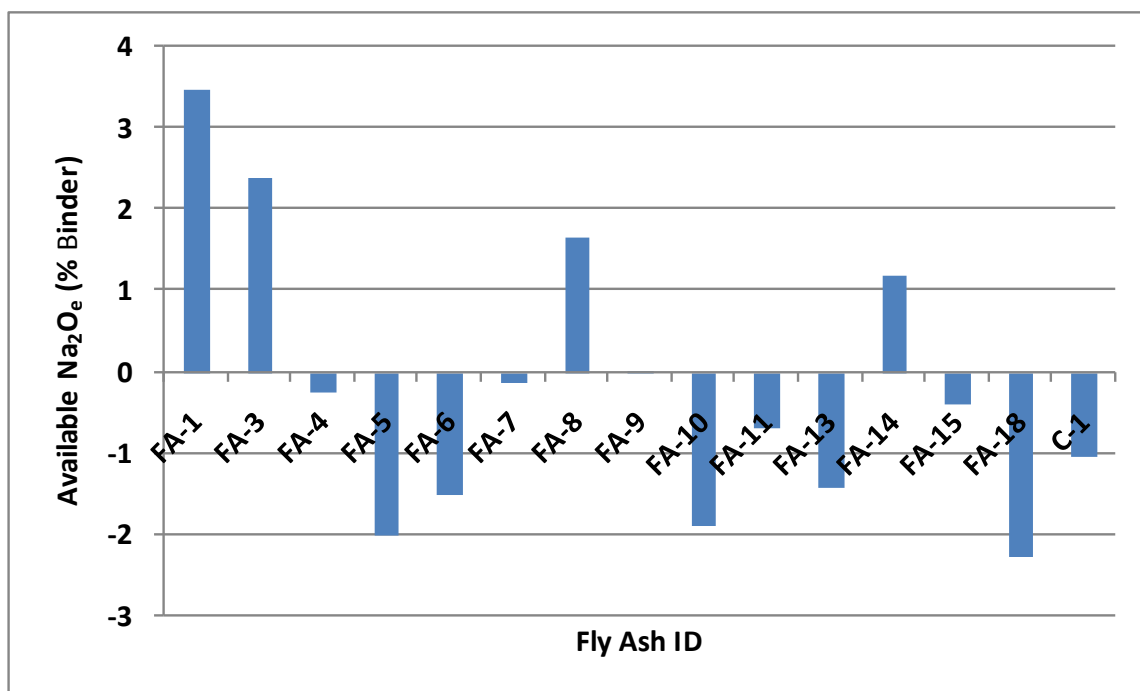


Figure C - 8: Leaching at 0.6 M  $\text{OH}^-$

## References

- ASTM Standard, C114. *Standard Test Methods for Chemical Analysis of Hydraulic Cement*. West Conshohocken, PA: ASTM International, 2011. Print. [www.astm.org](http://www.astm.org).
- ASTM Standard, C1260. *Standard Test Method for Potential Alkali Reactivity of Aggregates (Mortar-Bar Method)*. West Conshohocken, PA: ASTM International, 2007. Print. [www.astm.org](http://www.astm.org).
- ASTM Standard, C1567. *Standard Test Method for Determining the Potential Alkali-Silica Reactivity of Combinations of Cementitious Materials and Aggregate (Accelerated Mortar-Bar Method)*. West Conshohocken, PA: ASTM International, 2011. Print. [www.astm.org](http://www.astm.org).
- ASTM Standard, C305. *Standard Practice for Mechanical Mixing of Hydraulic Cement Pastes and Mortars of Plastic Consistency*. West Conshohocken, PA: ASTM International, 2012. Print. [www.astm.org](http://www.astm.org).
- ASTM Standard, C311. *Standard Test Methods for Sampling and Testing Fly Ash or Natural Pozzolans for Use in Portland-Cement Concrete*. West Conshohocken, PA: ASTM International, 2011. Print. [www.astm.org](http://www.astm.org).
- ASTM Standard, C430. *Standard Test Method for Fineness of Hydraulic Cement by the 45-Mm (No. 325) Sieve*. West Conshohocken, PA: ASTM International, 2003. Print. [www.astm.org](http://www.astm.org).

- ASTM Standard, C618. *Standard Specification for Coal Fly Ash and Raw or Calcined Natural Pozzolan for Use in Concrete*. West Conshohocken, PA: ASTM International, 2012. Print. [www.astm.org](http://www.astm.org).
- Baert, G., et al. "Interaction between the Pozzolanic Reaction of Fly Ash and the Hydration of Cement." *Ghent University*: n. pag. Print.
- Barlow, Donald F., and Peter J. Jackson. "The Release of Alkalis from Pulverised-Fuel Ashes and Ground Granulated Blastfurnce Slags in the Presence of Portland Cements." *Cement and Concrete Researach* (1988): n. pag. Print.
- Berube, M. A., et al. "Influence of Particle Size Distribution on the Effectiveness of Type-F Fly Ash in Suppressing Expansion Due to Alkali-Silica Reactivity." *SP 153-10 Milwaukee Conference*: n. pag. Print.
- Berube, Marc-Andre, and Charles Tremblay. "Chemistry of Pore Solution Expressed under High Pressure - Influence of Various Parameters and Comparasion with the Hot-Water Extraction." *CRIB*: n. pag. Print.
- Bleszynski, Roland F., and Michael D. Thomas. "Microstructural Studies of Alkali-Silica Reaction in Fly Ash Concrete Immersed in Alkaline Solutions." *Advn Cem Bas Mat* (1998): n. pag. Print.
- Brouwers, H. J., and R. J. Eijk. "Alkali Concentrations of Pore Solution in Hydrating OPC." *Cement and Concrete Research* (2003): n. pag. Print.
- Bulteel, D., et al. "Alkali-Silica Reaction A Method to Quantify the Reaction Degree." *Cement and Concrete Research* (2002): n. pag. Print.

- Canham, I., C. L. Page, and P. J. Nixon. "Aspects of the Pore Solution Chemistry of Blended Cements Related to the Control of Alkali Silica Reaction." *Cement and Concrete Research* (1987): n. pag. Print.
- Chancey, Ryan Thomas. "Characterization of Crystalline and Amorphous Phases and Respective Reactivities in a Class F Fly Ash." Diss. 2008. Print.
- Chen, W., and H. J. Brouwers. "Alkali Binding in Hydrated Portland Cement Paste." *Cement and Concrete Research* (2010): n. pag. Print.
- - -. "A Method for Predicting the Alkali Concentrations in Pore Solution of Hydrated Slag Cement Paste." *Journal of Material Science* (2011): n. pag. Print.
- "Determination of Sodium and Potassium Oxides by Flame Photometry." *Analytical Chemistry* (1954): n. pag. Print.
- Diamond, Sidney. "Effects of Two Danish Flyashes on Alkali Contents of Pore Solutions of Cement-Flyash Pastes." *Cement and Concrete Research* (1981): n. pag. Print.
- Duchesne, J., and M. A. Berube. "The Effectiveness of Supplementary Cementing Materials in Suppressing Expansion Due to ASR: Another Look at the Reaction Mechanisms Part 2: Pore Solution Chemistry." *Cement and Concrete Research* (1994): n. pag. Print.
- Duchesne, Josee, and Marc-Andre Berube. "Available Alkalies from Supplementary Cementing Materials." *ACI Materials Journal* (1994): n. pag. Print.
- "The Effectiveness of Supplementary Cementing Materials in Suppressing Expansion Due to ASR: Another Look at the Reaction Mechanisms Part 1: Concrete

- Expansion and Portlandite Depletion." *Cement and Concrete Research* (1993): n. pag. Print.
- Farbriar, Josef, and Ramon L. Carrasquillo. *Effectiveness of Fly Ash Replacement in the Reduction of Damage Due to Alkali-Aggregate Reaction in Concrete*. N.p.: n.p., 1986. Print.
- Fernandez-Jimenez, A., and A. Palomo. "Characterisation of Fly Ashes. Potential Reactivity as Alkaline Cements." *FUEL* (2003): n. pag. Print.
- Ferraris, Chiara F. *Alkali-Silica Reaction and High Performance Concrete*. N.p.: n.p., 1995. Print.
- FHWA. N.p., 2011. Web. <<http://www.fhwa.dot.gov/pavement/concrete/asr/history.cfm>>.
- Fournier, Benoit, and Marc-Andre Berube. "Alkali–Aggregate Reaction in Concrete: A Review of Basic Concepts and Engineering Implications." *Canadian Journal of Civil Engineering* (2000): n. pag. Print.
- Fraay, A. L., J. M. Bijen, and Y. M. Haan. "The Reaction of Fly Ash in Concrete. A Critical Examination." *Cement and Concrete Research* (1989): n. pag. Print.
- Garcia-Diaz, E., et al. "Mechanism of Damage for the Alkali-Silica Reaction." *Cement and Concrete Research* (2006): n. pag. Print.
- Geochemical Instrumentation and Analysis*. N.p., 2012. Web. <[http://serc.carleton.edu/research\\_education/geochemsheets/techniques/XRF.html](http://serc.carleton.edu/research_education/geochemsheets/techniques/XRF.html)>.
- Glasser, F. P., and J. Marr. "The Alkali Binding Potential of OPC and Blended Cements." *Cemento* (1985): n. pag. Print.

- Helmuth, Richard, comp. *Alkali-Silica Reactivity: A Overview of Research*. N.p.: n.p., 1993. Print. SHRP-C-342.
- Hemmings, R. T., and E. E. Berry. "On the Glass in Coal Fly Ashes: Recent Advances." *Materials Research Society* (1988): n. pag. Print.
- Hong, Sung, and F. P. Glasser. "Alkali Binding in Cement Pastes Part I. The C-S-H Phase." *Cement and Concrete Research* (1999): n. pag. Print.
- Hooton, R. D., and M. D. Thomas. "Pore Solution Analysis as a Tool for Studying Early –Age Hydration & Predicting Future Durability." Cement Hydration Summit. 2009. Print.
- Huffman, Morris, and Michael D. Thomas, comps. *Use of Fly Ash in Concrete*. N.p.: ACI Committee 232, 2003. Print. ACI Committee 232.
- Ideker, Jason H., et al. "Do Current Laboratory Test Methods Accurately Predict Alkali-Silica Reactivity?" *ACI Materials Journal* (2012): n. pag. Print.
- Junsomboon, Jaroon, and Jaroon Jamunee. "Determination of Potassium, Sodium, and Total Alkalies in Portland Cement, Fly Ash, Admixtures, and Water of Concrete by a Simple Flow Ime Photometric Systemnjection Fla." *Journal of Automated Methods and Management in Chemistry* (2011): n. pag. Print.
- Kutchko, Barbara G., and Ann G. Kim. "Fly Ash Characterization by SEM-EDS." *FUEL*: n. pag. Print.
- Lee, C. "Effects of Alkalies in Class C Fly Ash on Alkali-Aggregate Reaction." *Trondheim Conference* (1989): n. pag. Print.

- Lee, Chau. "Available Alkalis in Fly Ash and Their Effects on Alkali-Aggregate Reaction." Diss. 1986. Print.
- Lee, Chau, Scott Schlorholtz, and Turgut Demirel. "Available Alkalis in Fly Ash." *Materials Research Society* (1986): n. pag. Print.
- Lorenzo, P., et al. "Effect of Fly Ashes with High Total Alkalinity of the Pore Solution of Hydrated Portland Cement Paste." *Journal of the American Ceramic Society* (1996): n. pag. Print.
- Malvar, L. J., and L. R. Lenke. "Efficiency of Fly Ash in Mitigating Alkali Silica Reaction Based on Chemical Composition." *ACI Materials Journal* (2006): n. pag. Print.
- Malvar, L. J., and L. R. Lenke. "Minimum Fly Ash Cement Replacement to Mitigate Alkali Silica Reaction." *U.S. Navy*: n. pag. Print.
- Malvern. N.p., 2012. Web.  
<[http://www.malvern.com/processeng/systems/laser\\_diffraction/technology/technology.htm](http://www.malvern.com/processeng/systems/laser_diffraction/technology/technology.htm)>.
- Mings, M. L., et al. "Characterization of Fly Ash by X-Ray Analysis Methods." *Transportation Research Record*: n. pag. Print.
- Mitchell, L. D., et al. *The Mechanistic Differences between Alkali Silica and Alkali Carbonate Reactions as Studied by X-ray Diffraction*. N.p.: n.p., 2004. Print.  
NRCC.

- Nixon, P. J., et al. "The Effect of a Pfa with a High Total Alkali Content on Pore Solution Composition and Alkali Silica Reaction." *Magazine of Concrete Research* (1986): n. pag. Print.
- Pepper, Leonard, comp. *Influence of Alkali Content of Fly Ash on Effectiveness in Preventing Expansion of Concrete*. N.p.: n.p., 1963. Print.
- Rahhal, V., and R. Talero. "Fast Physics-Chemical Characterization of Fly Ash." *Journal of Thermal Analysis and Calorimetry* (2009): n. pag. Print.
- Ravina, Dan. "Optimized Determination of PFA (Fly Ash) Fineness with Reference to Pozzolanic Activity." *Cement and Concrete Research* (1980): n. pag. Print.
- Roy, Della, Karen Luke, and Sidney Diamond. "Characterization of Fly Ash and Its Reactions in Concrete." *Materials Research Society* (1985): n. pag. Print.
- Sakai, Etsuo, et al. "Hydration of Fly Ash Cement." *Cement and Concrete Research* (2005): n. pag. Print.
- Schulz, N. F. "Measurement of Surface Areas by Permeametry." *International Journal of Mineral Processing* (1974): n. pag. Print.
- Schure, Mark R., et al. "Surface Area and Porosity of Coal Fly Ash." *Environmental Science & Technology* (1985): n. pag. Print.
- Shehata, Medhat H. "The Effects of Fly Ash and Silica Fume on Alkali Silica Reaction in Concrete." Diss. 2001. Print.
- Shehata, Medhat H., and Michael Thomas. "The Effect of Fly Ash Composition on the Expansion of Concrete Due to Alkali-Silica Reaction." *Cement and Concrete Research* (2000): n. pag. Print.



- Shehata, Medhat H., and Michael D. Thomas. "Alkali Release Characteristics of Blended Cements." *Cement and Concrete Research* (2006): n. pag. Print.
- Shehata, Medhat H., Michael D. Thomas, and Roland F. Bleszynski. "The Effects of Fly Ash Composition on the Chemistry of Pore Solution in Hydrated Cement Pastes." *Cement and Concrete Research* (1999): n. pag. Print.
- Stanton, T. E. (1940). "Expansion of concrete through reaction between cement and aggregate." *Proc., ASCE*, 66, 1781–1811.
- Taylor, H. F. "A Method for Predicting Alkali Ion Concentrations in Cement Pore Solutions." *Advances in Cement Research* (1987): n. pag. Print.
- Thomas, Michael. "The Effect of Supplementary Cementing Materials on Alkali-Silica Reaction: A Review." *Cement and Concrete Research* (2010): n. pag. Print.
- Touma, Wissam Elias. "Alkali-Silica Reaction in Portland Cement Concrete: Testing Methods and Mitigation Alternatives." Diss. 2000. Print.
- Wang, Aiqin, Chengzhi Zhang, and Wei Sun. "Fly Ash Effects II. The Active Effect of Fly Ash." *Cement and Concrete Research* (2004): n. pag. Print.
- Wesche, K. "Test Methods for Determining the Properties of Fly Ash and of Fly Ash for Use in Building Materials." *Materials and Structures* (1989): n. pag. Print.
- Wesche, Karlhans. *Fly Ash in Concrete: Properties and Performance: Report of Technical Committee 67-FAB Use of Fly Ash in Building*. London: E & FN Spon, 1991. Print.